

**Fabrication of Biodegradable Graphene Crosslinked  
Polylactic Acid Nanocomposite with Enhanced Mechanical  
Strength**

by

MAJHARUL ISLAM SUJAN

STUDENT ID: 0416032702

MASTER OF SCIENCE IN CHEMISTRY



Department of Chemistry  
BANGLADESH UNIVERSITY OF ENGINEERING AND TECHNOLOGY

The thesis titled “Fabrication of Biodegradable Graphene Crosslinked Polylactic Acid Nanocomposite with Enhanced Mechanical Strength” submitted by Majharul Islam Sujan, Roll No: 0416032702, Session: April 2016, has been accepted as satisfactory in partial fulfillment of the requirement for the degree of Master of Science on June 3, 2018.

### BOARD OF EXAMINERS

1.

Dr. Md. Shafiul Azam  
Assistant Professor  
Department of Chemistry,  
BUET, Dhaka



Chairman

2.

Dr. Md. Abdur Rashid  
Professor & Head  
Department of Chemistry,  
BUET, Dhaka



Member  
(Ex-officio)

3.

Dr. Md. Nazrul Islam  
Professor  
Department of Chemistry,  
BUET, Dhaka



Member

4.


Dr. Chanchal Kumar Roy  
Assistant Professor  
Department of Chemistry,  
BUET, Dhaka



Member

5.

Dr. A. F. M. Mustafizur Rahman  
Professor  
Department of Applied Chemistry  
and Chemical Engineering,  
University of Dhaka, Dhaka



Member  
(External)

### **CANDIDATE'S DECLARATION**

It is hereby declared that this thesis or any part of it has not been submitted elsewhere for the award of any degree or diploma.

Majharul Islam Sujan

## DEDICATION

I dedicate this thesis to .....

*My Beloved Parents*  
&  
*Honorable supervisor*

**Table of Contents**

List of Figures ..... vi

List of Tables..... vii

List of Tables and Abbreviations of Technical Symbols and Terms .....viii

Acknowledgement ..... ix

Abstract ..... xi

# List of Tables and Figures

## Figures

<b>Figure 1.1.</b> Major Polyester Derived Biopolymers in the field of Engineering.....	22
<b>Figure 1.2.</b> Structural formula of Polydioxane.....	23
<b>Figure 1.3.</b> Major Players in Aliphatic Polycarbonate based Biopolymers in engineering field.....	24
<b>Figure 1.4.</b> Major Biopolyamides in engineering field .....	11
<b>Figure 1.5.</b> General Schemes of PLA.....	31
<b>Figure 1.6.</b> Different stereo forms of Lactide.....	32
<b>Figure 1.7.</b> General Scheme illustrating the basic principle of crosslinking and formation of high strength PLA .....	43
<b>Figure 2.2.1.</b> Schematic illustration of graphene oxide (GO) preparation.....	51
<b>Figure 2.2.2.</b> Schematic illustration of 2D-crosslinker preparation .....	52
<b>Figure 2.2.3.</b> Schematic illustration of GO-PLA preparation .....	53
<b>Figure 2.3.7.</b> Pellets preparation method in hot press by compression molding.....	58
<b>Figure 3.1.</b> Synthesis route of GO based 2D-crosslinker (GO-LA-LA).....	60
<b>Figure 3.2.</b> Schematic preparation route of GO based 2-D crosslinked (GO-LA-LA) Polylactic acid (GO-PLA).....	62
<b>Figure 3.3.</b> FTIR spectra of (a) GO, (b) GO-LA-LA, (c) PLA and (d) Crosslinked PLA.....	63
<b>Figure 3.4.1</b> XPS high resolution C1s spectra of GO and GO-LA-LA.....	65
<b>Figure 3.4.2</b> XPS high resolution C1s spectra of (a) PLA and (b) GO-PLA.....	66
<b>Figure 3.5.</b> EDX spectra of (a) PLA, (b) GO-PLA and (c) Crosslinked PLA.....	68
<b>Figure 3.6.1</b> AFM height sensor image of GO-LA-LA.....	70
<b>Figure 3.6.2</b> AFM height sensor images of (a) PLA and (b) crosslinked PLA.....	71
<b>Figure 3.6.3</b> Height profile image of GO-LA-LA.....	72
<b>Figure 3.6.4</b> Height profile images of (a, b) pristine PLA and	

(c, d) crosslinked PLA.....	73
<b>Figure 3.7</b> Typical SEM images for the surface of (a) pristine PLA and (b) crosslinked PLA.....	74
<b>Figure 3.8.</b> Thermogravimetric analysis of PLA, GO-PLA and crosslinked PLA...	75
<b>Figure 3.9.</b> DSC thermograms for the PLA, GO-PLA and crosslinked PLA.....	76
<b>Figure 3.10.</b> Stress vs. strain curve of pristine PLA and pure GO based PLA (GO-PLA).....	77
<b>Figure 3.11.</b> Stress vs. strain curve of pristine PLA and pure GO based PLA (GO-PLA), 0.1 and 0.2 % crosslinked PLA.....	78
<b>Figure 3.12.</b> Comparison of the compressive strength of PLA, GO-PLA, 0.1, 0.2% crosslinked PLA.....	80
<b>Figure 3.13.</b> Compressive stress vs. strain (%) curve of 0.33% crosslinked PLA.....	81
<b>Figure 3.14.</b> Compressive stress vs. strain (%) curve of 0.33% crosslinked PLA....	81
<b>References</b> .....	83

## Tables

<b>Table 1.1.</b> Major biodegradable polymers in the field of engineering materials .....	6
<b>Table 3.1.</b> Characteristic peak and interpretations correspond to GO, GO-LA-LA, PLA and crosslinked PLA.....	64
<b>Table 3.2.</b> XPS C1s peak information for four types of C bonds in GO and GO-LA-LA.....	66
<b>Table 3.3.</b> XPS C1s peak information for three types of C bonds in PLA and GO-PLA.....	67
<b>Table 3.4.</b> Elemental composition of PLA, GO-PLA and Crosslinked PLA.....	69
<b>Table 3.5.</b> Stress vs. strain curve of pristine PLA and pure GO based PLA (GO-PLA), 0.1 and 0.2 % crosslinked PLA.....	79

# **List of Abbreviations of Technical Symbols and Terms**

1. Graphene Oxide (GO).
2. Polylactic acid (PLA)
3. Lactic acid (LA)
4. 2D-Crosslinker (GO-LA-LA)
5. Pure GO polylactic acid (GO-PLA)
6. Compressive Strength (Comp. strength)
7. Abbreviation of Table 1.1 in page 7, and 8.



## Acknowledgement

At the very beginning, I humbly acknowledge my deepest gratitude to the almighty, the most gracious, benevolent and merciful creator for his infinite mercy bestowed on me in carrying out the research work presented in the dissertation.

It is a great pleasure for me to acknowledge my deepest sense of gratitude, sincere, appreciation, heartfelt indebtedness and solemn regards to my reverend teacher and supervisor Dr. Md. Shafiul Azam, Assistant Professor, Department of Chemistry, Bangladesh University of Engineering and Technology (BUET), for his kind supervision, indispensable guidance, valuable and constructive suggestions, liberal help and continuous encouragement during the whole period. It is obvious that his attributive contribution and efforts have greatly shaped me into what I am today. In fact, I am quite lucky to be a part of his ambitious research team.

It is my great honor to convey my sincere gratitude to my respected teacher Professor Dr. Md. Abdur Rashid, honorable Head of the Department of Chemistry, BUET for giving me his wonderful support to move through the academic processes during this M.Sc. program. I would like to convey my deepest gratitude to Professor, Dr. Md. Nazrul Islam, Dr. Md. Shakhawat Hossain Firoz, Dr. Abu Bin Imran, Dr. Chanchal Kumar Roy and Nahida Akter Department of Chemistry, BUET, for their valuable suggestions, appreciated comments, guidance and help during the research period.

I am thankful to all other respected teachers of the Department of Chemistry, BUET, for their time to time support. I would also like to thank all of the officers and staffs of the Department of Chemistry, BUET for their continuous help during my study period.

I am highly thankful to National Institute for Nanotechnology, University of Alberta, Edmonton, Canada, for the characterization of our samples using X-ray Photoelectron Spectroscopy (XPS), Atomic force microscopy (AFM) and FTIR.

I am grateful to Dr. Md. Abdul Gafur, Principal scientific officer, PP & PDC, BCSIR, Dhaka-1205 for his significant suggestions and lab facilities to make cylindrical pellets by using Hot Press.

I am highly grateful to all members of the board of examiners for their valuable suggestions and appreciated comments.

I am thankful to my dear colleagues and all the members of Azam Research Group for their friendly cooperation and lovely encouragement throughout my research period. Special thanks to Rizwan Tonoy, Mohammad Motiur Rahman Imon, Md. Ferdous and Fatema Zerine Farhana for their continuous help during the research.

I am also thankful to other fellows of Chemistry Materials Laboratory for their cooperation during the research period.

I am grateful to the authority of BUET and The World Academy of Sciences (TWAS) for providing financial support for this research work.

Finally, I would like to express my heartfelt indebtedness and profound gratitude to my beloved father, mother and all of my family members for their continuous inspiration and immeasurable sacrifices throughout the period of my study.

June, 2018

Majhual Islam Sujan

## Abstract

Intense research interest on development of biodegradable polymers as engineering material is backed by eco-friendliness of bio-based polymers; non-biodegradable nature of petroleum derived polymers; abundant bioavailability of precursor biomolecules in environment; involvement of relatively easy process parameters due to polymeric nature and finally possibility of incorporating multi-functional properties by exploiting advances in nanotechnology. Among synthetic biopolymers, PLA represents itself as a promising candidate to be used in packaging applications where absence of mechanical strength has been a noteworthy limitation. In order to overcome this limitation, incorporation of graphene-based material as filler in PLA has been a wide practice. However, in this experiment GO based 2D chemical crosslinker has been prepared and in situ polycondensation polymerization in presence of GO based 2D-crosslinker led to crosslinked PLA with higher molecular chain. The crosslinker, crosslinked PLA and neat PLA were characterized by XPS, AFM, SEM, TGA-DSC and FTIR. AFM analysis showed more than 10 times of thickness of crosslinked PLA than that of pristine form where an increase of 15 times in mechanical strength is observed. FE-SEM analysis showed that crosslinkers are dispersed homogeneously in PLA matrix without agglomeration and structural features also get improved due to overcoming of crosslinkers loading. Elemental composition and the presence of functional group was studied by FTIR and XPS analysis. Samples were also thermally characterized by TGA and DSC thermograms. The observations found that intelligent optimization in processing parameters pellet formation of GO crosslinked PLA would give high strength PLA with better packaging properties. Our crosslinked PLA exhibited first-rate mechanical properties compared to the neat PLA and pure GO based PLA. A comparison mechanical properties was also studied in different amount of crosslinkers loading.

CHAPTER 1 Introduction.....	1
1.1 Scope of Study: Plastic Pollution.....	2
1.2 Biopolymers and its Classification.....	3
1.3 Common Natural Biodegradable Polymers.....	8
1.3.1 Polysaccharides.....	8
1.3.1.1 Starch .....	8
1.3.1.2 Cellulose and its Derivative.....	11
1.3.1.3 Lignocellulosic Complexes.....	13
1.3.1.4 Chitin and Chitosan .....	14
1.3.2 Polypeptides /Proteins .....	15
1.3.2.1 Zein .....	15
1.3.2.2 Wheat Gluten .....	16
1.3.2.3 Collagen and Gelatin .....	17
1.3.2.4 Casein .....	19
1.3.2.5 Whey Protein .....	20
1.4 Synthetic Biopolymers Derived from Renewable Resources and Petroleum ...	20
1.4.1 Polyester Derived Biopolymers .....	21
1.4.2 Bio-Based Poly(ether-esters) based Polymers .....	22
1.4.3 Aliphatic Polycarbonate based Biopolymers .....	23
1.4.4 Polyamides based Biopolymers.....	25
1.4.5 Poly(ester amides) based Biopolymer.....	25
1.4.6 Poly(ether amides) based Biopolymer.....	26
1.4.7 Bio Polyurethane based Polymer.....	26
1.5 Light Weight Biodegradable Polymer based Packaging Material.....	27
1.6 Overview of Poly Lactic Acid as Packaging Material.....	29
1.6.1 PLA Production.....	30
1.6.1.1 Precursors.....	31
1.6.1.2 Polymerization of Precursors.....	33
1.6.2 PLA Properties.....	35
1.6.2.1 PLA Structure, Crystallinity and Physical Properties.....	36
1.6.2.2 Processing Properties.....	37

1.6.2.3 Mechanical Properties.....	39
1.6.2.4 Barrier Properties.....	40
1.7 Graphene Based Crosslinking of PLA: Motivation of Study.....	41
References .....	44

CHAPTER 2 Experimental .....	49
2.1 Materials and Instruments.....	50
2.1.1 Chemicals and Reagents.....	50
2.1.2 Instruments.....	50
2.2. Method of preparation .....	51
2.2.1. Preparation of Graphene Oxide (GO) .....	51
2.2.2. Preparation of GO based 2D-crosslinker (GO-LA-LA).....	52
2.2.3. Preparation of GO based 2D-crosslinked Polylactic acid (GO-PLA) .....	53
2.2.4. Preparation of neat Polylactic acid (PLA).....	54
2.2.5. Preparation of untreated GO grafted PLA .....	54
2.3 Sample characterization.....	54
2.3.1 Fourier transform infrared (FTIR) analysis.....	54
2.3.2 Scanning Electron Microscope (SEM).....	55
2.3.3 Atomic force microscope (AFM).....	55
2.3.4 X-ray Photoelectron Spectroscopy (XPS).....	56
2.3.5 Thermogravimetric analysis (TGA).....	56
2.3.6 Differential Scanning Calorimetry (DSC).....	56
2.3.7 Mechanical properties studies .....	57
References.....	58

CHAPTER 3 Results and Discussion.....	59
3.1 Synthesis route of GO based 2D-crosslinker (GO-LA-LA) .....	60
3.2 Synthesis route of GO based 2-D Crosslinked Polylactic acid.....	61
3.3 Functional Group Investigation by Fourier Transform Infrared Spectroscopy (FTIR) .....	63
3.4 X-ray photoelectron spectroscopy (XPS) analysis.....	65

3.4.1	High resolution C1s spectra analysis of GO and GO-LA-LA.....	65
3.4.2	High resolution C1s spectra analysis of PLA and crosslinked PLA (GO-PLA) .....	66
3.5	Energy-Dispersive X-ray Spectroscopy (EDXS).....	68
3.6	Surface Morphology study using Atomic force microscope (AFM).....	70
3.6.1	Surface morphology of GO-LA-LA.....	70
3.6.2	Surface morphology of neat PLA and crosslinked PLA.....	71
3.6.3	Height profile analysis of GO-LA-LA by Atomic force microscope.....	72
3.6.4	Height profile analysis of pristine PLA and crosslinked PLA by Atomic force microscope.....	73
3.7	Surface morphology of pristine PLA and crosslinked PLA using Field Emission Scanning Electron Microscopy (FE-SEM).....	74
3.8	Thermogravimetric analysis (TGA).....	75
3.9	Thermal behaviors of polymers using Differential scanning calorimetry (DSC).....	76
3.10.	Mechanical strength measurement.....	77
3.1.2	Conclusion.....	82
	References.....	83

# **Chapter 1**

## **Introduction**

## 1. Introduction

### 1.1 Scope of Study: Plastic Pollution

Intense research interest on development of biodegradable polymers as engineering material is backed by eco-friendliness of bio based polymers; non-biodegradable nature of petroleum derived polymers; abundant bioavailability of precursor biomolecules in environment; involvement of relatively easy process parameters due to polymeric nature and finally possibility of incorporating multi-functional properties by exploiting advances in nanotechnology. From supermarket bags to CDs, fossil derived plastic wastes have grabbed every sphere of our ecology becoming a marker of a new geological epoch. On average, more than 300 million tons of plastic is manufactured every year half of which is consigned to landfill or recycled. The remaining 150 million tons litter continents and oceans [1]. Although natural rubber has been known about since 1495, when Christopher Columbus landed on the island of Haiti but Charles Goodyear patented a method to sulfur vulcanize rubber in 1844 and since then it has been widely used in the tire industry. The first synthetic polymer was invented by Leo Hendrik Baekeland in 1907. This was a thermosetting phenol-formaldehyde resin called Bakelite. In recent decades, the rapid development of polymers has made a large contribution to technology with the invention of a highly effective catalytic polymerization process. Because commodity polymers like polyethylene, polypropylene, polystyrene, and polyvinyl chloride (PVC) can be produced very cheaply, their use has been exploited for the mass production of disposable packaging. Thus, around the world, polymer pollution has become a serious issue. These petroleum-derived commodity synthetic polymers require hundreds of years to fully degrade into harmless soil components. It is now almost impossible to walk in the countryside or on a beach without encountering bits of plastic. Such debris can kill or injure ecologically and commercially important species, including mussels, salt-marsh grasses and corals. Mammals, reptiles and birds can also be harmed through eating plastic or becoming entangled in it. Focusing on the most problematic materials is a realistic first step. Currently, just four plastics namely PVC, polystyrene, polyurethane and polycarbonate make up roughly 30% of production [2, 3]. These are particularly difficult to recycle and are made of potentially toxic materials. PVC is used in construction, such as in pipes that carry drinking water; polystyrene is used for food packaging; polyurethane in furniture; and polycarbonate in electronics. As plastic breaks into smaller pieces,



it is more likely to infiltrate food webs. In laboratory and field studies, fish, invertebrates and microorganisms ingest micrometer sized particles which also come from synthetic (polyester or acrylic) clothing and cleaning products containing plastics. Although steps have been taken to educate people about the environmental impact caused by the exploitation of plastics, these materials continue to represent the largest proportion of domestic waste. All these reasons together with reduction of reserve of crude oil has paved the way for searching renewable sources of raw materials for engineering polymers.

## **1.2 Biopolymers and its Classification**

In recent years, interest in protecting the environment by not only using products made from natural renewable resources but also products that decompose into environmentally friendly constituents has been steadily and rapidly increasing. Green movements, initiatives, and regulations have sprung up in almost every developed country to reduce the volume of solid polymers waste generated by consumers each year. Consumers have also expressed their desire for products that are environmentally friendly while providing the same results with products made from synthetic material.

In general biopolymer refers to polymeric biomolecules. From this viewpoint, three main biopolymers, classified according to the monomeric units used and the structure of the biopolymer formed: polynucleotides (RNA and DNA), which are long polymers composed of a number of nucleotide monomers; polypeptides, which are short polymers of amino acids; and polysaccharides, which are often linear bonded polymeric carbohydrate structures. However, from materials engineering perspective biopolymers are defined as polymers that are derived from renewable resources, as well as biological and fossil-based biodegradable polymers. Moreover, a number of terms such as “biodegradable,” “bio-based,” “compostable” are used in biopolymer engineering.

“Degradable” is a broad term applied to polymers or plastics that disintegrate by a number of processes including physical disintegration, chemical degradation and biodegradation by biological mechanisms. As result of this definition, a polymer may be degradable but not biodegradable. “Biodegradable” is a term focused on the functionality of a polymer, “biodegradability,” and it is applied to polymers that will degrade under the action of

microorganisms such as molds, fungi, and bacteria within a specific period of time and environment. According to the withdrawn standard ASTM D5488-94de1, biodegradable polymers refer to polymers that are capable of undergoing decomposition into carbon dioxide, methane, water, inorganic compounds, or biomass in which the predominant mechanism is the enzymatic action of microorganisms that can be measured by standard tests, over a specific period of time, reflecting available disposal conditions. The Japan Bioplastics Association (JBPA) defines the term “biodegradability” as the characteristics of material that can be microbiologically degraded to the final products of carbon dioxide and water, which in turn are recycled in the nature. Biodegradation should be distinguished from disintegration, which simply means the material is broken into small and separate pieces. Biodegradability of plastics is determined by the ISO methods and evaluated based upon the pre-established criteria. “Bio-based” is a term focused on the raw materials basis, and it is applied to polymers derived from renewable resources. Raw materials are defined as renewable if they are replenished by natural procedures at rates comparable or faster than their rate of consumption. ASTM defines a bio-based material as “an organic material in which carbon is derived from a renewable resource via biological processes. Bio-based materials include all plant and animal mass derived from carbon dioxide recently fixed via photosynthesis, per definition of a renewable resource”. Not every bio-based polymer is biodegradable (e.g., bio-based polyethylene or polyamide 11) and not every biodegradable polymer is bio-based ((e.g., poly( $\epsilon$ -caprolactone) (PCL) or poly(glycolic acid (PGA))), although some fall into both categories, such as polyhydroxyalkanoates (PHAs). “Compostable” polymer was defined by ASTM D6002-96(2002)e1 as “a plastic which is capable of undergoing biological decomposition in a compost site as part of an available program, such that the plastic is not visually distinguishable and breaks down to carbon dioxide, water, inorganic compounds, and biomass at a rate consistent with known compostable materials (e.g., cellulose) and leave no toxic residue.” The difference between biodegradable polymers and compostable polymers is determined by the rate of biodegradation, disintegration, and toxicity. All compostable polymers are by default biodegradable, but not vice versa [4].

The biopolymers can be classified according to their chemical composition, origin and synthesis method, processing method, economic importance, application, etc. However, two different criteria underline the definition of a “biopolymer”/“bioplastic”: (1) the source of the raw

materials and (2) the biodegradability of the polymer. Hence Niaounakis (2015) made classification on following basis:

- Type A: biopolymers made from renewable raw materials (bio-based) and being biodegradable
- Type B: biopolymers made from renewable raw materials (bio-based), and not being biodegradable
- Type C: biopolymers made from fossil fuels and being biodegradable.

The biopolymers of (type A) can be produced by biological systems (microorganisms, plants, and animals) or chemically synthesized from biological starting materials (e.g., corn, sugar, starch, etc.). Biodegradable bio-based biopolymers include (1) synthetic polymers from renewable resources such as poly (lactic acid) (PLA); (2) biopolymers produced by microorganisms, such as PHAs; (3) natural occurring biopolymers, such as starch or proteins—natural polymers are by definition those which are biosynthesized by various routes in the biosphere. The most used bio-based biodegradable polymers are starch and PHAs. The biopolymers of (type B) can be produced from biomass or renewable resources and are nonbiodegradable. Nonbiodegradable bio-based biopolymers include (1) synthetic polymers from renewable resources such as specific polyamides from castor oil (polyamide 11), specific polyesters based on biopropanediol, biopolyethylene (bio-LDPE, bio-HDPE), biopolypropylene (bio-PP), or biopoly(vinyl chloride) (bio-PVC) based on bioethanol (e.g., from sugarcane), etc.; (2) natural occurring biopolymers such as natural rubber or amber. The biopolymers of (type C) are produced from fossil fuel, such as synthetic aliphatic polyesters made from crude oil or natural gas, and are certified biodegradable and compostable. PCL, poly(butylene succinate) (PBS), and certain “aliphatic–aromatic” copolyesters are at least partly fossil fuel-based polymers, but they can be degraded by microorganisms.

Biopolymers can also be classified according to chemical nature of their backbone leading to differentiation in properties. For instance, Biopolymers can also be classified based on the ways in which they respond to heat as thermoplastics, thermosets or elastomers (niaounakis2015). Biopolymers are classified also on their composition as blends, composites, or laminates. Biopolymer blends are mixtures of polymers from different origins such as the commercial

**Table 1.1.** Major biodegradable polymers in the field of engineering materials

Biodegradable				Nonbiodegradable
Bio-based			Fossil-based	Bio-based
Plants	Microorganisms	Animal		
Cellulose and its derivatives (polysaccharide)	PHAs (e.g., P3HB, PHBHV, PHBHH <sub>X</sub> )	Chitin (polysaccharide)	Poly(alkylene dicarboxylates) (e.g., PBA, PBS, PBSA, PBSE, PEA, PES, PESE, PESA, PPF, PPS, PTA, PTMS, PTSE, PTT)	PE (LDPE, HDPE), PP, PVC
Lignin	PHF	Chitosan (polysaccharide)	PGA	PET, PPT
Starch and its derivatives (monosaccharide)	Bacterial cellulose	Hyaluronan (polysaccharide)	PCL	PU
Alginate (polysaccharide)	Hyaluronan (polysaccharide)	Casein (protein)	PVOH	PC
Lipids (triglycerides)	Xanthan (polysaccharide)	Whey (protein)	POE	Poly(ether-esters)

Wheat, corn, pea, potato, soy, potato (protein)	Curdlan (polysaccharide)	Collagen (protein)	Polyanhydrides	Polyamides (PA 11, PA 410, PA 610, PA 1010, PA 1012)
Gums (e.g., <i>cis</i> -1,4 polyisoprene)	Pullulan (polysaccharide)	Albumin (protein)	PPHOS	Polyester amides
Carrageenan	Silk (protein)	Keratin,PFF (protein)		Unsaturated polyesters
PLA (from starch or sugarcane)		Leather (protein)		Epoxy
				Phenolic resins

product Ecovio (BASF AG), which is a blend of PLA and poly(butylene adipate-co-terephthalate) (PBAT) (Ecoflex, BASF AG). The biopolymers can be classified into a chemical synthesis type, a microorganism production type and a natural type which are derived from the biomass, that is, materials derived from plants. Table 1.1 contains major biopolymers playing in the field of biodegradable polymer engineering [4].

**N.B Table 1.1:** HDPE, high-density polyethylene; LDPE, low-density polyethylene; P3HB, poly(3-hydroxybutyrate); P4HB, poly(4-hydroxybutyrate); PBA, poly(butylene adipate); PBS, poly(butylene succinate); PBSA, poly(butylene succinate-co-adipate); PBSE, poly(butylene sebacate); PC, polycarbonate; PCL, poly( $\epsilon$ -caprolactone); PE, polyethylene; PEA, poly(ethylene adipate); PES, poly(ethylene succinate); PESA, poly(ethylene succinate-co-adipate); PESE, poly(ethylene sebacate); PET, poly(ethylene terephthalate); PFF, poultry feather fiber; PGA,

poly(glycolic acid), polyglycolide; PHA, polyhydroxyalkanoate; PHBHH<sub>x</sub>, poly(3-hydroxybutyrate-co-3-hydroxyhexanoate); PHBV, poly(3-hydroxybutyrate-co-3-hydroxyvalerate); PHF, polyhydroxy fatty acid; PHH, poly(3-hydroxyhexanoate); PLA, poly(lactic acid), polylactide; POE, poly(ortho ester); PP, polypropylene; PPF, poly(propylene fumarate); PPHOS, polyphosphazenes; PPS, poly(propylene succinate); PTA, poly(tetramethylene adipate); PTMS, poly(tetramethylene succinate); PTSE, poly(tetramethylene sebacate); PTT, poly(trimethylene terephthalate); PU, polyurethane; PVC, poly(vinyl chloride); PVOH, poly(vinyl alcohol).

### 1.3 Common Natural Biodegradable Polymers

Biopolymers are formed in nature during the growth cycles of all organisms; hence, they are also referred to as natural polymers. Their synthesis generally involves enzyme catalyzed, chain growth polymerization reactions of activated monomers, which are typically formed within cells by complex metabolic processes.

#### 1.3.1 Polysaccharides

For materials applications, the principal polysaccharides of interest are cellulose and starch, but increasing attention is being given to the more complex carbohydrate polymers produced by bacteria and fungi, especially to polysaccharides such as xanthan, curdlan, pullulan and hyaluronic acid. These latter polymers generally contain more than one type of carbohydrate unit, and in many cases these polymers have regularly arranged branched structures. Because of this difference, enzymes that catalyze hydrolysis reactions during the biodegradation of each kind of polysaccharides are different and are not interchangeable. In this section a number of polysaccharides namely starch, cellulose and its derivatives, lignocellulosic materials and chitin are discussed.

##### 1.3.1.1 Starch

Starch is the major polysaccharide reserve material of photosynthetic tissues and of many types of plant storage organs such as seeds and swollen stems. The principal crops used for its

production include potatoes, corn and rice. In all of these plants, starch is produced in the form of granules, which vary in size and somewhat in composition from plant to plant. The starch granule is essentially composed of two main polysaccharides, amylose and amylopectin with some minor components such as lipids and proteins.

There are three types of crystallinity in starch. They are the 'A' type mainly cereal starches such as maize, wheat, and rice; 'B' type such as tuber starches (potato, sago); and finally the 'C' type crystallinity which is the intermediate between A and B type crystallinity, normally found in bean and other root starches. Another type of crystallinity is the Vh-type, which is the characteristic of amylose complexed with fatty acids and monoglycerides. Starch granules contain alternating 120-400 nm amorphous and semi-crystalline layers or growth rings. The semi-crystalline growth rings are composed of alternating amorphous and crystalline lamellae. The sum of one amorphous and one crystalline lamella is around 9-10 nm in size [5]. Amylopectin is often presumed to support the framework of the semi-crystalline layers in the starch granule. The short chains with polymerization degrees ranging between 15 and 18 form a double helical conformation and associating into clusters. These clusters pack together to produce a structure of alternating crystalline and amorphous lamellar composition. The side chains clusters which are predominantly linear and form double helices are responsible for the crystalline lamellae while the branching regions of the amylopectin molecule are responsible for the amorphous lamellae [6].

Thermoplastic starch is plasticized starch that has been processed (typically using heat and pressure) to completely destroy the crystalline structure of starch to form an amorphous thermoplastic starch. Thermoplastic starch processing typically involves an irreversible order-disorder transition termed gelatinization. Starch gelatinization is the disruption of molecular organization within the starch granules and this process is affected by starch-water interactions [7]. Thermoplastic starch is produced using dry native starch with a swelling or plastifying agent in compound extruders without adding water. In extrusion, starch is converted by application of both thermal and mechanical energy, and basically three phenomena occur at different structural levels: fragmentation of starch granules; hydrogen bond cleavage between starch molecules, leading to loss of crystallinity; and partial depolymerization of the starch polymers. Furthermore, the extrusion process ensures the very intimate mixing of the polymers and any additives. By

introduction of mechanical energy and heat in a temperature range of 120-220 °C, crystal starch, is homogenized and melted in an extrusion process with a plasticizer which lowers the melting point of the starch. With this process, a permanent conversion of the molecular structure to thermoplastic starch is performed [8].

Depending on the starch source and processing conditions, a thermoplastic material may be obtained with different properties suitable for various applications. Starch has been widely used as a raw material in film production because of increasing prices and decreasing availability of conventional film-forming resins. Potential applications of starch films include production of disposable food service-ware, food packaging, purchase bags, composting bags and loose fill product. Starch is also used in hygiene and cosmetics. Moreover, starch has been used for many years as an additive to plastic for various purposes. Starch was added as filler to various resin systems to make films that were impermeable to water but permeable to water vapor. Starch as biodegradable filler in LDPE was reported. A starch-filled polyethylene film was prepared which becomes porous after the extraction of the starch. This porous film can be readily invaded by microorganisms and rapidly saturated with oxygen, thereby increasing polymer degradation by biological and oxidative pathways [9]. Starch is also useful for making agricultural mulch films because it degrades into harmless products when placed in contact with soil microorganisms. Starch is also used in medical applications. For example, starch-based thermoplastic hydrogels for use as bone cements or drug-delivery carriers have been developed through blending starch with cellulose acetate [8].

Important properties of thermoplastic starch based materials include compostable in accordance with DIN 54900, high water vapor permeability, good oxygen barrier, not electrostatically chargeable and low thermal stability. In general, the low resistance to water and the variations in mechanical properties under humid conditions affect the use of starch for various applications. As water has a plasticizing power, the material behavior changes according to the relative humidity of the air. Strong hydrophilic character (water sensitivity) and poor mechanical properties compared to conventional synthetic polymers are the most important disadvantages of starch which make it unsatisfactory for some applications such as packaging purposes [4]. Generally, many approaches are suggested to mitigate these shortcomings. One approach is the modification of starch. Cross-linking can be produce low water sensitive and high strength



materials. The esterification of starch allows the increase of its thermoplastic characteristics, as well as its thermal stability. Other approach to improve the functional properties of the starch films is to blend starch with other polymers. Mao et al. (2000) examined the extrusion of thermoplastic cornstarch- glycerol-polyvinyl alcohol (PVOH) blends and noted the effect of PVOH to improve mechanical properties and slow biodegradation [10]. In terms of nanocomposite reinforcement of thermoplastic starch polymers there has been much exciting new developments. Dufresne and Cavaille (1998) and Angles and Dufresne (2000) highlight work on the use of microcrystalline whiskers of starch and cellulose as reinforcement in thermoplastic starch polymer and synthetic polymer nanocomposites. They find excellent enhancement of properties, probably due to transcrystallisation processes at the matrix/fibre interface [11, 12]. Almasi et al. (2010) examined the use of nanoscale montmorillonite into starch/carboxymethyl cellulose blends and finds excellent improvements in film impermeability and tensile properties [13].

### **1.3.1.2 Cellulose and its Derivatives**

After starch, prime attention has been paid to cellulose and its derivatives. At present, cellulose is the most abundant polymer available worldwide with an estimated annual natural production of  $1.5 \times 10^{12}$  tons and considered as an almost inexhaustible source of raw materials. Cellulose is composed of polymer chains consisting of unbranched D-glucopyranosyl units. Cellulose is the main constituent of cell wall in lignocellulosic plant, and its content depends on the plant species, growing environment, position, growth, and maturity. Generally, cellulose content in lignocellulosic plant is 23–53% on a dry-weight basis, less than that in cotton, which is almost made of pure fibrous cellulose. In most straw species, approximately 35–45% of the dry substance is cellulose. In the lignocellulosic materials, cellulose is embedded in a gel matrix composed of hemicelluloses, lignins, and other carbohydrate polymers [5].

Cellulose was isolated for the first time some 150 years ago. The combination of the chemical and the mechanical treatments is necessary for the dissolution of lignins, hemicelluloses, and other noncellulosic substances. A protocol based on acidified sodium chloride is frequently applied to de-lignify woody materials as an initial step in the isolation of cellulose. Alkali extraction to dissolve hemicelluloses before or after delignification is the common method. The

presence of high amounts of lignin in isolated cellulose fibers after delignification affects the structure and properties of the cellulose fibers. Fibers with high amounts of lignin are coarse and stiff, and have a brownish color. Therefore, it is challenging to obtain fibers that are relatively free of bound lignin. To achieve this aim, chemical bleaching, which is used to obtain fibers with higher cellulose content from de-lignified and unbleached fibers, is usually considered as a continuation of delignification process to isolate cellulose from woody raw materials. Nowadays, there are various procedures for extraction of cellulose micro-fibrils like pulping methods, acid hydrolysis, steam explosion etc. [14].

Many useful properties stem from unique functional characteristics related to the chemical structure of cellulose. These structural properties include an extended, planar chain conformation and oriented, parallel-chain packing in the crystalline state. The absence of branches in this 100% linear polymer contributes to efficient chain packing in the native crystalline state, resulting in stiff, dimensionally stable fibers. Cellulose fibers thus exhibit a high degree of crystallinity (upwards of 70%) when isolated and purified. However, cellulose fibers present in native woody biomass exhibit approximately 35% crystallinity, due to the presence of other lignocellulosic components. The crystal nature (monoclinic sphenodic) of naturally occurring cellulose is known as cellulose I. Cellulose is resistant to strong alkali (17.5 wt%) but is easily hydrolyzed by acid to water-soluble sugars. Cellulose is relatively resistant to oxidizing agents. The tight fiber structure created by hydrogen bonds results in the typical material properties of cellulose, such as high tensile strength and insolubility in most solvents. There are significant differences between the properties of straw cellulose, wood cellulose, and cotton cellulose. The cellulose crystallites are longer in straw pulps than in wood pulps, but they are not as long as in cotton cellulose. In addition, the degree of crystallinity of straw pulps appears to be less than that of wood cellulose. Low crystallinity can be useful when a cellulose derivative is to be manufactured. Cellulose has received more attention than any other polymer since it is attacked by a wide variety of microorganisms. The biodegradation of cellulose is complicated, because cellulose exists together with lignin however, it is fortunate that pure cellulose does decompose readily. Fermentation of cellulose has been suggested as a source of chemicals such as ethanol and acetic acid, but this has not achieved any commercial importance to date [15].

The most significant cellulosic applications are in the paper, wood product, textile, film, and fiber industries but recently it has also attracted significant interest as a source of biofuel production. The natural cellulosic carbon skeleton can be utilized in two major applications on an industrial scale. The first is as regenerated or mercerized cellulose (cellulose II, Rayon), which is not moldable and is used only for film and fiber production. The second represents a broader class of applications, which employs chemically modified celluloses, principally the cellulose esters [16]. As mentioned before, in all forms, cellulose is a very highly crystalline, high molecular weight polymer, which is infusible and insoluble in all but the most aggressive, hydrogen bond- breaking solvents such as N-methylmorpholine-N-oxide. Because of its infusibility and insolubility, cellulose is usually converted into derivatives to make it more processable. All of the important derivatives of cellulose are reaction products of one or more of the three hydroxyl groups, which are present in each glucopyranoside repeating unit [15]. These modified forms of cellulose can be tailored to exhibit particular physical and chemical properties by varying the pattern and degrees of substitution within the cellulose backbone. Industrial applications are numerous and widespread for cellulose derivatives owing to rigidity, moisture vapor permeability, grease resistance, clarity, and appearance [17]. Esterification of the cellulose backbone provides structural changes that allow for a greatly expanded range of applications, not available to the parent polysaccharide. Commercially available forms of cellulose acetate have degrees of substitution between 1.7 and 3.0 and are currently used in high volume applications ranging from fibers, to films, to injection molding thermoplastics, to low solids solvent-borne coatings for metal and automobile industries. Methylcellulose exhibits thermal gelation and has excellent film-forming properties. It has been widely used to prepare edible films. Carboxymethyl cellulose is also widely used in the pharmaceutical and food industries. It has good film forming properties. Carboxymethyl cellulose based film is a very efficient oxygen, carbon dioxide, and lipid barrier. However, it has poor resistance to water vapor transmission [18].

### **1.3.1.3 Lignocellulosic Complexes**

The lignocellulosic materials have the potential to be utilized as a feedstock for the production of a wide variety of industrial and commodity products, ranging from paper, lumber, and platform

chemicals to a variety of fuels and advanced materials, including biodegradable polymers. For example, HMP forms excellent films. Plasticized blends of citrus pectin and high amylase starch give strong, flexible films, which are thermally stable up to 180°C. Pectin is also miscible with poly(vinyl alcohol) in all proportions. Potential commercial uses for such films are water soluble pouches for detergents and insecticides, flushable liners and bags, and medical delivery systems and devices [19].

Hemicellulose can be utilized in microbial fermentations for the production of a variety of value-added products. Detoxified hemicellulosic hydrolysates have been used as xylose-rich feedstocks in a variety of biotechnological applications including the microbial production of ethanol, xylitol, and biodegradable polyhydroxyalkanoate (PHA) polymers. Production of PHAs based on renewable, bio-based substrates could make PHA-derived thermoplastic products more economically competitive with petroleum-based plastics, as the major costs in PHA production are the carbon source and the separation process. In the next section of this chapter we will describe the properties of this family of degradable microbial polyesters [15].

### **1.3.1.4 Chitin and Chitosan**

Chitin is a polysaccharide found in the shells of crabs, lobsters, shrimps and insects or can be generated via fungal fermentation processes. Chitosan is the deacylated derivative of chitin and forms the exoskeleton of arthropod. Structurally chitosan is a linear polysaccharide consisting of  $\beta$  D-glucosamine with randomly located N-acetylglucosamine groups depending upon the degree of deacetylation of the polymer.

Chitin is insoluble in its native form but chitosan, is water soluble. Chitosan is soluble in weakly acidic solutions resulting in the formation of a cationic polymer with a high charge density and can therefore form polyelectrolyte complexes with wide range of anionic polymers. Chitosan has been found to be non-toxic after oral administration in humans and is an FDA approved food additive. These biopolymers are biocompatible and have antimicrobial activities as well as the ability to absorb heavy metal ions. They also find applications in the cosmetic industry because of their water-retaining and moisturizing properties [15]. Chitosan has been formed into membranes and matrices suitable for several tissue-engineering applications. Chitin derivatives

can also be used as drug carriers. Chitosan was used to develop injectable thermo-sensitive carrier material for biomedical applications. Due to the mild gelling conditions, the hydrogel has been found to be a potential delivery vehicle for growth factors, small molecular weight drugs and cells for localized therapy. The high chemical reactivity of chitosan, has also led to several chitosan-drug conjugates for cancer therapy. Chitosan gels, powders, films, and fibers have been formed and tested for many applications such as encapsulation, membrane barriers, contact lens materials, cell culture, and inhibitors of blood coagulations. Chitosan has good film forming properties and therefore can be used as a food packaging material [20].

### **1.3.2 Polypeptides /Proteins**

Proteins can be defined as natural polymers able to form amorphous three-dimensional structures stabilized mainly by noncovalent interactions. The functional properties of these materials are highly dependent on structural heterogeneity, thermal sensitivity, and hydrophilic behavior of proteins. Numerous vegetable and animal proteins are commonly used as biodegradable polymers. Here discussions have been made on zein, gluten, soy, collagen and gelatin, casein and caeinates and whey proteins.

#### **1.3.2.1 Zein**

Zein comprises a group of alcohol-soluble proteins (prolamins) found in corn endosperm. It accounts for 50% or more of total endosperm protein, and it's only known role is the storage of nitrogen for the germinating embryo. It can be extracted with aqueous alcohol and dried to a granular powder. Based on solubility differences, zein consists of three protein fractions, i.e.,  $\alpha$ -zein,  $\beta$ -zein, and  $\gamma$ -zein. Due to the hydrophobic nature of zein, water sorption is extremely low in the low water activity range. Zein, although not soluble in water, is readily plasticized by it. Zein films are brittle at ambient temperature and need plasticization to become flexible. Plasticization increases polymer mobility, decreases glass transition temperature ( $T_g$ ), and markedly changes rheological properties. Common zein plasticizers include glycerol, glyceryl monoesters, poly ethylene glycol, and fatty acids [21].

Film-forming properties of zein have been recognized for decades, and they are the basis for its commercial utilization [22]. Coating films are formed on hard surfaces by covering them with zein solutions and allowing the solvent to evaporate off. The dried zein residue forms hard and glossy, scuff-proof, protective coatings that also are resistant to microbial attack. Zein coatings are used as oxygen, lipid, and moisture barriers for nuts, candies, confectionery products, and other foods. Rice fortified with vitamins and minerals has been coated with zein/stearic acid/wood resin mixtures to prevent vitamin and mineral losses during washing in cold water [23]. Pharmaceutical tablets are zein-coated for controlled ingredient release and protection. Use of zein-based coatings has been suggested for reducing oil uptake by deep-fat fried foods, for protecting active ingredients in chewing gum, for achieving controlled release of active ingredients in pharmaceutical tablets and for masking the taste of orally administered drugs. Zein, upon casting from aqueous aliphatic alcoholic solutions forms tough, glossy and grease resistant films. By cross-linking the tensile strength of the films is further improved. Zein films have water vapor permeability (WVP) values lower than or similar to those of other protein films, cellulose ethers, and cellophane. However, their WVP is notably higher than that of LDPE or ethylene-vinyl alcohol copolymer [5].

### **1.3.2.2 Wheat Gluten**

Wheat gluten consists mainly of wheat storage protein (70–80%, dry matter basis) with traces of starch and non-starch polysaccharides (10–14%), lipids (6–8%), and minerals (0.8–1.4%). Osborne distinguished four wheat protein classes based on their solubility in different solvents, namely, albumins, globulins, gliadins, and glutenins. The albumins and globulins (15–22% of total protein), which are, respectively, water- and salt-soluble, are removed with starch granules during gluten processing. In contrast, the gliadins, which are alcohol-soluble, and the glutenins, which are soluble (or at least dispersible) in dilute acid or alkali solutions, are being collected into gluten. Gliadin molecules may interact together or with glutenin molecules via hydrophobic interactions and hydrogen bonds. In the fully hydrated state, gliadin exhibits viscous flow properties without significant elasticity. For cereal technologists, gliadin accounts for the extensibility of wheat flour dough and acts as a filler diluting glutenin interactions. Contrary to gliadin, which is comprised of distinct polypeptide chains, glutenin consists of polymers made

from polypeptide chains (also named subunits) linked end-to-tail by SS bonds. Vital wheat gluten is the cohesive and elastic mass that is leftover after starch is washed away from wheat flour dough. Commercially, it is an industrial by-product of wheat starch production via wet milling [5]. Wheat gluten is suitable for numerous food and nonfood uses. Its main application is in the bakery industry, where it is used to strengthen weak flours rendering them suitable for bread Biodegradation. The other potential applications of gluten are very diverse: windows in envelopes, surface coatings on paper, biodegradable plastic films for agricultural uses, water-soluble bags with fertilizers, detergents, cosmetics, cigarette filters and additives and molded objects. Wheat gluten-based materials are homogeneous, transparent, mechanically strong, and relatively water resistant. They are biodegradable and a priori biocompatible, apart from some wheat gluten-specific characteristics such as allergenicity. The moisture barrier properties of wheat gluten-based films are relatively poor as compared to synthetic films, such as LDPE. The gas (O<sub>2</sub>, CO<sub>2</sub>, and ethylene) barrier properties of wheat gluten-based films are highly interesting, as they are exceptionally good at low relative humidity conditions. Water and other plasticizers can lower the glass transition temperature ( $T_g$ ) of the wheat gluten and enable processing at temperatures below those that lead to protein decomposition, which means that protein-based films can be formed by using techniques that are conventionally used with synthetic polymers e.g., extrusion, injection, and molding [24].

### 1.3.2.3 Collagen and Gelatin

Collagen is an abundant protein constituent of connective tissue in vertebrate (about 50% of total human protein) and invertebrate animals. Similar to cellulose in plants, collagen molecules support mechanical stresses transferred to them by a low-modulus matrix. Collagen is a rod-type polymer nearly 300 nm long with a molecular weight of 300,000. There have been more than twenty two different types of collagen identified so far in the human body, with the most common being Type I–IV [5]. Type I collagen is the single most abundant protein present in mammals and is the most thoroughly studied protein. The Type I collagen is composed of three polypeptide subunits with similar amino acid compositions. Each polypeptide is composed of about 1050 amino acids, containing approximately 33% glycine, 25% proline and 25% hydroxyproline with a relative abundance of lysine. Collagen is a hydrophilic protein because of

the greater content of acidic, basic, and hydroxylated amino acid residues than lipophilic residues. Therefore, it swells in polar liquids with high solubility parameters. Collagen undergoes enzymatic degradation within the body via enzymes, such as collagenases and metalloproteinases, to yield the corresponding amino acids. Due to their enzymatic degradability, unique physico-chemical, mechanical and biological properties collagen has been extensively investigated for various applications. Collagen is mostly soluble in acidic aqueous solutions and can be processed into different forms such as sheets, tubes, sponges, foams, nanofibrous matrices, powders, fleeces, injectable viscous solutions and dispersions. Studies have also shown that the degradation rate of collagen used for biomedical applications can be significantly altered by enzymatic pre-treatment or cross-linking using various cross-linking agents. The major sources of collagen currently used for industrial applications are bovine or porcine skin or bovine or equine Achilles tendons [5].

Thermal or chemical dissociation of collagen polypeptide chains forms products known as gelatin. Insoluble collagen is converted to soluble gelatin by acid or alkaline/lime (mild and slow) processing. Two processes are mainly used for commercial production of gelatin. In the first process, the collagen in hide or demineralized bone is partly depolymerized by prolonged liming that breaks down covalent cross-links. The occurring hydrolysis results in extensive release of collagenous material, which is solubilized at near neutral pH at temperatures of 60–90 °C (Type B gelatin). The acid process (Type A gelatin) involves soaking skin or bone in a dilute acid followed by extraction at acid pH [5]. The properties of collagen and gelatin are of great interest to various fields, such as surgery, implantations; wound dressings, leather chemistry (tanning), pharmacy (capsule production; tablet binding), and food science (gels; edible films). Reportedly, about 65% of gelatin manufactured worldwide is used in foods, 20% in photographic applications, 10% in pharmaceutical products, and 5% in other specialized and industrial applications.

Collagen has been extensively investigated for the localized delivery of low molecular weight drugs including antibiotics. Collagen films have traditionally been used for preparing edible sausage casing. Gelatin has been successfully used to form films that are transparent, flexible, water-resistant, and impermeable to oxygen. These films were made by cooling and drying an



aqueous film-forming solution based on gelatin. Gelatin is also used as a raw material for photographic films, and to microencapsulate aromas, vitamins, and sweeteners [25].

#### 1.3.2.4 Casein

Casein is the main protein of milk, representing 80% of the total milk proteins. Casein exists in the form of micelles containing all four casein species complexed with colloidal calcium phosphate. The casein micelles are stable to most common milk processes such as heating, compacting, and homogenization. Micellar integrity is preserved by extensive electrostatic and hydrogen bonding, and hydrophobic interactions. Two principal methods have been established for the production of casein on commercial scale, i.e., isoelectric precipitation (acid casein) and enzymatic coagulation (rennet casein). Though water insoluble casein has some applications, most food application would require casein with high water solubility. This is achieved by dispersing the casein in water and adjusting the pH to between 6.5 and 7.0 with an alkali. The most commonly used soluble caseinate is sodium caseinate. It is normally manufactured by dissolving fresh acid casein curd in sodium hydroxide followed by spray drying. Other soluble caseinates prepared in a similar manner include potassium, calcium, magnesium, and ammonium caseinates. Its relative simple isolation and the useful properties of casein as an industrial material and food ingredient have led to commercial production of casein and caseinates since the 19<sup>th</sup> century.

Casein and caseinates are suitable for numerous food and nonfood uses such as in industrial applications (especially in glues, paper coatings, paints, leather finishing, textile fibers, and plastics), and in various food products. The end-uses of casein and caseinates have gradually shifted from industrial to food applications [26]. About 70 to 80% of the casein produced worldwide is used as a food ingredient. Film-forming properties of caseins have been used to improve the appearance of numerous foods, to produce water soluble bags, and to produce origin or quality identification labels inserted under pre-cut cheeses, to ensure the surface retention of additives on intermediate-moisture foods, and to encapsulate polyunsaturated lipids for animal feeds. Casein-based edible films are attractive for food applications due to their high nutritional quality, excellent sensory properties and potential to adequately protect food products from their surrounding environment. The mechanical properties of casein and caseinate films, being neither

too tough nor too fragile, also make them suitable for edible purposes. Though more permeable to water vapor than plastic films, they are capable of retarding moisture transfer to some degree. Casein and caseinate films dissolve nearly instantaneously in water and this is desirable for many food applications [27].

### **1.3.2.5 Whey Protein**

Whey protein, a byproduct of the cheese industry, has excellent nutritional and functional properties and the potential to be used for human food and animal feed. Whey proteins are those proteins that remain in milk serum after pH/rennet coagulation of casein during cheese or casein manufacture. The industrial processes used for whey protein recovery are ultrafiltration, reverse osmosis, gel filtration, electrodialysis, and ion exchange chromatography. Fractionated whey constituents of various degrees of concentration can be obtained by combining two or more of the above recovery processes [28]. The film-forming properties of whey proteins have been used to produce transparent, flexible, colorless, and odorless films, such as those produced from caseins. The use of whey proteins to make an edible packaging film material brings several environmental advantages because of the film's biodegradability and its capacity to control moisture, carbon dioxide, oxygen, lipid, flavor and aroma transfer. These properties offer the potential to extend the shelf-life of many food products avoiding quality deterioration [29].

### **1.4 Synthetic Biopolymers Derived from Renewable Resources and Petroleum**

Unlike the aforementioned natural polymers, which can be harvested directly from the nature, some polymers are not available (or available in meaningful quantity) from the nature but can be produced with human intervention from naturally occurring bio-sources. PLAs and PHAs are the two most important polymers within this category. They have received intensive research interests in the past two decades and are finding more and more applications due to their unique combinations of properties. Biodegradable polymers can be derived not only from renewable bioresources but also from petroleum. Some synthetic aliphatic polyesters have been known to be biodegradable for decades. Petroleum based biodegradable polyesters are synthesized by polycondensation reaction between aliphatic diacids and aliphatic diols or by ring-opening polymerization of lactones. Aliphatic acids and terephthalic acids can also be used together to

react with aliphatic diols to produce biodegradable aliphatic-aromatic co- polyesters. Typical synthetic aliphatic polyesters include PCL, PBS, and their copolymers. However, biopolymers are discussed in this section in terms of chemical functional groups so that a well arranged overview of common players in the field engineering biopolymers can be summarized.

### 1.4.1 Polyester Derived Biopolymers

Polyesters, especially the aliphatic ones, are the most extensively studied class of biopolymers. Polyesters can be classified into two groups according to the bonding of the constituent monomers. The first group consists of the poly(hydroxy acids). These are polyesters synthesized from hydroxy acids and/or esters or by ring-opening polymerization (ROP) of cyclic esters. The second group consists of the poly(alkylene dicarboxylates) (PADCs). These are polyesters prepared by polycondensation of diols and dicarboxylic acids. The condensation reaction of a hydroxy acid and/or ester, and the ROP of a cyclic ester provides a polymer having a repeat unit with a head-tail-head-tail configuration of the general structure:  $[(CR''_2)_y-CO-O]-$ . In contrast, the condensation of a diol and a dicarboxylic acid, provides a polymer having a repeat unit with a head-tail-tail-head configuration of the general formula:  $[(CR_2)_x-O-CO-(CR'_2)_y-CO-O]-$  [30]. Figure 1.1 shows major biopolymers of this family.

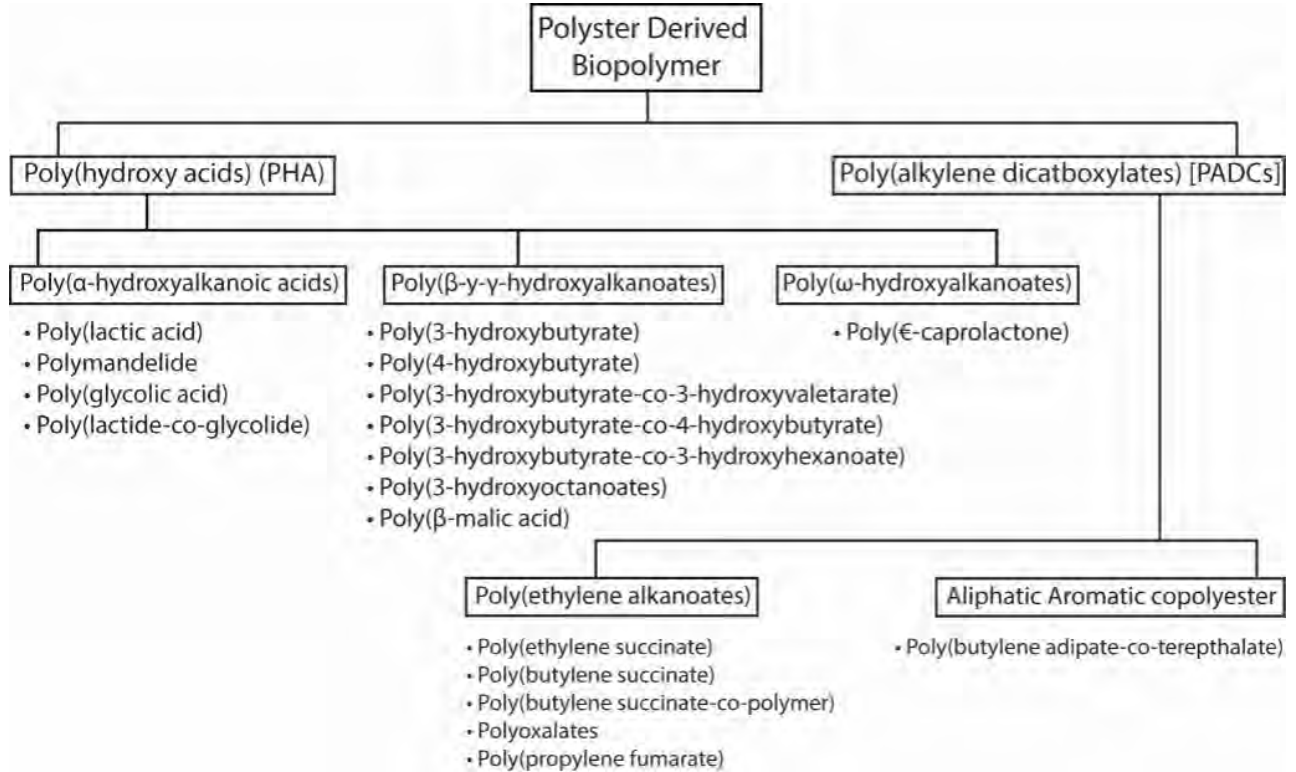


**Figure 1.1.** Major Polyester Derived Biopolymers in the field of Engineering

#### 1.4.2 Bio-Based Poly(ether-esters) based Polymers

Bio-based poly(ether-esters) are thermoplastic elastomers prepared by a two-stage melt transesterification process from readily available starting materials such as alkylene terephthalate, an alkane diol, and a poly(alkylene glycol ether) derived from renewable resources. The resulting poly(ether-esters) consist of crystallizable alkylene terephthalate sequences (hard segments) and elastomeric poly(alkylene oxide) sequences (soft segments). These materials show a wide range of properties depending upon the content of alkylene terephthalate segments and the length of poly(alkylene oxide). Several commercially available bio-based block poly(ether-esters) based on PBT and poly(tetramethylene oxide) are known, such as Hytel and Arnitel Eco. These block copolyesters combine many interesting properties, including a high-temperature  $T_m$ , a low  $T_g$ , and high yield stress, elongation at break and

elasticity along with ease of processing [31]. Hytrel RS grades contain rubbery soft blocks made from Cerenol, a polyether diol containing 20–60 wt% renewably sourced 1,3-propanediol derived from corn. According to Du Pont, Hytrel RS thermo- plastic elastomers have many applications including hoses and tubing for automotive and industrial uses, boots for constant-velocity joints (CVJ), air bag doors, and energy dampers. According to DSM, Arnitel Eco is suitable for applications in consumer electronics, sports and leisure, automotive interiors and exteriors, furniture, alternative energy and special packaging. The material is designed for a long service lifetime under extreme conditions. Polydioxanone (PDO, PDS) is a colorless, crystalline, biodegradable synthetic polymer of multiple repeating ether-ester units (Figure 1.2). Referred as poly(oxyethylene glycoate) and poly(ether ester), PDO is synthesized by the ring-opening polymerization of p-dioxanone. The polymer is processed at the lowest possible temperature to prevent depolymerization back to monomer. A commercially available PDO for medical devices is X206 S. PDO is mainly used for making biodegradable sutures. A commercial monofilament absorbable suture made of PDO is PDS™ Plus Antibacterial Suture.

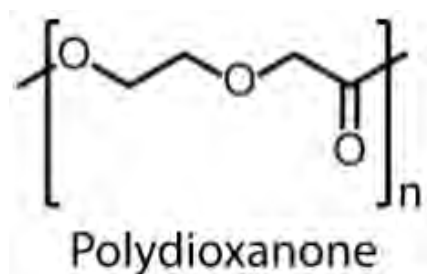


**Figure 1.2.** Structural formula of Polydioxane

### 1.4.3 Aliphatic Polycarbonate based Biopolymers

The synthesis of high molecular weight poly(alkylene carbonates) was first reported by Inoue et al. in the late 1960 [32]. These rather new polymers are derived from carbon dioxide and are produced through the copolymerization of CO<sub>2</sub> with one or more epoxy compounds (ethylene oxide or propylene oxide). They can contain up to 50 wt% CO<sub>2</sub> or CO and sequester this harmful greenhouse gas permanently from the environment. Aliphatic polycarbonates (APCs), as another

important class of biodegradable polymers, are widely used in the areas of packaging materials, drug carriers and tissue engineering for their favorable biodegradability, biocompatibility, and nontoxicity. Various aliphatic polycarbonate based biopolymers are depicted in figure 1.3.

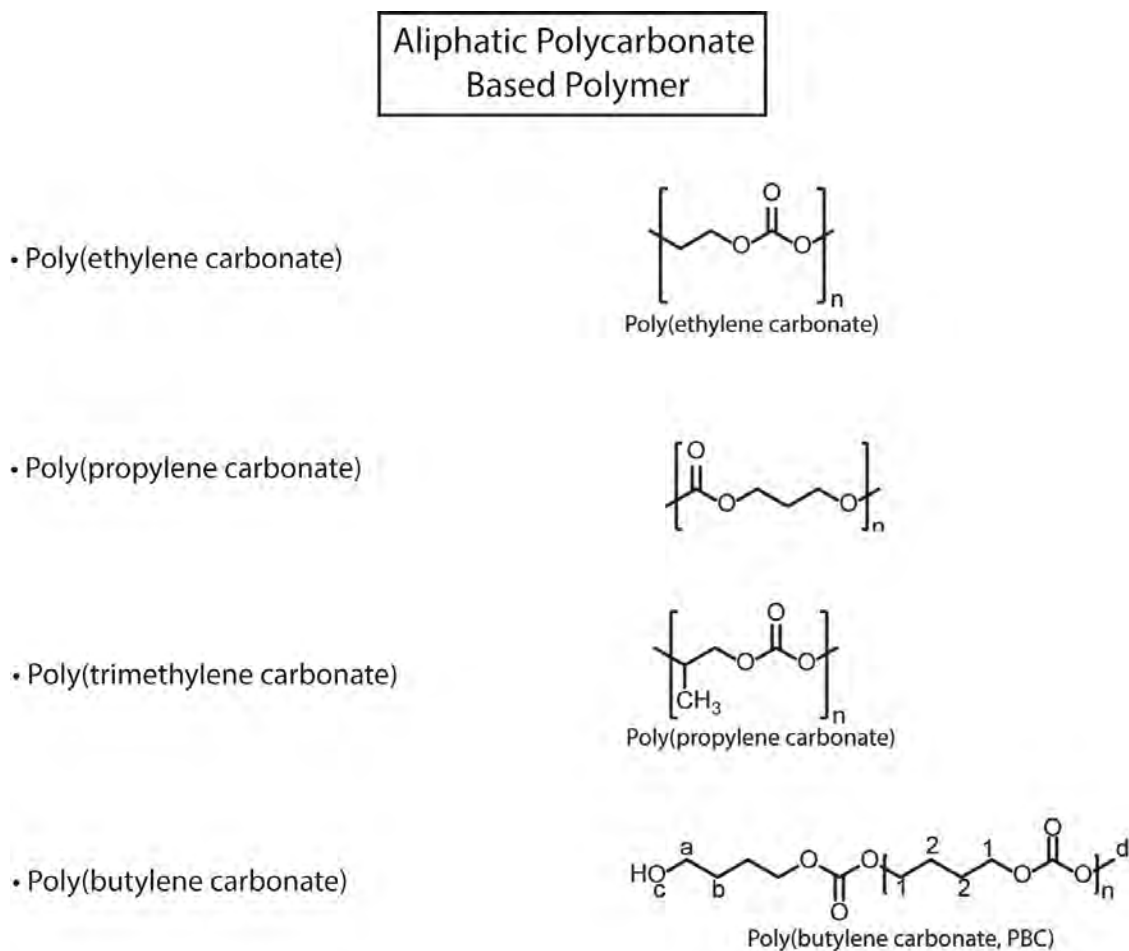


**Figure 1.3.** Major Players in Aliphatic Polycarbonate based Biopolymers in engineering field

### 1.4.4 Polyamides based Biopolymers

Polyamides are polymers with amide groups (R–CO–NH–R') as integral parts of the main polymer chain. Polyamides are basically formed from polycondensation of (1) diamines and dicarboxylic acids, (2)  $\omega$ -amino carboxylic acids as bifunctional monomers and (3)  $\alpha$ -amino carboxylic acids as bifunctional monomers. Biopolyamides include both bio-based polyamides and biodegradable fossil fuel based polyamides [14]. Figure 1.4 depicts various biopolyamides in terms of organic groups taking place in polycondensation.

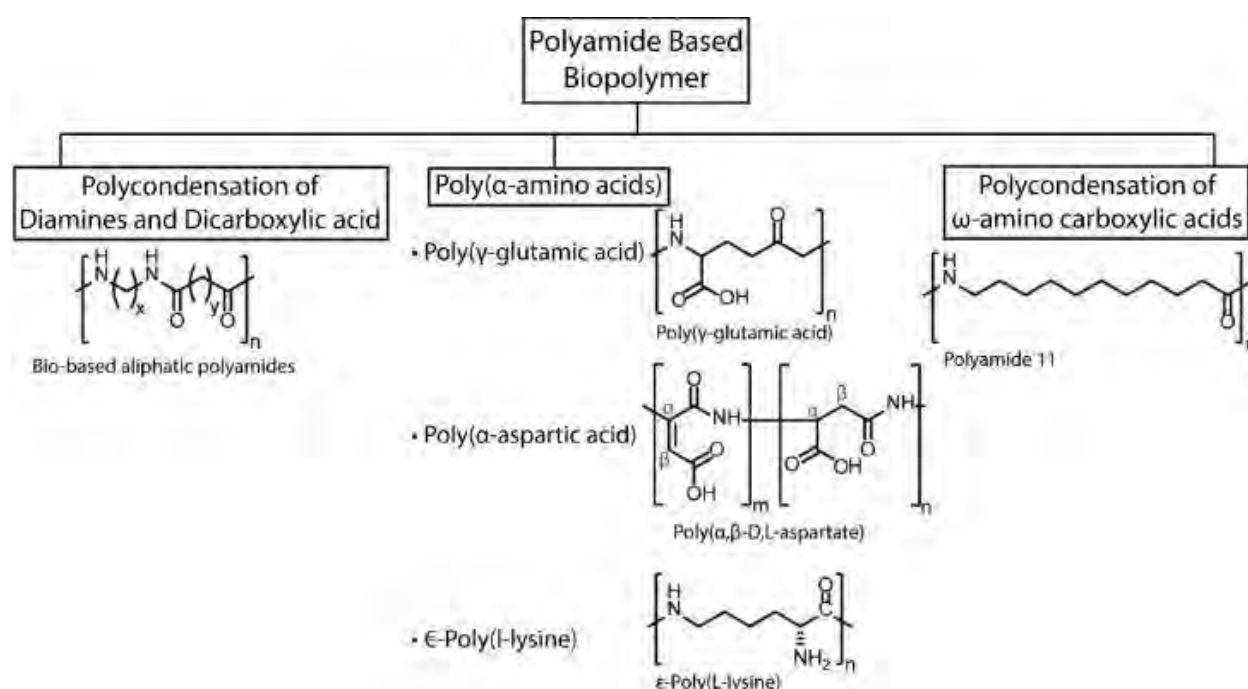


**Figure 1.4.** Major Biopolyamides in engineering field

### 1.4.5 Poly(ester amides) based Biopolymer

Poly(ester amides) constitute a promising family of biodegradable materials since they combine a degradable character, afforded by the easily hydrolyzable ester groups (–COO–), with relatively good thermal and mechanical properties given by the strong intermolecular hydrogen

bonding interactions that can be established between their amide groups ( $-\text{NHCO}-$ ) [33]. In 1995, Bayer AG introduced a series of biodegradable poly(ester amides) for film and molding applications. The poly(ester amides) of Bayer are based on the following combinations of monomers: (1) adipic acid, 1,4-butanediol and  $\epsilon$ -caprolactam; (2) adipic acid, 1,4-butanediol, diethylene glycol, and hexamethylenediamine. The various commercial products, which result from the combination of monomers (1) are based on polyamide. The products, which result from the combination of monomers (2) are based on polyamide-6, 6. Hyperbranched poly(ester amides) are produced on an industrial scale and commercialized by DSM. These poly(ester amides) are intrinsically biodegradable and synthesized from cyclic anhydride (e.g., succinic anhydride) and a diisopropanol amine. Hyperbranched poly(ester amides) are used as performance additive in many applications such as oil field chemicals, demulsifiers, drug carriers, paper coatings, etc.

#### 1.4.6 Poly(ether amides) based Biopolymer

Poly(ether amides) are thermoplastic elastomers (TPEs) that can be processed by injection molding and profile or film extrusion. A commercially available product of bio-based poly(ether amides) is the Pebax Rnew (Arkema). Pebax Rnew is a plasticizer-free poly(ether-b-amide) TPE from renewable sources (up to 90% derived from castor oil), made up of a block copolymer consisting of a sequence of polyamide 11 (PA 11) and polyether segments [4].

#### 1.4.7 Bio Polyurethane based Polymer

The term “polyurethane” includes all polymers incorporating more than one urethane group ( $-\text{NH}-\text{CO}-\text{O}-$ ) in the polymer backbone. Polyurethanes are commonly formed by the polyaddition reaction of a poly-isocyanate such as a diisocyanate with a polyol such as a diol, resulting in the formation of linear, branched, or crosslinked polymers. Other low molecular weight reagents such as chain extenders or crosslinking agents may be added during the polyaddition process. As polyol components used as raw materials of bio-based polyurethanes (bio-based PUs), there are used polyether and polyester polyols derived from natural resources. Polyether polyols are produced from sucrose, glucose, fructose, and glycerol. Polyester polyols are made from diacids and di- or tri-functional polyols [34]. The isocyanate component is not



produced from renewable resources. Aliphatic polyisocyanates, such as hexamethylene diisocyanate, butane diisocyanate, lysine diisocyanate ethyl ester, and lysine diisocyanate methyl ester, are used for the production of bio-based PUs. The poly(ester urethanes) are more liable to biodegradation than the poly(ether urethanes). Polyester polyols such as polycaprolactone, polylactide, and polyglycolide are the most widely used polyols in biodegradable polyurethanes. In a thermoplastic elastomer polyurethane (TPU) the polyester polyol forms the “soft” segment of the polymer while the diisocyanate and the chain extender form the hard segment. The hard segment forms ordered domains due to hydrogen bonding and imparts high mechanical strength to the material. The soft domains are formed mainly by the polyester polyol and provide elastic properties to the polymer. The biodegradation of these polymers occurs largely due to the hydrolytic degradation of the ester, urethane, and urea linkages of the polymer. The urethane or urea linkages in the hard segment degrade by hydrolysis at a significantly slower rate than ester linkages. Because of the relatively slow degradation rates of these linkages compared with ester linkages, the polymer degradation may lead to oligomers containing mainly hard segments. The soft segment of the TPU degrades significantly faster than the hard segment as result of the presence of relatively easily hydrolysable ester linkages and the amorphous nature of the soft segment. PUs have a broad spectrum of types and properties (soft and flexible foams, coatings, elastomers, and fibers) and used in a very wide range of applications. The market for bio-based PUs is small and premium applications are being targeted. As an example, Biodegradable PUs are used as “shock absorber” materials in shoes soles and heels and as a carpet backing using PU derived from soy. Biodegradable polyurethanes find applications also in regenerative medicine. Examples include the fabrication of porous scaffolds for use in soft tissue engineering and cartilage repair. Other medical applications include bone graft substitutes and wound dressings [4].

### **1.5 Light Weight Biodegradable Polymer based Packaging Material**

Plastic packaging offers protection against moisture and dirt, safeguards hygiene, provides an attractive appearance and protects the packaged goods against misuse with use of a comparatively small amount of material. The use of plastic packaging has increased considerably in recent decades. In many cases, packaging materials are intended for only a single use, such as

boxes, cartons, pouches, and wraps. Disposal of these materials has now become a problem, which is growing in the same way. In view of the rising tide of disposable packaging materials, some countries, particularly those in Europe, have put restrictions either on the use and disposal of packaging materials by mandating their recycling, or promoting the use of packaging materials which are “biodegradable” or “compostable.” Recycling systems are being developed only very slowly, have questionable effectiveness, and are often only implemented regionally. In addition, fossil fuel resources for most synthetic polymers are limited. These circumstances were the motivating force for the development of alternative packaging materials derived from renewable resources, which can in addition be disposed of in an environmentally friendly manner. Lightweight materials are materials with reduced weight. They are important for the packaging industry since they can reduce the cost of materials and transport, and therefore reduce the waste and energy used. Lightweight can be achieved by using low density materials, and by designing novel thin film or foamed structures.

Packaging materials made of bio-based polymers address the concerns about depletion of natural resources and greenhouse gas generation effects. Bio-based polymers are believed—once fully scaled up—to help reduce reliance on fossil fuels, reduce production of greenhouse gases, and can be biodegradable or compostable as well. Among numerous kinds of biopolymers, polylactic acid (PLA), sometimes called polylactide, an aliphatic polyester and biocompatible thermoplastic, is currently the most promising and popular material. Commercially available PLA packaging can provide better mechanical properties than polystyrene and have properties more or less comparable to those of PET. Market studies show that PLA is an economically feasible material for packaging. With its current consumption, it is at the present the most important market in volume for biodegradable packaging. Due to its high cost, the initial use of PLA as a packaging material has been in high value films, rigid thermoforms, food and beverage containers, and coated papers. One of the first companies to use PLA as a packaging material was Danone (France) in yoghurt cups for the German market at the end of the 1990s. But the production of these cups was rapidly stopped. In 2011, Danone launched new yoghurt cups for German market, 100% compostable, with a bigger success. During the last decade, the use of PLA as a packaging material has increased all across Europe, Japan, and the United States, mainly in the area of fresh products, where PLA is being used as a food packaging for short shelf-life products, such as fruit and vegetables. Package applications include containers,

drinking cups, sundae and salad cups, wrappings for sweets, lamination films, blister packages, and water bottles. Currently, PLA is used in compostable yard bags to promote national or regional composting programs. In addition, new applications such as cardboard or paper coatings are being pursued, e.g., for the fast-food market (cups, plates, and the like). However, to cater for a larger market, some PLA drawbacks must be overcome, such as its limited mechanical and barrier properties and heat resistance, and, in order to meet market expectations, the world production of PLA must be increased [35].

### **1.6 Overview of Poly Lactic Acid as Packaging Material**

Environmental, economic, and safety challenges have provoked packaging scientists and producers to partially substitute petrochemical-based polymers with biodegradable ones. In this list Poly Lactic acid has taken the position of most feasible candidate owing to a number reasons. For instance; 1) it can be obtained from a renewable agricultural source (e.g.: corn or potato); 2) it provides significant energy savings; 3) it is recyclable and compostable; 4) it is helpful for improving agricultural economies and 5) their physical and mechanical properties can be tailored through design the different polymer architectures or processing methods. PLA or poly-lactide was discovered in 1932 by Carothers (at DuPont). He was only able to produce a low molecular weight PLA by heating lactic acid under vacuum while removing the condensed water. The problem at that time was to increase the molecular weight of the products; and, finally, by ring-opening polymerization of the lactide, high-molecular weight PLA was synthesized. PLA was 1st used in combination with polyglycolic acid (PGA) as suture material and sold under the name Vicryl in the U.S.A. in 1974. Briefly, PLA is based on agricultural (crop growing), biological (fermentation), and chemical (polymerization) sciences and technologies. It is classified as generally recognized as safe (GRAS) by the United State Food and Drug Administration (FDA) and is safe for all food packaging applications [36].

Production steps, general properties, applications, processing technologies, modifications, and biodegradability of PLA are presented in this section. Consequently, migration and release studies of active compounds and PLA abilities making it a potential active food packaging are also discussed; finally, recent different types of nanocomposites used for improving PLA applications are summarized.

### 1.6.1 PLA Production

The basic building block for PLA is lactic acid, which was first isolated in 1780 from sour milk by the Swedish chemist Scheele and first produced commercially in 1881. Lactic acid (2-hydroxy propionic acid) is the simplest hydroxy acid with an asymmetric carbon atom and exists in two optically active configurations. The L(+)-isomer is produced in humans and other mammals whereas both the D(-) and L(+)-enantiomers are produced in bacterial systems. The majority of the world's most commercially produced lactic acid is made by the bacterial fermentation of carbohydrates, using homolactic organisms such as various optimized or modified strains of the genus *Lactobacilli*, which exclusively form lactic acid [37].

PLA has a variable molecular weight and only its high molecular weight polymer is used in the packaging industry. Three ways are possible for the polymerization of lactic acid are depicted in figure 1.5. Lactic acid is condensation polymerized to yield a low-molecular-weight, brittle polymer, which, the most part, is unusable, unless external coupling agents are employed to increase its chain length. The second route is the azeotropic dehydrative condensation of lactic acid. It can yield high molecular-weight PLA without the use of chain extenders or special adjuvants. The third and main process is ring-opening polymerization (ROP) of lactide to obtain high-molecular-weight PLA, patented by Cargill (US) in 1992. Finally, lactic acid units can be part of a more complex macromolecular architecture as in copolymers [38].

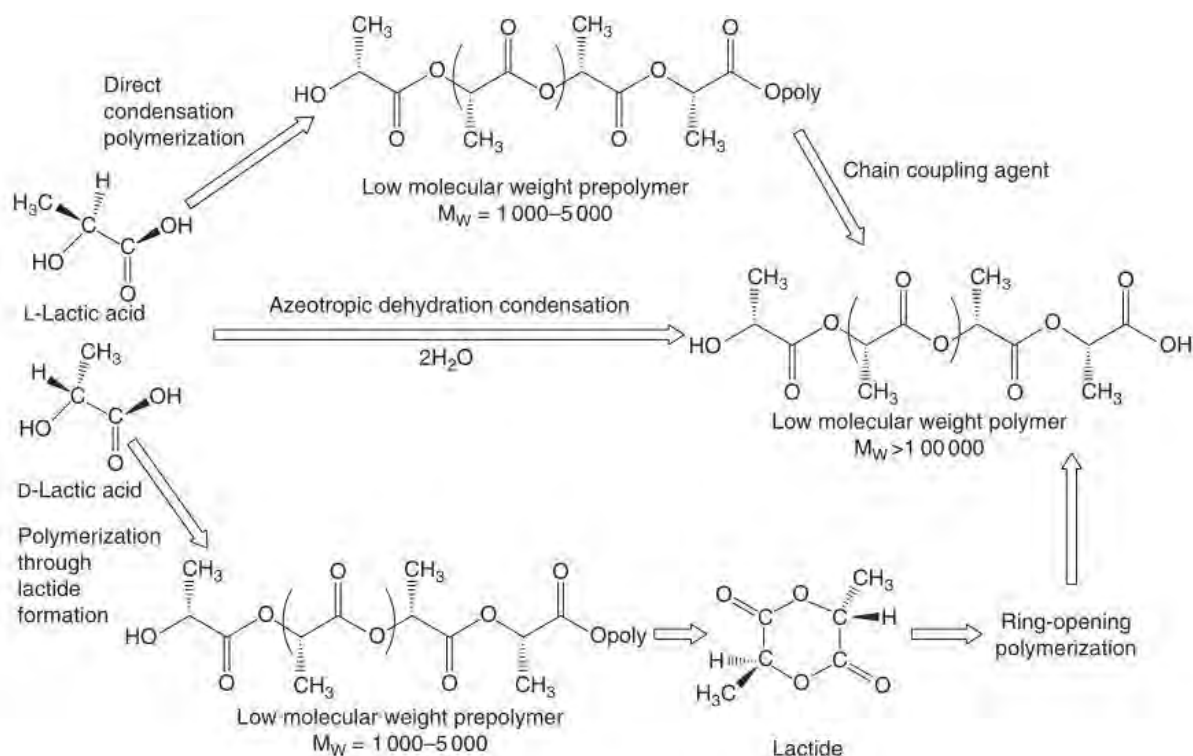


**Figure 1.5.** General Schemes of PLA

### 1.6.1.1 Precursors

**Lactic Acid:** Lactic acid is a compound that plays a key role in several biochemical processes. For instance, lactate is constantly produced and eliminated during normal metabolism and physical exercise. Lactic acid has been produced on an industrial scale since the end of the nineteenth century and is mainly used in the food industry to act, e.g., not only as an acidity regulator, but also in cosmetics, pharmaceuticals, and animal feed. It is, additionally, the monomeric precursor of PLA. It can be obtained either by carbohydrate fermentation or by common chemical synthesis. Lactic acid is mainly prepared in large quantities (estimated to more than 250 kT per year, in 2011) by the bacterial fermentation of carbohydrates. These fermentation processes can be classified according to the type of bacteria used: (i) the heterofermentative method, which produces less than 1.8 mole of lactic acid per mole of hexose, with other metabolites in significant quantities, such as acetic acid, ethanol, glycerol, mannitol, and carbon dioxide; (ii) the homo-fermentative method, which leads to greater yields of lactic acid

and lower levels of by-products, and is mainly used in industrial processes. The conversion yield from glucose to lactic acid is more than 90%. The homo-fermentative method is preferably used for industrial production because its pathways lead to greater yields of lactic acid and to lower levels of by-products. The general process consists of using species of the *Lactobacillus* genus such as *Lactobacillus delbrueckii*, *L. amylophilus*, *L. bulgaricus*, and *L. leichmanii*, a pH range of 5.4 to 6.4, a temperature range of 38 to 42° C, and a low oxygen concentration. If the lactic acid is used in pharmaceutical and food applications, it is further purified to remove the residual byproducts. If it is to be polymerized, it is purified by separation techniques including ultrafiltration, nanofiltration, electrodialysis, and ion-exchange processes [39].

**Lactide:** Figure 1.6 shows the different stereoisomers of lactide. The cyclic dimer of lactic acid combines two of its molecules and gives rise to L-lactide or LL-lactide, D-lactide or DD-lactide, and meso-lactide or LD-lactide. A mixture of L and D-lactides is a racemic lactide (rac-lactide). Lactide is usually obtained by the depolymerization of low-molecular-weight PLA under reduced pressure to give a mixture of L-, D-, and meso-lactides. The different percentages of the lactide isomers formed depend on the lactic acid isomer feedstock, temperature, and the catalyst's nature and content. A key point in most of the processes is the separation between each stereoisomer to control the final PLA structure (e.g., by vacuum distillation), which is based on the boiling point differences between the meso- and the L- or D-lactide [39].

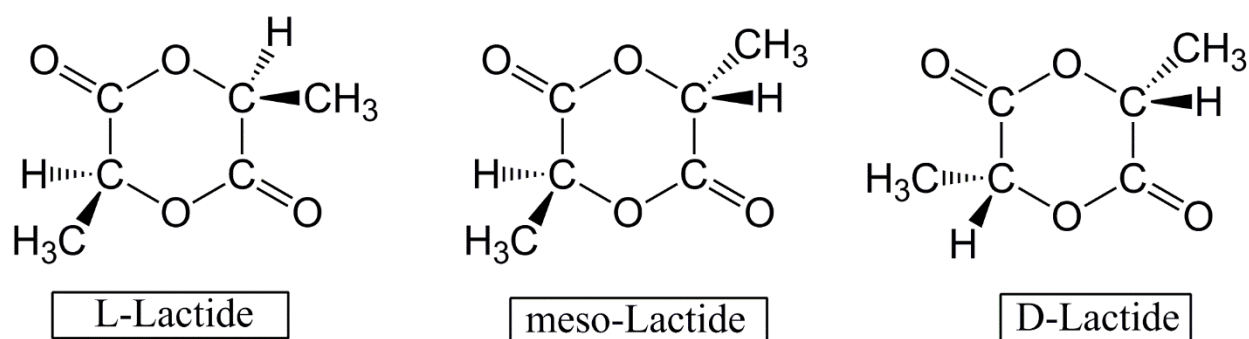


**Figure 1.6.** Different stereo forms of Lactide

### 1.6.1.2 Polymerization of Precursors

**Lactic Acid Condensation and Coupling:** The condensation polymerization is the least expensive route, but it is difficult to obtain high molecular weights by this method. The use of coupling or esterification-promoting agents is required to increase chain length, but at the expense of an increase in both cost and complexity (multistep process). The role of chain coupling agents is to react with either the hydroxyl (OH) or the carboxyl end-groups of the PLA, thus giving telechelic polymers. The nature of the chain end- groups should be fully controlled. The use of chain-extending agents brings some advantages, because reactions involving small amounts of them are economical and can be carried out in the melt without the need of separating the different process steps. The tunability to design copolymers with various functional groups is also greatly expanded. The disadvantages are that the final polymer may contain unreacted chain-extending agents, oligomers, and residual metallic impurities from the catalyst. Moreover, some extending agents could be associated with a lack of biodegradability. Examples of chain-extending agents are anhydrides, epoxides, and isocyanates. Similar products are used to develop compatibilization for PLA-based blends. The disadvantages of using isocyanates as chain extenders are their eco-toxicity. The advantages of esterification-promoting adjuvants are that the final product is highly purified and free from residual catalysts and/or oligomers. The disadvantages are higher costs due to the number of steps involved and the additional purification of the residual by-products, since these additives produce by-products that must be neutralized or removed [37].

**Azeotropic Dehydration and Condensation:** The azeotropic condensation polymerization is a method used to obtain high chain lengths without the use of chain extenders or adjuvants and their associated drawbacks. Mitsui Chemicals (Japan) has commercialized a process wherein lactic acid and a catalyst are azeotropically dehydrated in a refluxing, high boiling and aprotic solvent under reduced pressures to obtain high-molecular-weight PLA ( $M_w$  300,000). A general procedure consists in the reduced pressure distillation of lactic acid for 2-3 h at 130<sup>0</sup> C to remove most of the condensation water. The catalyst and diphenyl ether are then added and a tube packed with molecular sieves is attached to the reaction vessel. The refluxing solvent is returned to the vessel by way of the molecular sieves during 30-40 h at 130<sup>0</sup> C. Finally, the ensuing PLA is purified. This polymerization gives considerable catalyst residues because of its high

concentration needed to reach an adequate reaction rate. This can cause many drawbacks during processing, such as degradation and hydrolysis. For most biomedical applications, the catalyst toxicity is a highly sensitive issue. The catalyst can be deactivated by the addition of phosphoric acid or can be precipitated and filtered out by the addition of strong acids such as sulfuric acid. Thus, residual catalyst contents can be reduced to some ppm [38].

**ROP of Lactide:** The lactide method is the only method for producing pure high-molecular-weight PLA ( $M_w$  100,000). The ROP of lactide was first demonstrated by Carothers in 1932, but high molecular weights were not obtained until improved lactide purification techniques were developed by DuPont in 1954. This polymerization has been successfully carried out calling upon various methods, such as solution, bulk, melt, or suspension process. The mechanism involved in ROP can be ionic (anionic or cationic) or coordination insertion, depending on the catalytic system. The role of the racemization and the extent of trans-esterification in the homo or copolymerization are also decisive for the enantiomeric purity and chain architecture of the resulting macromolecules. It has been found that trifluoromethane sulfonic acid and its methyl ester are the only cationic initiators known to polymerize lactide. Lactide anionic polymerizations proceed by the nucleophilic reaction of the anion with the carbonyl group and the subsequent acyloxygen bond cleavage, which produces an alkoxide end group, which continues to propagate. Some authors have shown that the use of alkoxides, such as potassium methoxide, can yield well-defined polymers with negligible racemization. Both the anionic and cationic ROPs are usually carried out in highly purified solvents, and although they show a high reactivity, they are susceptible to give racemization, trans-esterification, and high impurity levels. For industrial and large commercial use, it is preferable to do bulk and melt polymerization with low levels of nontoxic catalysts. The use of less-reactive metal carboxylates, oxides, and alkoxides has been extensively studied in this context, and it has been found that high-molecular-weight PLA can be readily obtained in the presence of transition metal compounds of tin, zinc, iron and aluminum, among others. A systematic investigation has led to the wide use of tin compounds, namely tin(II) bis-2-ethylhexanoic acid (stannous octoate) as a catalyst in PLA synthesis. This is mainly due to its high catalytic efficiency, low toxicity, food and drug contact approval, and ability to give high molecular weights with low racemization. The mechanisms of the polymerization with stannous octoate have been studied in detail, and it is now widely accepted that this ROP is actually initiated from compounds containing hydroxyl



groups, such as water and alcohols, which are either present in the lactide feed or can be added upon demand. First, a complex between monomer and initiator is formed followed by a rearrangement of the covalent bonds. Second, the monomer is inserted within the oxygen-metal bond of the initiator, and its cyclic structure is thus opened through the cleavage of the acyloxygen link, thus, the metal is incorporated with an alkoxide bond into the propagating chain. It was found that the polymerization yield and the trans-esterification effect are affected by different parameters, such as the polymerization temperature and time, the monomer/catalyst ratio, and the type of catalyst. The interaction between the time and temperature is very significant in terms of limiting the degradation reactions, which affect the molecular weight and the reaction kinetics. It has also been shown that the chain length is directly controlled by the amount of OH impurities [39].

### 1.6.2 PLA Properties

The properties of a polymer can be distinguished in three broad classes: (1) intrinsic properties, which refer to the polymer itself; (2) processing properties, which refer to the behavior of the polymer during forming; and (3) product properties, which refer to the properties of the polymer as an entity. These three categories of properties are interrelated with each other; for example, an increase in melting temperature ( $T_m$ ), which is an intrinsic property, is accompanied by an increase in heat resistance, which is a product property. Intrinsic properties can be classified further into molecular and bulk properties. Intrinsic molecular properties depend mainly on the chemical nature of the constituting monomer units, while intrinsic bulk properties depend mainly on the polymer structure. The properties of high molecular weight PLA are determined by the polymer architecture (i.e. the stereochemical makeup of the backbone) and the molecular mass, which is controlled by the addition of hydroxylic compounds. The ability to control the stereochemical architecture permits precise control over the speed of crystallization and finally the degree of crystallinity, the mechanical properties and the processing temperatures of the material. In addition, the degradation behavior strongly depends on the crystallinity of the samples. PLA has unique properties like good appearance, high mechanical strength, and low toxicity; and good barrier properties have broadened its applications. In this section, the PLA

polymer structure, physical, mechanical, rheological, processing, solubility, barrier, and degradation properties are presented [4].

### 1.6.2.1 PLA Structure, Crystallinity and Physical Properties

Unmodified polylactides are linear macromolecules having a molecular architecture that is determined by their stereochemical composition. The repeat unit of PLA (72 g/mol) contains one stereocenter that is either L (S) or D (R) in configuration. PLA derived from greater than 93% L-lactic acid can be semicrystalline whereas PLA from between 50 and 93% L-lactic acid is strictly amorphous. Both meso- and D-lactide induce twists in the otherwise very regular poly(L-lactide) molecular architecture. Molecular imperfections are responsible for the decrease in both the rate and extent of poly(L-lactide) crystallization. Since polylactide production always contains some amount of meso-lactide impurities, practically all PLAs are made up of L- and D,L-lactide copolymers. It is known that poly(L-lactide) and poly(D-lactide) form an equimolar stereocomplex crystalline structure (i.e., racolactides) having a significantly higher melting temperature (230 °C) than the homopolymers. Dimeric polymerization imparts some order to the otherwise random distribution of L- and D-stereocenters in PLA chains. Hence, the lactide ring-opening polymerization process gives a fundamentally different molecular architecture for PLA polymers derived from lactic isomeric mixtures other than 100% L- and 50/50 D,L-lactic acid. High molecular weight bulk lactide polymerization should be conducted at high temperatures (e.g. 190–200 °C) to maintain the appropriate viscosity, and at these temperature racemization can become an important side reaction. However, a laboratory scale polymerization of lactide at low reaction temperature such as 120–140 °C gives a high molecular weight PLA.

Depending on the preparation conditions, poly(L-lactide) crystallizes in three forms ( $\alpha$ ,  $\beta$  and  $\gamma$ ). The stable  $\alpha$ -form exhibits a well-defined diffraction pattern. It has been analyzed the  $\alpha$ -form of poly(L-lactide) using linked-atom least squares refinements for X-ray fiber diffraction data, and found that the  $\alpha$ -form has an orthorhombic  $P2_12_12_1$  space group, with a unit cell containing two antiparallel chains. The chain conformation was the 2-fold helix distorted periodically form of the regular helix. The lattice parameters were  $a=10.66 \text{ \AA}$ ,  $b=6.16 \text{ \AA}$  and  $c$  (chain axis)= $28.88 \text{ \AA}$  with a crystal density of  $1.26 \text{ g/cm}^3$ . The  $\beta$ -form can be prepared at a high draw ratio and high drawing temperature. The chain conformation is a left-handed 3-fold helix. The  $\beta$  form of poly(L-

L-lactic acid) has an orthorhombic unit cell (containing 6 chains) containing polymeric helix. The unit cell dimensions are as follows:  $a=10.31 \text{ \AA}$ ,  $b=18.21 \text{ \AA}$ ,  $c=9.0 \text{ \AA}$ . The  $\alpha$ -structure is more stable than the  $\beta$ -structure, with a melting point of  $185^\circ \text{ C}$  compared to  $175^\circ \text{ C}$  for the  $\beta$ -structure. Chain packing in the  $\beta$ -form has been termed a frustrate structure where the crystal structure rests on a frustrated packing of three three-fold helices in a trigonal unit-cell of parameters  $a=b=10.52 \text{ \AA}$ ,  $c=8.8 \text{ \AA}$ . The  $\gamma$ -form, found by epitaxial crystallization, contains two antiparallel  $s(3/2)$  helices in the pseudo-orthorhombic unit cell ( $a=9.95 \text{ \AA}$ ,  $b=6.25 \text{ \AA}$ ,  $c=8.8 \text{ \AA}$ ) and it assumes the known three-fold helix of polylactides. Following table shows the unit cell parameters for non-blended PLLA [37].

PLLA crystals have been grown in different solvents to study the morphology and the rate of crystallization. PLLA crystals are highly dependent on the L- concentration. The rate and extent of crystallization also depend on the presence of nucleating agents as well as on the time and temperature. Long annealing times at temperatures higher than the glass transition temperature ( $T_g$ ). The crystallization kinetics of PLA have been extensively studied and found to be rather slow, as in the case of poly(ethylene terephthalate) (PET). The rate of crystallization increases with a decrease in the molecular weight and is strongly dependent on the (co)polymer composition. PLLA can crystallize in the presence of D-lactide; however, as the structure becomes more disordered, the rate of crystallization decreases. It has been reported that the crystallization rate is essentially determined by the decrease in the melting point of the different copolymers. PDLA/PLLA stereocomplexes are very efficient nucleating agents for PLLA, with increases in both crystallization rate and crystallinity, the latter of up to 60%. Quenching decreases the time taken for crystallization. As PET, PLA can be oriented by processing, and the chain orientation increases the mechanical strength of the polymer. If orientation is performed at low temperature, the resulting PLLA has a higher modulus without any significant increase in crystallinity. To determine the crystallinity levels by differential scanning calorimetry (DSC), the value most often referred to in the literature concerning the PLA melt enthalpy at 100% crystallinity is  $93 \text{ J/g}$ . The crystallization of the thermally crystallizable, but amorphous, PLA can be initiated by annealing it at temperatures between  $75^\circ \text{ C}$  and the melting point. Annealing crystallizable PLA copolymers often produces two melting peaks and different hypotheses have been put forward to explain this feature. It has been found that a double melting point in PLLA polymers and attributed them to slow rates of crystallization and recrystallization. The typical

PLA glass transition temperature ranges from 50 °C to 80 °C, whereas its melting temperature ranges from 130 °C to 180 °C. For instance, enantiomerically pure PLA is a semicrystalline polymer with a  $T_g$  of 55 °C and a  $T_m$  of 180 °C. For semicrystalline PLA, the  $T_m$  is a function of the different processing parameters and the initial PLA structure. According to Ikada and Tsuji,  $T_m$  increases with increasing molecular weight ( $M_w$ ) to an asymptotic value, but the actual crystallinity decreases with increasing  $M_w$ .  $T_m$ , moreover, decreases with the presence of meso-lactide units in its structure. Both, the degree of crystallinity and the melting temperature of PLA-based materials can be reduced by random copolymerization with different co-monomers (e.g., GA, CL, or valerolactone). The  $T_g$  of PLA is also determined by the proportion of the different types of lactide in its macro-molecular chain. The density of amorphous poly(L-lactic acid) has been reported as 1.248 g/ml and for crystalline PLLA as 1.290 g/ml. The density of solid polylactide was reported as 1.36 g/cm<sup>3</sup> for L- lactide, 1.33 g/cm<sup>3</sup> for meso-lactide, 1.36 g/cm<sup>3</sup> for crystalline polylactide and 1.25 g/cm<sup>3</sup> for amorphous polylactide [4].

Surface energy is critically important to many processes (printing, multilayering, etc.) and it influences the interfacial tension. The surface energy of a PLA made up of 92% L-lactide and 8% meso-lactide was found to be 49 mJ/m<sup>2</sup>, with dispersive and polar components of 37 and 11 mJ/m<sup>2</sup>, respectively, which suggests a relatively hydrophobic structure compared with that of other biopolyesters. A good solvent for PLA and for most of the corresponding copolymers is chloroform. Other solvents are chlorinated or fluorinated organic compounds, dioxane, dioxolane, and furan. Poly(rac-lactide) and poly(meso-lactide) are soluble in many other organic solvents like acetone, pyridine, ethyl lactate, tetra-hydrofuran, xylene, ethyl acetate, dimethylformamide, and methyl ethyl ketone. Among nonsolvents, the most relative compounds are water, alcohols (e.g., methanol and ethanol), and alkanes (e.g., hexane and heptane).

### 1.6.2.2 Processing Properties

PLA can be processed by injection molding, sheet extrusion, blow molding, thermoforming and film forming. Cargill Dow LLC commercialized PLA polymer under the name of Natureworks for extrusion, thermoforming, cast film, blown film and injection stretch blow molded bottles and containers. Mitsubishi Plastics in Japan also commercialized PLA polymers for different applications under the brand name of LACEA. Hartmann reported that the molecular weight for

polymers used in extrusion and injection molding is usually reduced over the virgin material. PLA quickly loses its thermal stability when heated above its melting point. Significant molecular weight degradation occurred when PLA was held 10 °C above its melting point for a substantial period of time. Migliaresi et al. measured the reduction in molecular weight due to thermal degradation and attributed it to chain splitting and not to hydrolysis as had been previously reported. They did not observe oxidation of PLA. The degradation of PLA is not only a consequence of the thermal degradation of the PLA, but the amount of residual monomer in the resin also has an important effect in inducing early degradation of the polymer. PLLA polymers have a narrow processing window (12 °C) although a 90/10 L- to D- copolymer has a much wider window of processing conditions (40 °C) due to its lower melting temperature. PLA can be plasticized with lactides, oligomeric lactic acid and a wide variety of conventional plasticizers. In general, PLA plasticizing agents are low molecular weight lactide and glycol acids. However, Bechtold et al. found that a copolymer made from lactic acid and ethylene oxide could be used as a macromolecular plasticizing agent for commercial PLA. Other biocompatible plasticizers such as glycerol, citrate ester, polyethylene glycol, PEG monolaurate and oligomeric lactic acid have also been used to improve the brittle behavior of PLA. Glycerol is the least efficient of these plasticizing agents, and polyethylene glycol is the most efficient. A reduction in the glass transition temperature from 58 °C to 12 °C was found when plasticizers were used. No reduction in the melt temperature was observed. PLA polymers start to thermally degrade at 300 °C and completely decompose at 400 °C when tested under dried conditions by thermal gravimetric analysis (TGA) with a heating ramp of 10 °C/min and purged with nitrogen at 50 ml/min. Zero-order kinetics are followed between 40 and 80% volatilization, which are consistent with a depolymerization phenomenon. Thermal decomposition is independent of initial lactide isomer distribution. The activation energy for PLA weight loss is 139 kJ/mol between 186 °C and 257 °C. Polylactide has a similar thermal stability to PVC but is considerably less stable than PS, PP, PE and PET [37].

### 1.6.2.3 Mechanical Properties

The mechanical properties of PLA can vary to a large extent, ranging from soft and elastic materials to stiff and high strength materials, according to different parameters, such as

crystallinity, polymer structure and molecular weight, material formulation (plasticizers, blend, composites, etc.), and processing (e.g., orientation). For instance, commercial PLA, such as poly(92% L-lactide, 8% meso-lactide), has a modulus of 2.1 GPa and an elongation at break of 9%. After plasticization, its Young's modulus decreases to 0.7 MPa and the elongation at break rises to 200%, with a corresponding  $T_g$  shift from 58 °C to 18 °C. This example indicates that mechanical properties can be readily tuned to satisfy different applications. The mechanical properties of PLA-related polymers were recently reviewed by Sodergard and Stolt, who showed, among other features, that the PLLA fiber modulus can be increased from 7-9 GPa to 10-16 GPa by going from melt to solution spinning. The mechanical behavior can also be modified by preparing suitable copolymers, as in the case of the use of CL, which, with its soft segments, induces a decrease in modulus and an increase in the elongation at break, respectively [39].

#### 1.6.2.4 Barrier Properties

Because PLA finds a lot of applications in food packaging, its barrier properties (mainly to carbon dioxide, oxygen, and water vapor) have been largely investigated. The CO<sub>2</sub> permeability coefficients for PLA polymers are lower than those reported for crystalline polystyrene at 25 °C and 0% relative humidity (RH) and higher than those for PET. Since diffusion takes place through the amorphous regions of a polymer, an increase in the extent of crystallization will inevitably result in a decrease in permeability. A significant increase in the oxygen permeability coefficient is shown as the temperature is increased, but its decrease with water activity at temperatures close to  $T_g$  and its stabilization at temperatures well below  $T_g$  are clearly visible. PET and PLA are both hydrophobic and the corresponding films absorb very low amounts of water, showing similar barrier properties, as indicated by the values of their water vapor permeability coefficient determined from 10 °C to 37.8 °C in the range of 40-90% RH. Auras et al. have shown that the permeability for 98% L-lactide polymers is almost constant over the range studied, despite PLA being a rather polar polymer [37].

### 1.7 Graphene Based Crosslinking of PLA: Motivation of Study

Graphene's invention has catalyzed many new material applications in different fields. It has been used in combination with different biopolymers to design nanocomposites with improved mechanical, thermal, electrical, as well as, gas and water vapor-barrier properties. The major pathways for graphene incorporation into biopolymers include (1) solution intercalation, (2) melt intercalation, and (3) in situ polymerization. The fabrication, application, and mechanisms of bonding between biodegradable biopolymers, like poly (lactic acid), cellulose, starch, chitosan, alginates, polyamides, and other biodegradable materials, with different forms of graphene including graphene oxide (GO), reduced graphene oxide (RGO), graphene nanoplatelets (GNP), etc. have been the focus of most researchers.

Even though the history of graphene traces back to 1840, room temperature stable graphene was not invented until 2004. Andre K. Geim and Konstantin S. Novoselov were the first to produce room temperature stable graphene and received the highly prestigious Nobel Prize in 2010, for their innovative research with this amazing material. Graphene consists of a unit hexagonal cell, organized in a repeating honeycomb structure. In a unit cell of graphene, the subunits of carbon atoms are joined by sigma ( $\sigma$ ) bonds (length 0.142 nm), and the p-orbital from each carbon atom in the lattice contributes to a network of delocalized electrons, ensuring enhanced stability of the nanosystems. The original definition of graphene was of a single carbon layer, but now the definition has broadened. If the number of carbon layers is less than ten, it is still considered graphene, but if the layer number is ten or more, it is then known as graphite nanoplatelet GNP, or exfoliated graphite nanoplatelet (xGNP). GNPs have also been defined as a graphite base nanofiller, whose thickness can vary between 30 and 80 nm, depending on the synthesis method. However, if the thickness is even lower than 30 nm, the form of graphene is then referred as graphene nanosheet (GNS). GNP or GNS contain a very small number of functional groups (carboxyl, epoxy, and hydroxyl). As a result, GNP and GNS do not go into polar interactions or hydrogen bonding, so they are considered hydrophobic. A useful derivative of graphene that has found application in nanocomposites, due to its numerous and diverse functional groups, is graphene oxide (GO). GO is polar in nature and bears a negative charge, due to many epoxy and hydroxyl groups on its surface and carboxyl ( $-\text{COOH}$ ) group on the edges and as a result, it interacts better with polar polymers [40].

PLA is considered biodegradable and biocompatible, which has made it possible to be used in short-term packaging, tissue scaffolds, internal sutures, implant devices etc. Different studies have incorporated graphene nanofiller into the PLA matrix, in order to overcome its shortcomings like poor mechanical property, low crystallization rate, and thermal resistance. In the case of solution casting of PLA-graphene nanocomposites, a similar trend is observed as the previous studies where using the same percentage of nanofiller with different solvents has yielded significantly different property enhancements in the nanocomposites. Solvents like N, N-dimethyl-formamide (DMF), chloroform and acetone were used in dispersing graphene derivative in PLA matrices. The dispersibility of graphene varies depending on the solvents Hydrogen Component, also known as Hansen solubility parameter HSP and polar surface energy [36].

Majority of works based on intercalation of GO and PLA involve formation of graphene based PLA composites. For instance; Cao and co-workers made successful use of lyophilized graphene nanosheets to improve the mechanical and thermal properties of PLA in some degree [41]. Yang et al. prepared a series of PLA/thermally reduced graphene oxide composites via the in situ ring-opening polymerization of lactide, using thermally reduced graphene oxide as the initiator [42]. The thermal stability, crystallization rate and electrical conductivity of PLA were increased. Although in situ polymerization is an effective way to disperse the fillers in the matrix uniformly and generate better interfacial interactions with the host polymer, the synthesis of high molecular weight PLLA requires severe conditions and expensive precursor (lactide) [37]. However, controlled functionalization of carbonaceous materials and intercalation of functional carbon and PLA provide better results. In the works of Song et al [43, 44]. and Yoon et al [45]., PLA was successfully covalently grafted onto the convex surfaces and tips of the carboxylated multi-walled carbon nanotubes (MWNTs) via one step based on in situ polycondensation of lactic acid monomers. The resulting MWNTs-g-PLA were mixed with commercially available neat PLA to prepare PLA/MWCNTs-g-PLA nanocomposites and improved the initial modulus, tensile strength and crystallization rate of PLLA. Chemical crosslinking of linear polymers may provide feasible routes for the improvement of the mechanical properties and thermal stability. Several crosslinking methods have been published for different uses, since as a rule, all multifunctional compounds capable of reacting with hydroxyl groups can be used to obtain three dimensional



networks in polymers. Already cross linked PVA find a very promising application in the preparation of biomedical materials and of magnetic-field-sensitive gel.

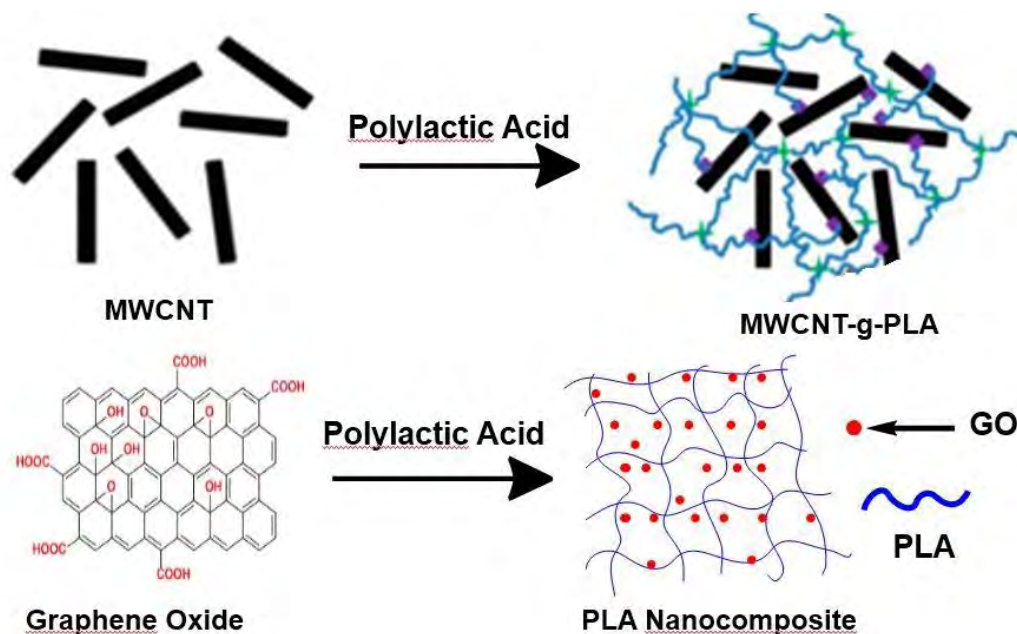


**Figure 1.7.** General Scheme illustrating the basic principle of crosslinking and formation of high strength PLA

Figure 1.7 depicts schematically the incorporation of MWCNT on PLA as discussed in above literature review. On the other hand, incorporation of GO on PLA should provide more hopeful output due to higher content of oxygen-containing functional groups [46] and higher specific surface area than that of MWCNTs-COOH. Thus it is expected to be more promising than MWCNTs-COOH in polycondensation of L-lactic acid as well as monomers of other similar biopolymers [47]. Achieving motivation from the concept stated above, a two dimensional GO based functionalized crosslinker will be prepared. After obtaining GO based functionalized 2D-crosslinker, it will be further functionalized in order to increase the length of reactive sites that should minimize the steric hindrance for crosslinking. It is expected that in situ polycondensation of lactic acid in presence of that 2D-crosslinker would provide uniformly crosslinked PLA having better mechanical properties.

## References

- [1] J. Zalasiewicz, M. Williams, W. Steffen and P. Crutzen “The New World of the Anthropocene,” *Environmental Science & Technology*, vol. 44, pp. 2228-2231, (2010).
- [2] R. A. Gross and B. Kalra, “Biodegradable polymers for the environment,” *Science*, vol. 297, pp. 803-7, (2002).
- [3] C. M. Rochman, M. A. Browne, B. S. Halpern, B. T. Hentschel, E. Hoh, H. K. Karapanagioti, L. M. Rios-Mendoza, H. Takada, S. Teh and R. C. Thompson, “Classify plastic waste as hazardous,” *Nature*, vol. 494, pp. 169, (2013).
- [4] M. Niaounakis, "1 - Definitions of Terms and Types of Biopolymers," *Biopolymers: Applications and Trends*, pp. 1-90, Oxford: William Andrew Publishing, 2015.
- [5] B. Ghanbarzadeh and H. Almasi, “Biodegradable Polymers,” *Biodegradation- Life of Science*, pp. 141-185, (2013).
- [6] A. Buléon, P. Colonna, V. Planchot and S. Ball, “Starch Granules: Structure and Biosynthesis,” *International Journal Biological Macromolecules*, vol. 23, pp. 85-112, (1998).
- [7] L. S. Lai and J. L. Kokini’, “Physicochemical Changes and Rheological Properties of Starch during Extrusion (A Review),” *Blotechnology Progress*, vol. 7, pp. 251-266, (1991)
- [8] W. Wiedmann and Strobe, E., “Compounding of Thermoplastic Starch with Twin-screw Extruders,” *Starch*, vol. 43, pp. 138-145, (1990).
- [9] E. M. Nakamura, L. Cordi, G. S. G. Almeida, N. Duran and L. H. I. Mei *et al.*, “Study and Development of LDPE/starch Partially Biodegradable Compounds,” *Journal of Materials Processing Technology*, vol. 162-163, pp. 236-241, (2005).
- [10] L. Mao, S. Imam, S. Gordon, P. Cinelli and E. Chiellini, “Extruded Cornstarch-Glycerol-Polyvinyl Alcohol Blends: Mechanical Properties, Morphology, and Biodegradability,” *Journal of Polymers and the Environmen.*, vol. 8, pp. 205-211, (2000).
- [11] A. Dufresne and J. Y. Cavailee., “Clustering and Percolation Effects in Microcrystalline Starch-Reinforced Thermoplastic,” *Journal of Polymer Science Part B: Polymer Physics*, vol. 36, pp. 2211-2224, (1998).

- [12] M. N. Anglès and A. Dufresne, "Plasticized Starch/Tunicin Whiskers Nanocomposites. 1. Structural Analysis," *Macromolecules*, vol. 33, pp. 8344-8353, (2000).
- [13] H. Almasi, B. Ghanbarzadeh and A. A. Entezami, "Physicochemical properties of starch–CMC–nanoclay biodegradable films," *International Journal of Biological Macromolecules*, vol. 46, pp. 1-5, (2010).
- [14] O. Brendel, P. P. M. Lannetta and D. Stewart, "A Rapid and Simple Method to Isolate Pure Alpha-Cellulose," *Phytochemical Analysis*, vol. 11, pp. 7-10, (2000).
- [15] R. Chandra, and R. Rustgi, "Biodegradable Polymers," *Progress in Polymer Science*, vol. 23, pp. 1273-1335, (1998).
- [16] F. P. La Mantia, and M. Morreale, "Green Composites: A Brief Review," *Composites Part A: Applied Science and Manufacturing*, vol. 42, pp. 579-588, (2011).
- [17] K. J. Edgar, C. M. Buchanan, J. S. Debenham, P. A. Rundquist, B. D. Seiler, M. C. Shelton and D. Tindall, "Advances in Cellulose Ester Performance and Application," *Progress in Polymer Science*, vol. 26, pp. 1605-1688, (2001).
- [18] B. Ghanbarzadeh, M. Musavi, A. R. Oromiehie, K. Rezayi, E. R. Rad and J. Milani, "Effect of Plasticizing Sugars on Water Vapor Permeability, Surface Energy and Microstructure Properties of Zein Films," *LWT - Food Science and Technology*, vol. 40, pp. 1191-1197, (2007).
- [19] R. N. Tharanathan, "Biodegradable Films and Composite Coatings: Past, Present and Future," *Trends in Food Science and Technology*, pp. 71-78, (2003).
- [20] C. Shi, Y. Zhu, X. Ran, M. Wang, Y. Su and T. Cheng, "Therapeutic Potential of Chitosan and Its Derivatives in Regenerative Medicine," *Journal of Surgical Research*, vol. 133, pp. 185-192, (2006).
- [21] B. Ghanbarzadeh, A. R. Oromiehie, M. Musavi, P. M. Falcone, Z. E. D-Jomeh and E. R. Rad, "Study of Mechanical Properties, Oxygen Permeability and AFM Topography of Zein Films Plasticized by Polyols," *Packaging Technology and Science*, vol. 20, pp. 155-163, (2007).
- [22] H-M. Li and G. W. Padua, "Properties and Microstructure of Plasticized Zein Films," *Cereal Chemistry Journal*, vol. 74, pp. 771-775, (1997).
- [23] B. Ghanbarzadeh, A. R. Oromiehie, M. Musavi, Z. E. D-Jomeh, E. R. Rad and J. Milani, "Effect of Plasticizing Sugars on Rheological and Thermal Properties of Zein Resins and

- Mechanical Properties of Zein films,” *Food Research International*, vol. 39, pp. 882-890, (2006).
- [24] S. Guilbert, N. Gontard and L. G. M. Gorris, “Prolongation of the Shelf-life of Perishable Food Products using Biodegradable Films and Coatings,” *LWT-Food Science and Technology*, vol. 29, pp. 10-17, (1996).
- [25] I. S. Arvanitoyannis, A. Nakayama, and S. I. Aiba, “Chitosan and Gelatin based Edible Films: State Diagrams, Mechanical and Permeation Properties,” *Carbohydrate Polymers*, vol. 37, pp. 371-382, (1998).
- [26] S. Nakai, “Structure-Function Relationships of Food Proteins: With an Emphasis on the Importance of Protein Hydrophobicity,” *J. Agricultural and Food Chemistry*, vol. 31, pp. 676-683, (1983).
- [27] G. G. Buonocore, M. A. Del Nobile, C. Di Martino, G. Gambacorta, E. L. Notte and L. Nicolais, “Modeling the Water Transport Properties of Casein-Based Edible Coating,” *Journal of Food Engineering*, vol. 60, pp. 99-106, (2003).
- [28] M. Ozdemir, and J. D. Floros, “Optimization of Edible Whey Protein Films Containing Preservatives for Mechanical and Optical Properties,” *Journal of Food Engineering*, vol. 84, pp. 116-123, (2008).
- [29] M. E. Gounga, S. Y. Xu, and Z. Wang, “Whey Protein Isolate-Based Edible Films as Affected by Protein Concentration, Glycerol Ratio and Pullulan Addition in Film Formation,” *Journal of Food Engineering*, vol. 83, pp. 521-530, (2007).
- [30] M. Muchizuki and M. Hiram, “Structural Effects on the Biodegradation of Aliphatic Polyesters,” *Polymers Advanced Technologies*, vol. 8, pp. 203-209, (1997).
- [31] E. J. Tijsma, L. van der Does, A. Bantjes, A. Bantjes and I. Vulic, “Mechanical Properties and Chemical Stability of Pivalolactone-Based Poly(ether ester)s,” *Polymer*, vol. 35, pp. 5483-5490, (1994).
- [32] I. Shohei, K. Hideomi, and T. Teiji, “Copolymerization of Carbon Dioxide and Epoxide With Organometallic Compounds,” *Die Makromolekulare Chemie*, vol. 130, pp. 210-220, (1969).
- [33] A. Rodriguez-Galan, L. Franco, and J. Puiggali, “Degradable Poly(ester amide)s for Biomedical Applications,” *Polymers*, vol. 3, pp. 65, (2011).

- [34] M. Desroches, M. Escouvois, R. Auvergne, S. Caillol and B. Boutevin, "From Vegetable Oils to Polyurethanes: Synthetic Routes to Polyols and Main Industrial Products," *Polymer Reviews*, vol. 52, pp. 38-79, (2012).
- [35] B. Hu, "Biopolymer-Based Lightweight Materials for Packaging Applications," *Lightweight Materials from Biopolymers and Biofibers*, ACS Symposium Series 1175, pp. 239-255: American Chemical Society, (2014).
- [36] J. Majid, T. E. Arab, I. Muhammad, J. Muriel and D. Stephane, "Poly-Lactic Acid: Production, Applications, Nanocomposites, and Release Studies," *Comprehensive Reviews in Food Science and Food Safety*, vol. 9, pp. 552-571, (2010).
- [37] D. Garlotta, "A Literature Review of Poly(Lactic Acid)," *Journal of Polymers and the Environment*, vol. 9, pp. 63-84, (2001).
- [38] L. Avérous, "9 - Synthesis, Properties, Environmental and Biomedical Applications of Polylactic Acid A2 - Ebnesajjad, Sina," *Handbook of Biopolymers and Biodegradable Plastics*, pp. 171-188, Boston: William Andrew Publishing, 2013.
- [39] A. Rafael, H. Bruce, and S. Susan, "An Overview of Polylactides as Packaging Materials," *Macromolecular Bioscience*, vol. 4, pp. 835-864, (2004).
- [40] T. B. Rouf, and J. L. Kokini, "Biodegradable Biopolymer-Graphene Nanocomposites," *Journal of Materials Science*, vol. 51, pp. 9915-9945, (2016).
- [41] Y. Cao, J. Feng, and P. Wu, "Preparation of Organically Dispersible Graphene Nanosheet Powders Through a Lyophilization Method and Their Poly(lactic acid) Composites," *Carbon*, vol. 48, pp. 3834-3839, (2010).
- [42] J. H. Yang, S. H. Lin, and Y. D. Lee, "Preparation and Characterization of Poly(l-lactide)-Graphene Composites Using the in Situ Ring-Opening Polymerization of PLLA With Graphene as the Initiator," *J. Materials Chemistry*, vol. 22, pp. 10805-10815, (2012).
- [43] S. Qin, D. Qin, W. T. Ford, D. E. Resasco and J. E. Herrera, "Functionalization of Single-Walled Carbon Nanotubes with Polystyrene via Grafting to and Grafting from Methods," *Macromolecules*, vol. 37, pp. 752-757, (2004).
- [44] W. Song, Z. Zheng, W. Tang and X. Wang, "A Facile Approach to Covalently Functionalized Carbon Nanotubes With Biocompatible Polymer," *Polymer*, vol. 48, pp. 3658-3663, (2007).

- [45] Y. J. Tae, J. Y. Gyu, L. S. Cheol and B. M. Gil, “Influences of Poly(lactic acid)-Grafted Carbon Nanotube on Thermal, Mechanical, and Electrical Properties of Poly(lactic acid),” *Polymers for Advanced Technologies*, vol. 20, pp. 631-638, (2009).
- [46] D. C. Marcano, D. V. Kosynkin, J. M. Berlin, A. Sinitskii, Z. Sun, A. Slesarev, L. B. Alemany, W. Lu and J. M. Tour, “Improved Synthesis of Graphene Oxide,” *ACS Nano*, vol. 4, pp. 4806-4814, (2010).
- [47] H. Hu, Z. Zhao, Q. Zhou, Y. Gogotsi and J. Qiu “The Role of Microwave Absorption on Formation of Graphene From Graphite Oxide,” *Carbon*, vol. 50, pp. 3267-3273, (2012).

## **Chapter 2**

### **Experimental**

### 2.1.1 Chemicals and Reagents

The chemicals and reagents in this research were analytical grade and used without further purification. Deionized water was used as solvent to prepare most of the solutions of this work. The chemicals and reagents which were used in the research are given below:

- i. Lactic acid (Scharlau, Spain)
- ii. Xylene (BDH, England)
- iii. Stannous Chloride ( $\text{SnCl}_2 \cdot 2\text{H}_2\text{O}$ ), (Sigma-Aldrich, USA)
- iv. Graphite flake (325 mesh), (Merck, Germany)
- v. Thionyl Chloride (BDH, England)
- vi. Methanol (Merck, Germany)
- vii. Potassium permanganate (Merck, Germany)
- viii. Sulfuric acid (Merk, Germany)
- ix. Hydrogen peroxide (Sigma-Aldrich)
- x. Chloroform (Merk, India)
- xi. Dimethylformamide (DMF), (Merk, India)
- xii. Sodium nitrate (Merk, Germany)
- xiii. Cellulose nitrate filter paper  $0.45\mu\text{m}$  (sartorius stedim, Germany)

### 2.1.2 Instruments

**Synthesis, characterization and data analysis was performed by using the following instruments:**

- i. Fourier Transform Infrared Spectrophotometer (SHIMADZU FTIR-8400)
- ii. Field Emission Scanning Electron Microscopy (JSM-7600F, Tokyo, Japan)
- iii. X-ray photoelectron Spectroscopy (XPS)
- iv. Atomic Force Microscopy (AFM)
- v. Thermogravimetric Analysis (TGA)
- vi. Differential Scanning Calorimetry (DSC)
- vii. Centrifuge machine (Hettich, Universal 16A)
- viii. Hot press (P/O/WEBER, Germany)
- ix. Universal testing machine (UTM)
- x. Digital Balance (AB265/S/SACT METTLER, Toletto, Switzerland)



- xi. Freeze Dryer (Heto FD3)
- xii. Oven (Lab Tech, LDO-030E)
- xiii. Dean Stark apparatus

## 2.2. Method of preparation

### 2.2.1. Preparation of Graphene Oxide (GO)

A modified Hummer's method was applied to synthesize graphene oxide (GO) [1]. Graphite (2g) and  $\text{NaNO}_3$  (1.5g) were mixed in 500 mL two-necked round bottom flask in an ice water bath, and  $\text{H}_2\text{SO}_4$  (98%, 150 mL) was added slowly into the mixture with magnetic stirring. Then,  $\text{KMnO}_4$  (9g) was then added slowly over the mixture. Stirring and ice bath were maintained during the addition of  $\text{KMnO}_4$ , which were kept for another 2 h after the addition. The ice bath was removed while the stirring was kept vigorously for 5 days at room temperature.  $\text{H}_2\text{O}_2$  solution (6 mL) was then added into the mixture with another 2 h agitation. Consecutively, 250 mL solution of deionization (DI) water mixed with  $\text{H}_2\text{SO}_4$  (98%, 7.5 mL) and  $\text{H}_2\text{O}_2$  (30 wt%, 4.17 mL) was added to dilute and wash the mixture.

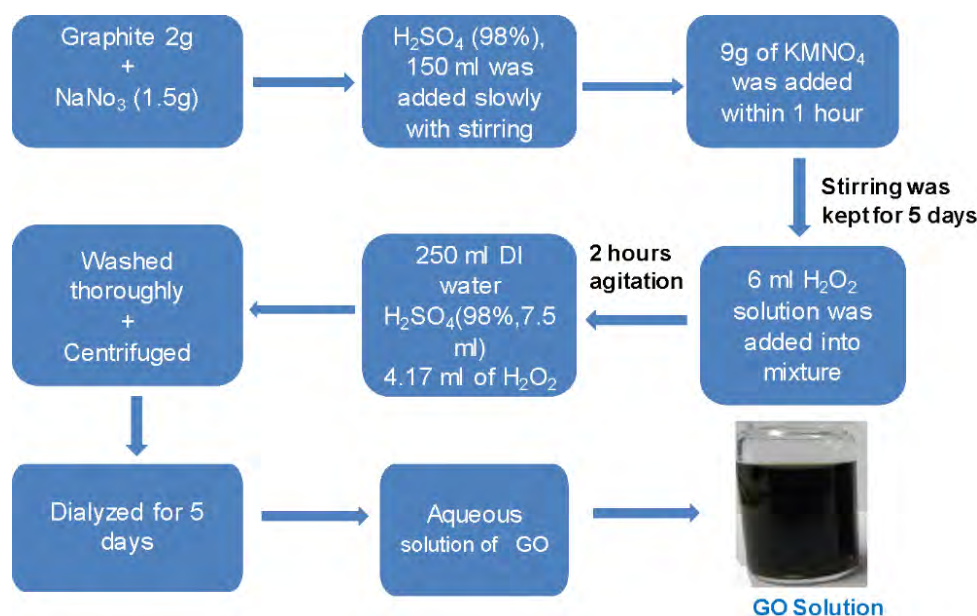


**Figure 2.2.1.** Schematic illustration of graphene oxide (GO) preparation

The resulted mixture was carefully washed by DI water, centrifuged, and then dialyzed for 5 days. Finally, the GO aqueous solution was lyophilized and fluffy black dried GO was

obtained.

### 2.2.2. Preparation of GO based 2D-crosslinker (GO-LA-LA)

GO (32 mg) and DMF (2 mL) were sonicated for 30 min in a 50 mL flask. Then, the homogeneous solution was kept in oil bath for 120 °C for 1 h, in which if any water remains to evaporate. The solution will reach then in room temperature, after then thionyl chloride ( $\text{SOCl}_2$ , 6 mL) was added in order to convert the carboxyl group into acyl chlorides. Then, the solution was kept for 24 h in 70 °C under reflux and the residual  $\text{SOCl}_2$  was evaporated by rotatory evaporator. The resultant and chloroform (3 mL) were sonicated 30 min to create a homogeneous dispersion. Lactic acid (LA, 100 g) was then added to the mixture, and the reactor was then immersed in an oil bath at 70 °C with magnetic stirring for 1 h to remove the solvent. Then, the reaction was allowed to proceed for 24 h at 60 °C under magnetic stirring. Finally, the resulting reaction medium was dissolved in excess chloroform and vacuum filtered three times through 0.2 nylon membrane to remove unbound LA [2]. To increase the crosslinker (GO-LA) length above discussed procedure was repeated.

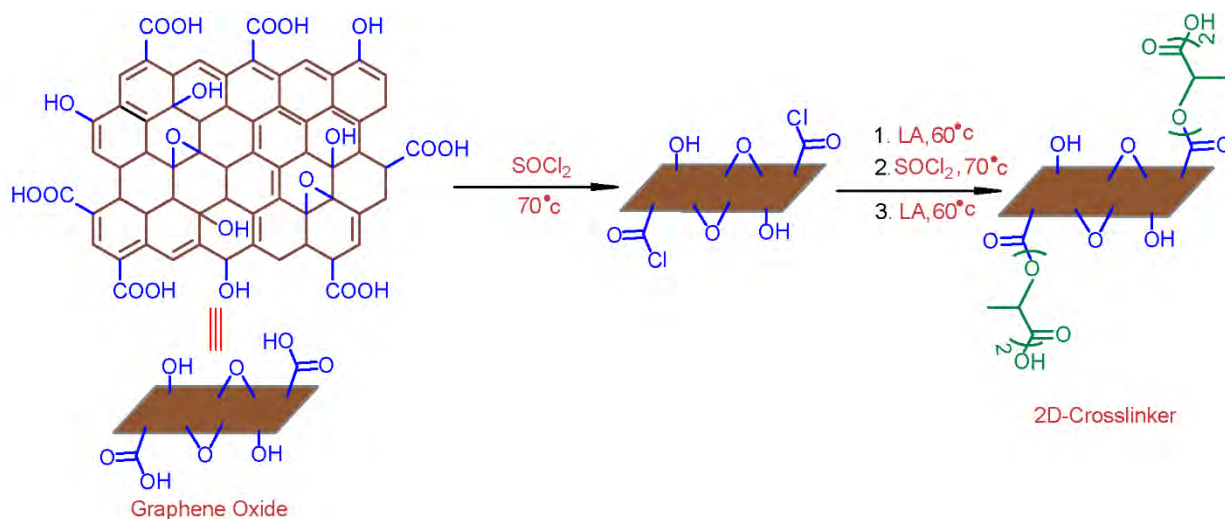


**Figure 2.2.2.** Schematic illustration of 2D-crosslinker preparation

### 2.2.3. Preparation of GO based 2D-crosslinked Polylactic acid (GO-PLA)

L-lactic acid (9 g) and GO-LA (0.33%, 0.03 g) was added to a round bottom flask (100 mL) and sonicated 30 min to get a homogeneous dispersion which was immersed in an oil bath at 100 °C for 1 h in order to remove the water. Stannous chloride ( $\text{SnCl}_2 \cdot 2\text{H}_2\text{O}$ , 0.02 g, 0.2 wt%) was added to the reactor as a catalyst, and the flask reactor was heated in an oil bath to 138-140 °C. The azeotrope dehydration was carried out for 30 h using a Dean-Stark trap which removed trace amount of water produced in situ polycondensation reaction, while m-xylene (20 mL) was used as a solvent. The reaction mixture was concentrated to about half of the volume, and then the resulting mixture was poured into methanol. Precipitated polymers were collected by suction filtration and dried under reduced pressure, and finally GO-PLA powders were obtained [3]. Besides, 2D-crosslinked (GO-PLA) was synthesized in various amount (0.2 and 0.1 wt%) of crosslinker loadings.

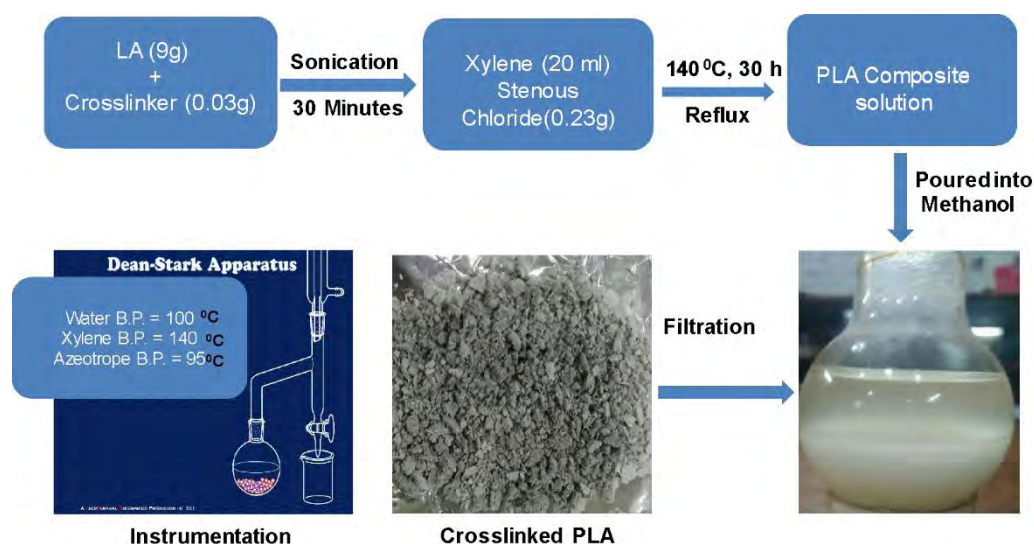


**Figure 2.2.3.** Schematic illustration of GO-PLA preparation

#### **2.2.4. Preparation of neat Polylactic acid (PLA)**

For comparison with the crosslinked PLA (GO-PLA), PLA also was synthesized by polycondensation reaction. L-lactic acid (9 g) was taken in a round bottom flask, which was immersed in an oil bath at 100 °C for 1 h in order to remove the water. Stannous chloride ( $\text{SnCl}_2 \cdot 2\text{H}_2\text{O}$ , 0.02 g, 0.2 wt%) was added to the reactor as a catalyst, and the flask reactor was heated in an oil bath to 138-140 °C. The azeotrope dehydration was carried out for 30 h using a Dean-Stark trap which removed trace amount of water produced in situ polycondensation reaction, while m-xylene (20 mL) was used as a solvent. The reaction mixture was concentrated to about half of the volume, and then the resulting mixture was poured into methanol. Precipitated polymers were collected by suction filtration and dried under reduced pressure, and finally PLA white powders were obtained [3].

#### **2.2.5. Preparation of untreated GO grafted PLA**

Untreated GO grafted PLA has been prepared by condensation reaction. 9g LA was taken in a round bottom flask, which was heated at 100°C for 1 h into oil bath in order to remove water. 0.33 g GO (0.33 wt%) was then added into the reactor and sonicated for 30 minutes to get homogeneous dispersion. 0.02 g (0.2wt%) stannous chloride ( $\text{SnCl}_2 \cdot 2\text{H}_2\text{O}$ ) similarly added into the mixture as a polymerization catalyst, and the flask reactor was immersed into an oil bath heated 138-140 °C. Azeotropic dehydration reaction was carried out for 30 h with the help of Dean-Stark trap where 20 ml Xylene was added as solvent in this in-situ polymerization. The reaction mixture was concentrated to about half of the volume, and then the resulting mixture was poured into methanol. Precipitated polymers were collected by suction filtration and dried under reduced pressure, and finally untreated GO grafted PLA powders were obtained [3].

### **2.3 Sample characterization**

#### **2.3.1 Fourier transform infrared (FTIR) analysis**

The infrared spectra of graphene oxide (GO), GO based 2D-Crosslinker (GO-LA-LA), neat polylactic acid (PLA) and 2D-crosslinked polylactic acid (GO-PLA) were investigated on a FTIR spectrometer in the region of 4000-1000  $\text{cm}^{-1}$ . After preparation, all of the samples were oven dried at 60<sup>0</sup>c and small portion of samples were taken into vial. GO flakes are

mechanically very strong so, it was grinded into a mortar with a pestle to get GO powder. Rest of the samples were not grinded because they were physically granule and powder after complete drying. FTIR spectra of the solid samples were frequently obtained by mixing and grinding a small amount of materials with dry and pure KBr crystals. The mixing and grinding were done in a mortar by a pestle. The powder mixture was then compressed in a metal holder under a pressure of 8–10 tons to make a pellet. The pellet was then placed in the path of IR beam for measurements.

### 2.3.2 Scanning Electron Microscope (SEM)

The surface morphology of the synthesized GO, GO based 2D-crosslinker (GO-LA-LA), neat PLA and crosslinked PLA (GO-PLA, 0.33 wt%, 0.2 wt% and 0.1 wt%) was conducted using Field Emission Scanning Electron Microscopy (FE-SEM). The completely air dried samples were glued on a conducting carbon strip. The sample loaded strip was then mounted to a chamber that evacuated to  $\sim 10^{-3}$  to  $10^{-4}$  torr and then a very thin platinum layer ( $\sim$ few nanometers thick) were sputtered on the sample to ensure the conductivity of the sample surface. The sample was then placed in the main SEM chamber to view its surface. The microscope was operated at an accelerating voltage of 5.0 kV. The system was computer interfaced and thus provides recording of the surface images in the computer file for its use as hard copy.

### 2.3.3 Atomic force microscope (AFM)

AFM experiments were performed on samples of 2D-crosslinker (GO-LA-LA), neat PLA and 0.33wt% crosslinked PLA (GO-PLA). The experiments were done using a MFP-3D (Asylum) operated in tapping mode with commercially available Si cantilevers (Olympus, 300 kHz frequency). The force constant of the cantilevers was 42 N/m. The oscillation frequency used for tapping mode was  $310 \pm 5$  kHz.

### 2.3.4 X-ray Photoelectron Spectroscopy (XPS)

Most surface sensitive analytical technique XPS measurements were performed on samples that had been prepared within 4 days using the AXIS ULTRA spectrometer (Kratos Analytical). The base pressure in the analytical chamber was  $<3 \times 10^{-8}$  Pa. The

monochromatic AlK $\alpha$  source ( $h\nu=1486.6$  eV) was used at a power of 210 W. The photoelectron exit angle was  $90^\circ$ , and the incident angle was  $35.3^\circ$  from the plane of the surface. The analysis spot was  $400 \times 700$   $\mu\text{m}$ . The resolution of the instrument was 0.55 eV for Ag 3d peaks. Survey scans were collected for binding energies from 1100 to 0 eV with an analyzer pass energy of 160 eV and a step of 0.35 eV. The high-resolution spectra were run with a pass-energy of 20 eV and a step of 0.1 eV. Relative sensitivity factors (RSFs) for different elements were as follows: 1 for F (1s), 0.477 for N (1s), 0.955 for Br (3d). Only one set of XPS scans was performed on a given sample; therefore, XPS analysis before and after surface reactions were performed on different samples.

### 2.3.5 Thermogravimetric analysis (TGA)

TGA is the study of weight loss of a specimen with respect to the temperature increasing. The quantities are recorded for a TGA; they are the weight, the temperature and temperature change rate. The weight loss and weight loss rate are usually plotted for further analysis. TGA system usually consists of a high precision with pans, an oven and a closed chamber. The balance must be able to sustain high temperature up to  $100^\circ\text{C}$ .

The thermal stability of neat PLA, (0.33%, 0.2%, 0.1 wt% crosslinked PLA) and 0.33wt% GO filled PLA were studied by a thermo-gravimetric analyzer (TGA) in a nitrogen atmosphere. Approximately 3-10 mg freeze dried samples taken into an aluminum cell and heated from 30 to  $800^\circ\text{C}$  at a heating rate of  $10^\circ\text{C}/\text{min}$  under a nitrogen flow of 10 mL/ min. Before the data acquisition segment, the sample was equilibrated at  $25^\circ\text{C}$  for 5 min to obtain an isothermal condition.

### 2.3.6 Differential Scanning Calorimetry (DSC)

Differential scanning calorimetry (DSC) is a technique used to investigate the response of polymers to heating. The aim of this experiment is to find  $T_g$ ,  $T_c$ , and  $T_m$  as well as the latent heats of crystallization and melting for the specimens. The DSC set-up is composed of a measurement chamber and a computer. Two pans are heated in the measurement chamber. The sample pan contains the material being investigated. A second pan, which is typically empty, is used as a reference. The computer is used to monitor the temperature and regulate

the rate at which the temperature of the pans changes. A typical heating rate is around 10 °C/min.

The  $T_g$ ,  $T_c$ , and  $T_m$  of neat PLA, (0.33%, 0.2%, 0.1 wt%) crosslinked PLA and 0.33wt% GO filled PLA were recorded by a DSC in a nitrogen atmosphere. Approximately 3-10 mg freeze dried samples taken into an aluminum pan and heated from 30 to 800 °C at a heating rate of 10 °C/min under a nitrogen flow of 10 mL/ min.

### 2.3.7 Mechanical properties studies

Mechanical test (compressive) were carried out using universal testing machine (UTM) with 1 KN load cell in room temperature. For compressive test, the cylinder-shaped pellets of polymer with height  $10 \pm 0.5$  mm and diameter of  $10 \pm 0.2$  mm were used to conduct compressive tests and the compression rate was fixed at 10 mm/min. A 45 mm height and 10 mm whole diameter mold was designed in order to fabricate cylindrical pellets, which is as like as figure 2.3.7. The compressive strain ( $\epsilon$  %) was defined as the length change ( $\Delta l$ ) divided by initial length ( $l_0$ ) of the specimen and the stress ( $\sigma$ ) was obtained by utm data. The Young's modulus was determined from the slope of the initial linear regions ( $\epsilon_t = 10\% \sim 20\%$ ) of the stress-strain curves. The toughness was calculated by the area under the compressive stress-strain profiles.

The mold was filled with the 1g of 0.33% crosslinked PLA sample and was placed in hot press which heated at 120°C. A pressure of 2 KN was applied for 2 min to soften the powder like sample at 60°C and then a pressure of 5 KN was applied for 25 min. Finally, the mold was quenched to room temperature with the water recycle system and removed the mold from hot press to obtain the cylindrical pellets. For comparison, (0.1 %, 0.2%) GO-PLA, neat PLA and 0.33% GO filled PLA pellets were also prepared by same method.



**Figure 2.3.7.** Pellets preparation method in hot press by compression molding

### References

- [1] J. Zhang, M. S. Azam, C. Shi, J. Huang, B. Yan, Q. Liu and H. Zeng, “Poly(acrylic acid) Functionalized Magnetic Graphene Oxide Nanocomposite for Removal of Methylene Blue,” *RSC Advances*, vol. 5, pp. 32272-32282, (2015).
- [2] G. X. Chen, H. S. Kim, B. H. Park and J. S. Yoon, “Controlled Functionalization of Multiwalled Carbon Nanotubes with Various Molecular-Weight Poly(l-lactic acid),” *The Journal of Physical Chemistry B*, vol. 109, pp. 22237-22243, (2005).
- [3] K. K. Woong and W. S. Ihl, “Synthesis of High- Molecular- Weight Poly(L- lactic acid) by Direct Polycondensation,” *Macromolecular Chemistry and Physics*, vol. 203, pp. 2245-2250, (2002).



## **CHAPTER 3**

### **Result and Discussion**

### 3.1 Synthesis route of GO based 2D-crosslinker (GO-LA-LA)

Graphene, which consists of a one-atom-thick planar sheet comprising a  $sp^2$ -bonded carbon structure is a novel material that has emerged as a rapidly rising star in the field of material science [1-3]. One specific branch of graphene research deals with graphene oxide (GO). Recently, GO has attracted much research interest for its outstanding electrical, thermal, and mechanical properties [4, 5]. GO has 2-D structure with high surface area (theoretically  $2630 \text{ m}^2/\text{g}$  for single-layer graphene) and oxygen containing rich functional group such as carboxylic, hydroxyl and epoxide groups, which confirms the availability of further modification [1, 6, 7]. The synthesis route of 2D-crosslinker (GO-LA-LA) has been illustrated in Figure 3.1. At first GO was treated by thionyl chloride in order to convert all of the carboxylic groups (-COOH) into acyl chloride groups (-COCl). Then the resulting system was functionalized by lactic acid (LA) and an ester forms between acyl group (-COCl) and hydroxyl group (-OH) of LA. In the same time, carboxylic groups (-COOH) has become free from LA in basal plane of GO surface, which will act as the active functional group of crosslinker. In order to increase the length of GO-LA to GO-LA-LA above discussed procedure was repeated, so that it is possible to avoid the steric barrier among GO and LA molecules.

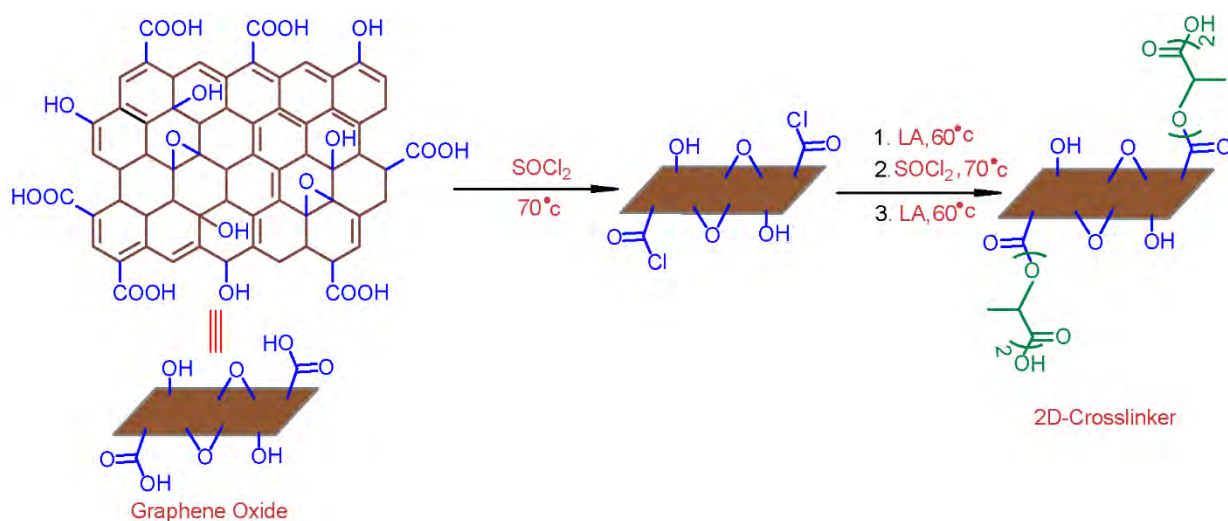


**Figure 3.1.** Synthesis route of GO based 2D-crosslinker (GO-LA-LA)

### 3.2 Synthesis route of GO based 2-D Crosslinked Polylactic acid

Poly(lactic acid) (PLA) is a plant-derived biodegradable polymer that is widely used as an alternative of widely used to petroleum-derived polymers [8]. In recent years PLA has received much research interest because of its degradability and wide range of application, such as food packaging, drug delivery, biomedical, agriculture, tissue engineering etc [9, 10]. However, its wider range of application has been limited by its relatively poor mechanical strength and thermal stability. To overcome this drawbacks herein we propose a new synthetic route to fabricate GO based 2-D crosslinked PLA in Figure 3.2. However, PLA has been produced by a multi-step process called ring-opening polymerization, including the production and the isolation of intermediate lactide [11]. PLA production has been restricted by ring-opening polymerization because of its high process cost of synthesizing and purifying lactide. To overcome this problem we preferred one step direct polycondensation polymerization reaction. It was reported that it is very difficult to obtain high-molecular-weight PLA by direct polycondensation because of equilibrium between free acids, water and polyesters causing difficulty in removing water as a byproduct [12]. Aqueous LA was used as a starting material and 0.2 wt% stannous chloride ( $\text{SnCl}_2 \cdot 2\text{H}_2\text{O}$ ) of monomer was used as a catalyst. To extract water produced in condensation reaction Dean-Stark apparatus was used as a water separator and m-xylene was also used as solvent [12]. GO based 2-D Crosslinked Polylactic acid (GO-PLA) was synthesized by direct noble *in situ condensation* reaction. This *in situ* polymerization was firstly reported by Imai et al., where carbon black and nylonsalt- type monomer/carbon black were used as conductive fillers. Again, *in situ* polymerization is an effective way to disperse the fillers in the matrix uniformly and generate better interfacial interactions with the host polymer. For homogeneous crosslinking in PLA matrix GO based crosslinked PLA was synthesized following *in situ condensation* reaction. It is desirable to use GO based 2-D crosslinker (GO-LA-LA) as the reactants or initiators in the *in situ* polymerization of L-lactic acid monomers to prepare GO based 2-D crosslinked PLA (GO-PLA). Finally crosslinked PLA was prepared by esterification polycondensation reaction between oxygen containing functional groups from both 2-D crosslinker (GO-LA-LA) and LA.

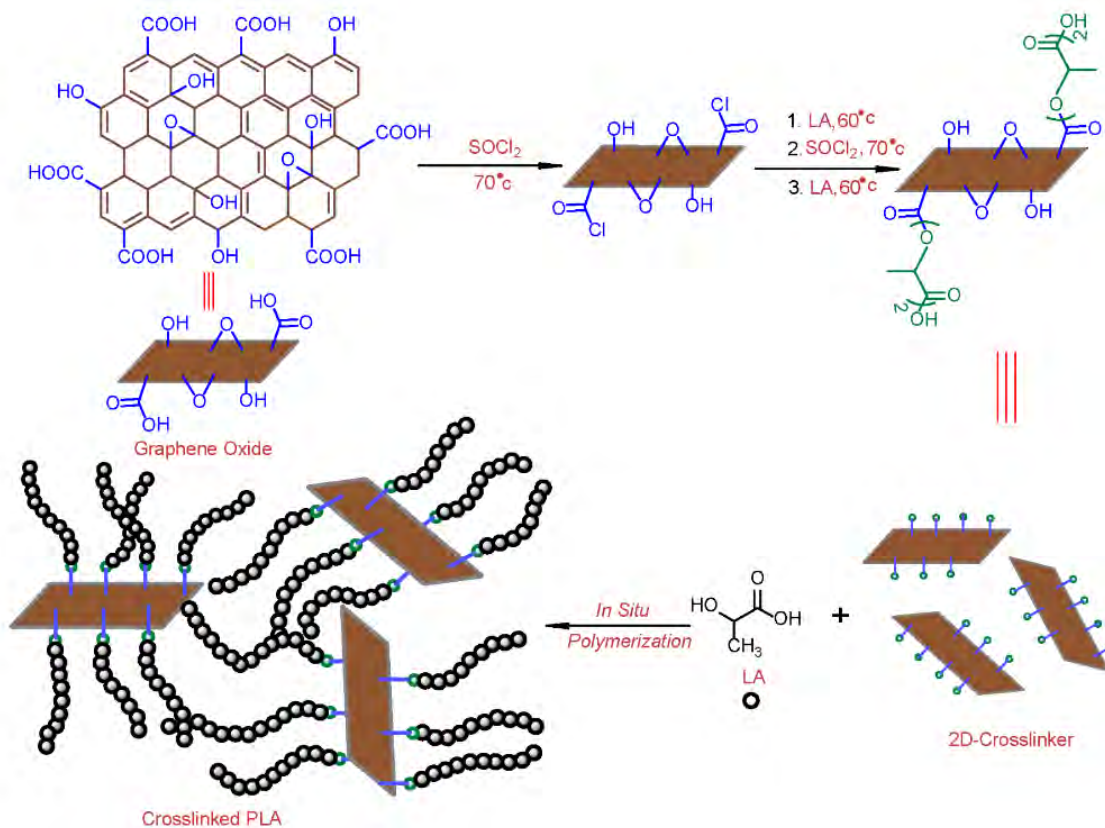


**Figure 3.2.** Schematic preparation route of GO based 2-D crosslinked (GO-LA-LA) Poly(lactic acid) (GO-PLA).

### 3.3 Functional Group Investigation by Fourier Transform Infrared Spectroscopy

#### (FTIR)

FTIR spectra was conducted to authorize the presence of functional groups on the surface of GO, GO-LA-LA, crosslinked PLA and pure PLA. The FTIR spectra of synthesized GO, GO-LA-LA, crosslinked PLA and PLA were displayed in Figure. 3.3. In GO spectra (Figure 3.3a) the characteristic peaks were band at  $3430\text{ cm}^{-1}$  (O-H stretching vibration),  $1728\text{ cm}^{-1}$  (C=O stretching vibration from carboxylic acid groups). The spectrum also shows a C=C peak at  $1620\text{ cm}^{-1}$  corresponding to unoxidized graphite powder or to the remaining  $\text{sp}^2$  character [13-15]. For GO-LA-LA, more intense C=O stretching band appeared at  $1740\text{ cm}^{-1}$ .

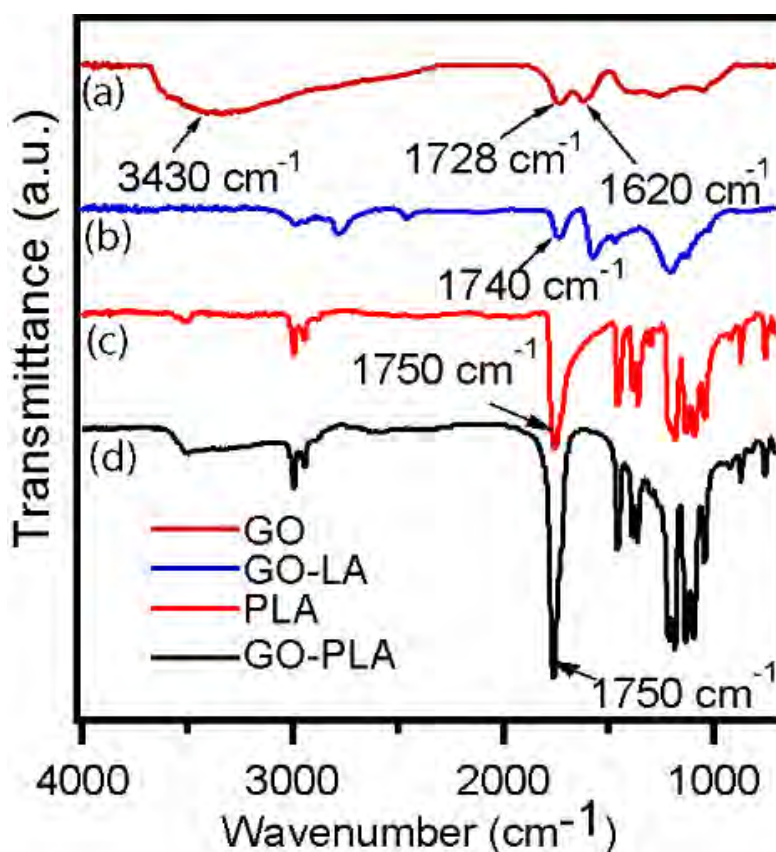


**Figure 3.3.** FTIR spectra of (a) GO, (b) GO-LA-LA, (c) PLA and (d) Crosslinked PLA

The wavenumber of C=O shifted from 1728  $\text{cm}^{-1}$  (GO) to 1740  $\text{cm}^{-1}$  (GO-LA-LA), which could be elucidated that the band at 1728  $\text{cm}^{-1}$  corresponds to carboxylic acid group from GO, while the band at 1740  $\text{cm}^{-1}$  corresponds to ester group of GO-LA-LA (Figure 3.3 a and b) [16, 17]. On the other hand, the intensity of O-H bands at 3430  $\text{cm}^{-1}$  (Figure. 1d) which corresponded to hydroxyl groups decreased clearly because the PLA chains were covalently bonded to GO surface (the esterification reaction between carboxyl groups or hydroxyl groups on lactic acid and hydroxyl groups or carboxyl groups on GO) [18]. In PLA, the peak was band at 1750  $\text{cm}^{-1}$  which demonstrate the C=O vibration from ester. The resonance due to C-CH<sub>3</sub> stretching mode, -CH<sub>3</sub> rocking mode and -CH<sub>3</sub> asymmetric bending mode of PLA were at 1090, 1185 and 1454  $\text{cm}^{-1}$  respectively. We have also found more intense C-CH<sub>3</sub> stretching mode, -CH<sub>3</sub> rocking mode and -CH<sub>3</sub> asymmetric bending mode in the case of GO-PLA in figure 3.3d [16]. Therefore, FTIR spectra indicate clearly that GO was successfully functionalized LA and PLA chains also covalently bonded in the surface of GO based 2D-crosslinker.

**Table 3.1.** Characteristic peak and interpretations correspond to GO, GO-LA-LA, PLA and crosslinked PLA.

Functional Group	Wavenumber ( $\text{cm}^{-1}$ )
O-H stretching vibration	3430
C=O (-COOH) stretching vibration	1728
C=O (-COOR) stretching vibration	1740, 1750
C=C (SP <sup>2</sup> ) character	1620
C-CH <sub>3</sub> stretching mode	1090
-CH <sub>3</sub> rocking mode	1185
CH <sub>3</sub> asymmetric bending	1454

### 3.4 X-ray photoelectron spectroscopy (XPS) analysis.

#### 3.4.1 High resolution C1s spectra analysis of GO and GO-LA-LA

The functionalization of GO with lactic acid was confirmed by XPS, which is the most surface sensitive technique. The C1s core-level spectra of both samples GO and GO-LA were presented in Figure 3.4.1. The spectrum of GO (Figure 3.4.1a) is demonstrated four types of carbon bond, they are C-C/C=C, C-O, C=O and O-C=O in the binding energy of 284.7 eV, 286.6 eV, 287.7 eV and 289.0 eV respectively. After the functionalization with LA, -OH group of GO was reduced and at the same time C-C/C-H (284.6 eV) and O-C=O (289.0 eV) corresponding to lactic acid were increased significantly in GO-LA-LA (Figure 3.4.1b), which is attributed in Table 1 [19, 20].

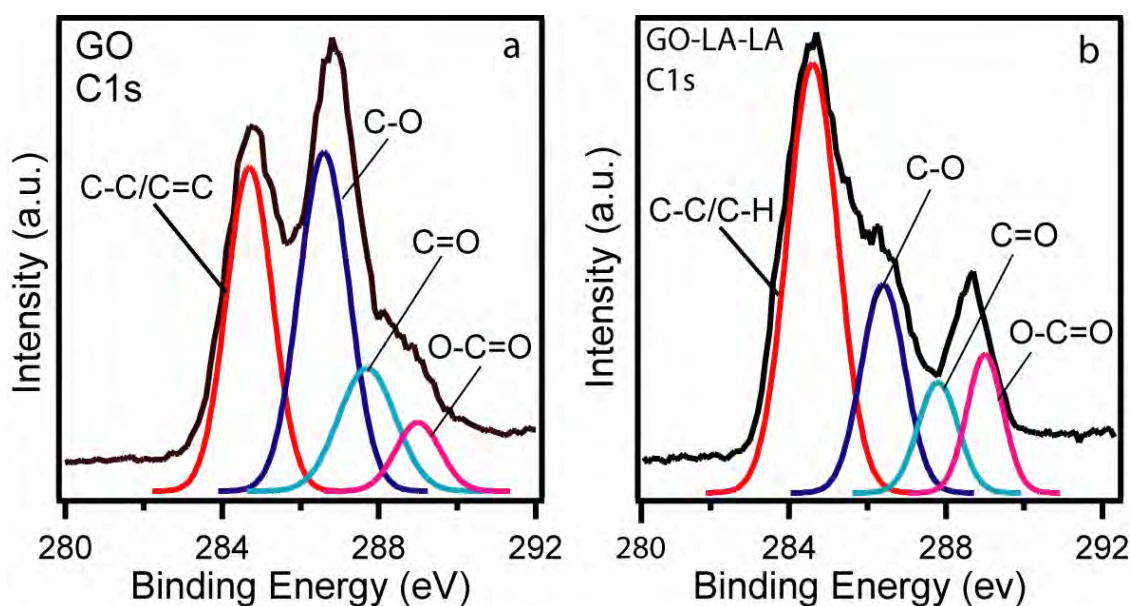


**Figure 3.4.1** XPS high resolution C1s spectra of GO and GO-LA-LA.

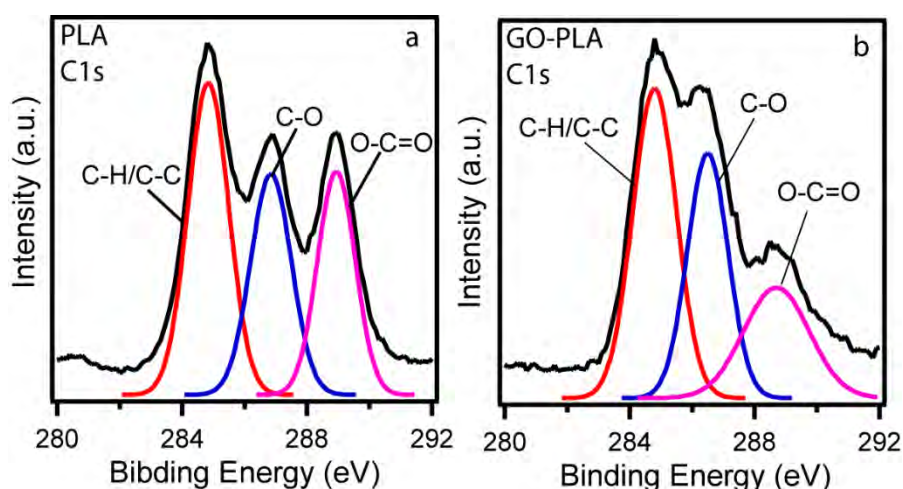
The bond percentage and binding energy of different bonds based on C1s spectra for GO and GO-LA are summarized in Table 3.2. Table 3.2 Shows that after the functionalization of GO by LA, the percentage of C-C/C-H and O-C=O is increased from 35.6% to 53.6% and 7.3%-12.4% respectively and C-O was decreased 40.4% to 22.7% simultaneously. The increasing of C-C/C-H and O-C=O bond percentage in GO to GO-LA resultant to GO was successfully functionalized by LA.

**Table 3.2.** XPS C1s peak information for four types of C bonds in GO and GO-LA-LA.

Materials	B.E.	%	B.E.	%	B.E.	%	B.E.	%
	O-C=O		C=O		C-O		C-C/C=C/C-H	
GO	289.0	7.3	287.7	16.7	286.6	40.4	284.7	35.6
GO-LA	289.0	12.4	287.8	11.0	286.4	22.7	284.6	53.9

### 3.4.2 High resolution C1s spectra analysis of PLA and crosslinked PLA (GO-PLA)

The crosslinking of PLA with graphene based 2D-crosslinker was also confirmed by XPS analysis. The C1s core-level spectra of both samples neat PLA and crosslinked PLA (GO-PLA) were showed in figure 3.4.2. The spectrum of PLA is convoluted into three components in different binding energy and they are O-C=O (288.9 eV), C-O (286.8 eV) and C-C/C-H (284.8 eV) [21, 22].

**Figure 3.4.2** XPS high resolution C1s spectra of (a) PLA and (b) GO-PLA.

The bond percentage, binding energy of different bonds based on C1s spectra and the ratio of C-O and O-C=O for PLA and GO-PLA are summarized in Table 3.3. Table 3.3 shows that the bond



Percentage are 29.9 and 28% corresponding to C-O and O-C=O respectively and the ratio is 1.07. After crosslinking the bond percentage of C-O is increased from 29.9% to 32.3% because crosslinker contains 22.7% (Table 3.2) of C-O bond. According to the mechanism of

**Table 3.3.** XPS C1s peak information for three types of C bonds in PLA and GO-PLA.

Materials	B.E.	%	B.E.	%	B.E	%	Ratio
	O-C=O		C-O		C-C/C-H		C-O and O-C=O
PLA	288.9	28	286.8	29.9	284.8	42.2	1.07
GO-PLA	288.7	23.6	286.5	32.3	284.8	44.1	1.37

polycondensation reaction of lactic acid, this reaction is well-thought-out to involve both “grafted from” and “grafted to approaches” [16, 23]. “Grafted to” approach means the monomers are in situ polymerized from initiator or catalyst on GO surface and again GO is bonded with polymeric molecules whose terminal functional groups react with the functional groups on GO corresponding to “grafted to” approach [24]. In our reaction system, the lactic acid monomer reacted with the carboxyl acid and hydroxyl group on the surface of GO based crosslinker through the in situ surface initiated polymerization reaction which attributed to “grafted from” approach, and at the same time free lactide added with the functional group supported by the surface of GO based crosslinker, which is attributed to “grafted to” approach. Now it can be said that most of the surface of crosslinker was coated by PLA chains, which made it more difficult for free oligomer to attack the surface of GO based crosslinker. During this stage, the chain length of the PLA chains were continuously increased [25]. Furthermore, the bond ratio of C-O and O-C=O is increased from 1.07 to 1.37 which corresponds to crosslinker was successfully incorporated into the PLA matrix.

### 3.5 Energy-Dispersive X-ray Spectroscopy (EDXS)

Energy-Dispersive X-ray Spectroscopy (EDXS) sometimes called energy dispersive X-ray analysis (EDXA), is an analytical technique used for the elemental analysis or chemical characterization of samples. EDX was conducted to investigate the elemental composition of three samples namely neat PLA, GO-PLA and crosslinked PLA, which are seen in figure 3.5.

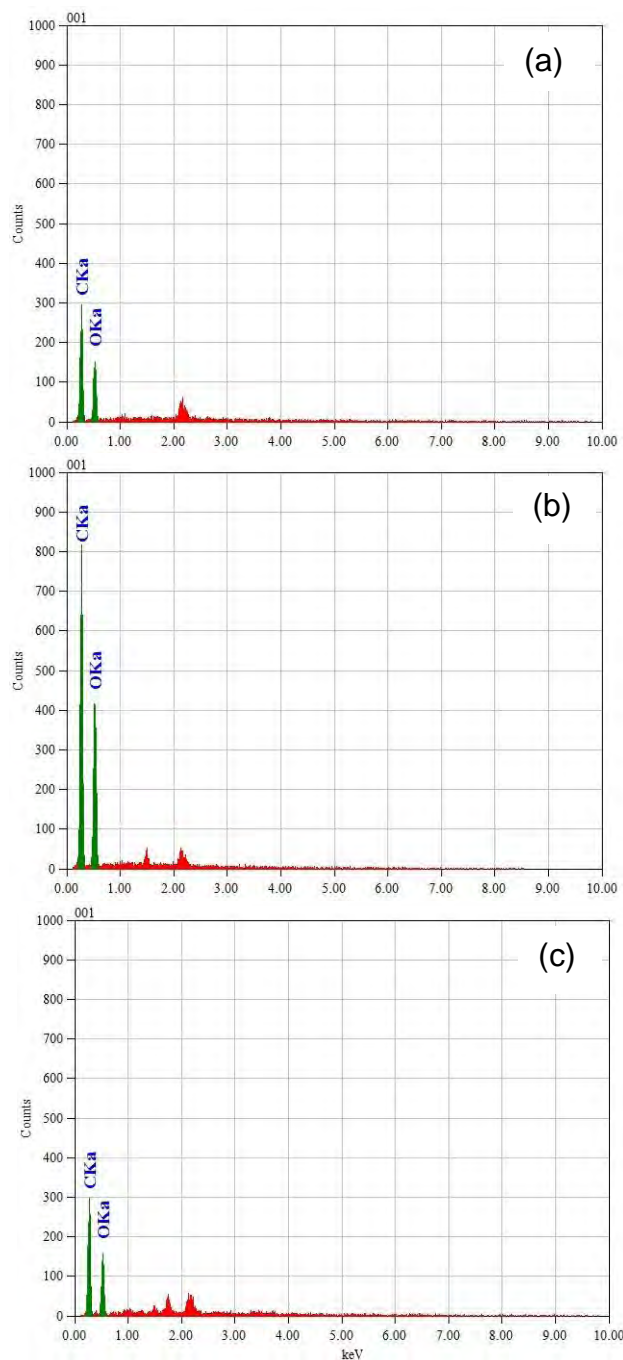


**Figure 3.5.** EDX spectra of (a) PLA, (b) GO-PLA and (c) Crosslinked PLA

Figure 3.5 (a) shows that PLA contains two desired atom carbon (C) and oxygen (O), and the atom percentage was 65.68% and 34.32% respectively. In the case of GO-PLA (b), same atom were found and the atom percentage was 65.17% and 34.83%. We also got same atom for crosslinked PLA (c) in the percentage of 66.09% and 33.91% respectively. All of the atoms and their percentages are summarized in table 3.4.

**Table 3.4.** Elemental composition of PLA, GO-PLA and Crosslinked PLA.

Samples	C %	O %
PLA	65.68	34.32
GO-PLA	65.17	34.83
Crosslinked PLA	66.09	33.91

### 3.6 Surface Morphology study using Atomic force microscope (AFM)

#### 3.6.1 Surface morphology of GO-LA-LA

In order to get three dimensional images with high resolution, GO based 2D-crosslinker, neat PLA and 0.33% crosslinked PLA was characterized by atomic force microscopy. We analyzed atomic force microscopy images using AFM Nanoscope software. AFM height sensor image of 2D-crosslinker which, corresponds to GO-LA-LA is shown in Figure 3.6.1 in the scale of  $3\mu\text{m}$ . According to literature the average thickness of GO surface is 1.37 nm [26]. When GO was functionalized by LA monomer in order to fabricate crosslinker, then the average thickness was found 2.73 nm which is increased significantly from 1.37 nm to 2.73 nm. This thickness changing of GO indicated clearly that LA monomer was on the GO surface.

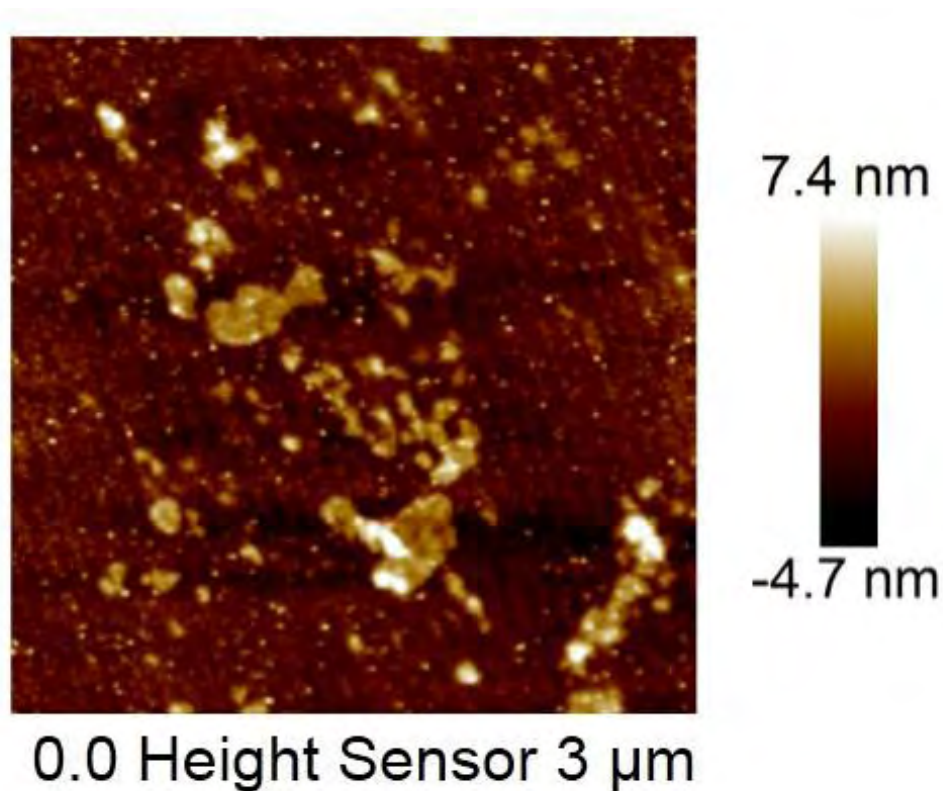


**Figure 3.6.1** AFM height sensor image of GO-LA-LA

### 3.6.2 Surface morphology of neat PLA and crosslinked PLA

Atomic force microscope was also conducted to get surface dependent information of neat PLA and crosslinked PLA. The height sensor atomic force microscope images of both sample are shown in figure 3.6.2. It has measured the average thickness of PLA surface is 3.1 nm in the scale of 1  $\mu\text{m}$  (Figure 3.6.2(a)). When we fabricated crosslinked PLA, than the average surface thickness was found 35 nm in the scale of 50  $\mu\text{m}$ . and the height sensor image is shown in figure 3.6.2 (b). It is a very interesting matter that, after crosslinking the thickness of PLA was increased tremendously from 3.1 nm to 35 nm and the scale was shifted simultaneously from 1  $\mu\text{m}$  to 50  $\mu\text{m}$ . Here it is clearly seen that the thickness of graphene crosslinked PLA is increased by 10~ folds. To the best of our knowledge, this kind of observation has never been reported before.

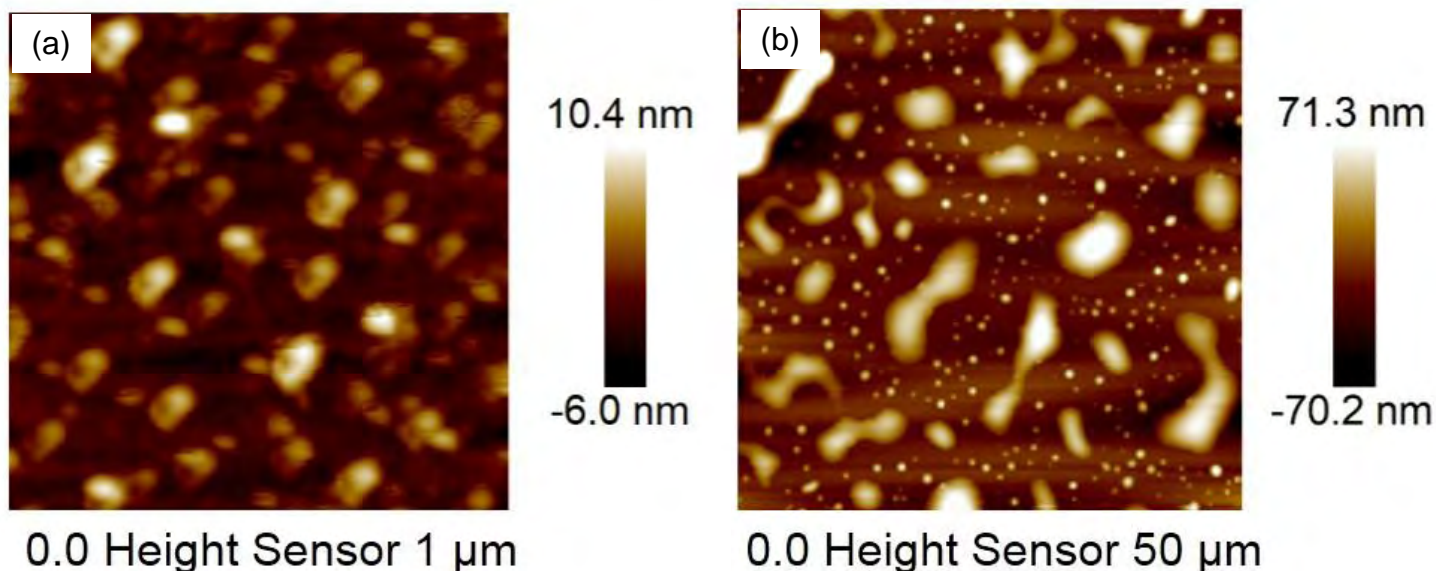


**Figure 3.6.2** AFM height sensor images of (a) PLA and (b) crosslinked PLA

### 3.6.3 Height profile analysis of GO-LA-LA by Atomic force microscope

For getting more surface information of GO-LA-LA, neat PLA and crosslinked PLA, the height profiles also have been analyzed by using mostly surface sensitive analytical technique atomic force microscope (AFM).

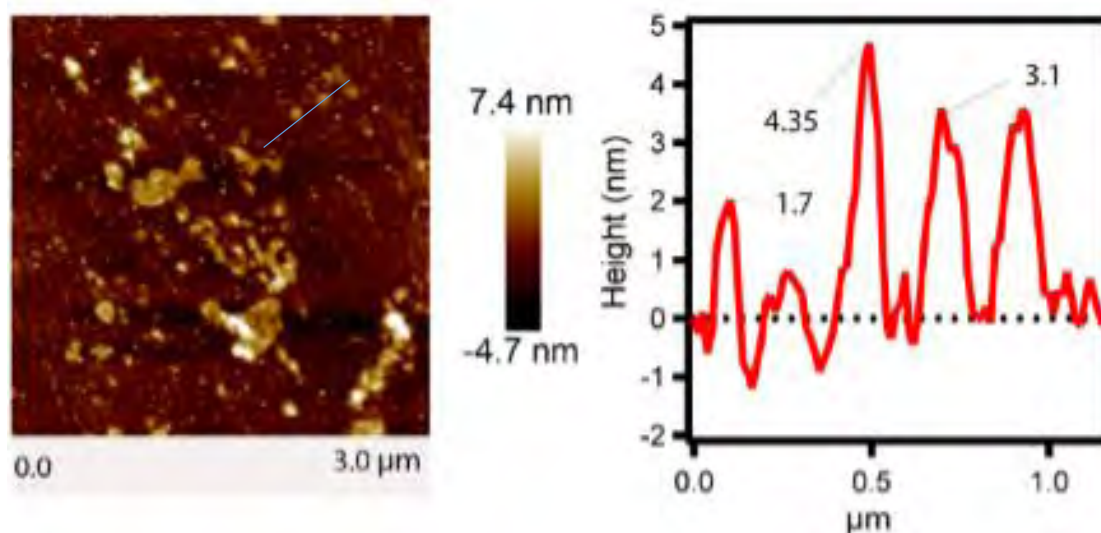


**Figure 3.6.3** Height profile image of GO-LA-LA

Figure 3.6.3 shows that the maximum height of GO-LA-LA is 4.35 nm and the height range is (1.6-4.2) nm, maximum diameter is  $96 \pm 237$  nm where diameter range (67-237) nm.

### 3.6.4 Height profile analysis of pristine PLA and crosslinked PLA by Atomic force microscope

For pristine PLA the maximum height was measure 10.8 nm (Figure 3.6.4 (b)) and the height range was from 0.1 to 5  $\mu\text{m}$ . Figure 3.6.4 (b) also shows that the diameter is  $71 \pm 31$  nm and the diameter range (22-137) nm. It is very clearly seen from figure 3.6.3 (d) that the maximum height of crosslinked PLA surface is 93.3 nm and the height was at the range of 7.5 to 97.5 nm, whereas the  $(1.4 \pm 0.2)$   $\mu\text{m}$  and  $(1.1-2.3)$   $\mu\text{m}$  was the diameter and the diameter range respectively.

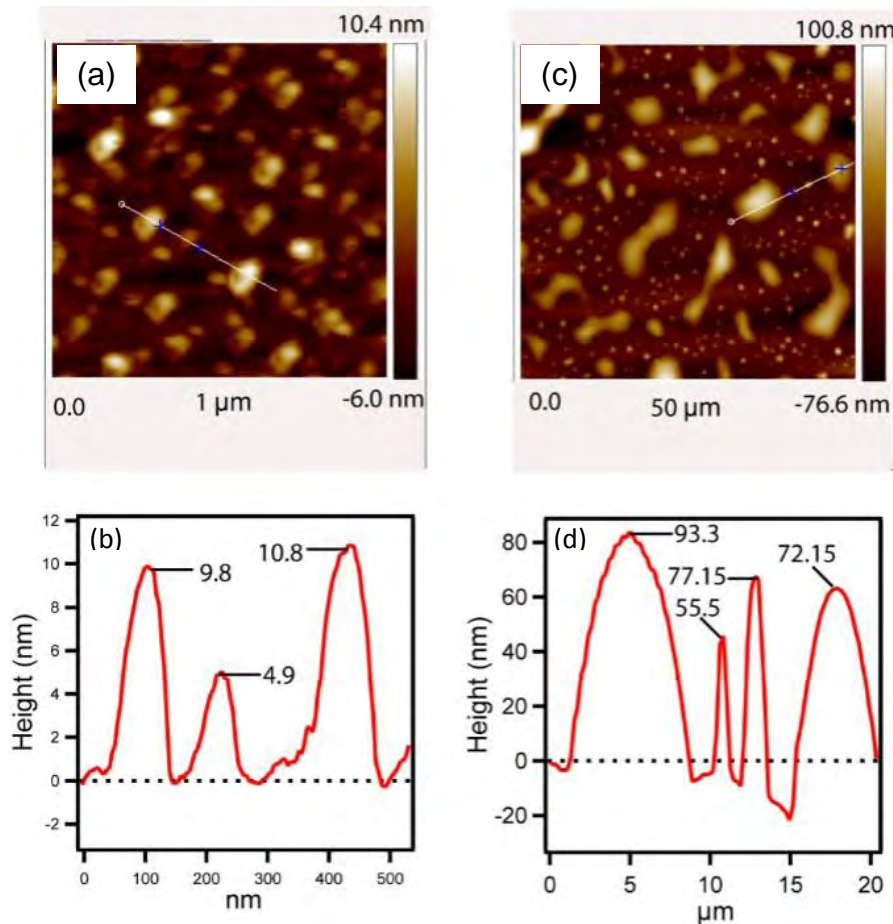


**Figure 3.6.4.** Height profile images of (a, b) pristine PLA and (c, d) crosslinked PLA.

From the surface topography of crosslinked PLA (Figure 3.6.4 (c)) we see that it contains some large, some are medium and some are small polymer chain. It is a very interesting matter that the



small chains are larger than the polymer chain of pristine PLA. It elucidates visibly us that after crosslinking the chain length of PLA was increased significantly.

### 3.7 Surface morphology of pristine PLA and crosslinked PLA using Field Emission Scanning Electron Microscopy (FE-SEM).

Phases are very vital to understand the polymer behavior. Field emission scanning electron microscopy (FE-SEM) was performed to observe the surface morphology of pure PLA and crosslinked PLA and the FE-SEM images are shown in figure 3.7. Cylindrical pellets of PLA and crosslinked PLA was made applying same pressure and temperature in the purposes to compare surface structure. In figure 3.7 (a), FE-SEM image of PLA shows very porous and irregular surface.

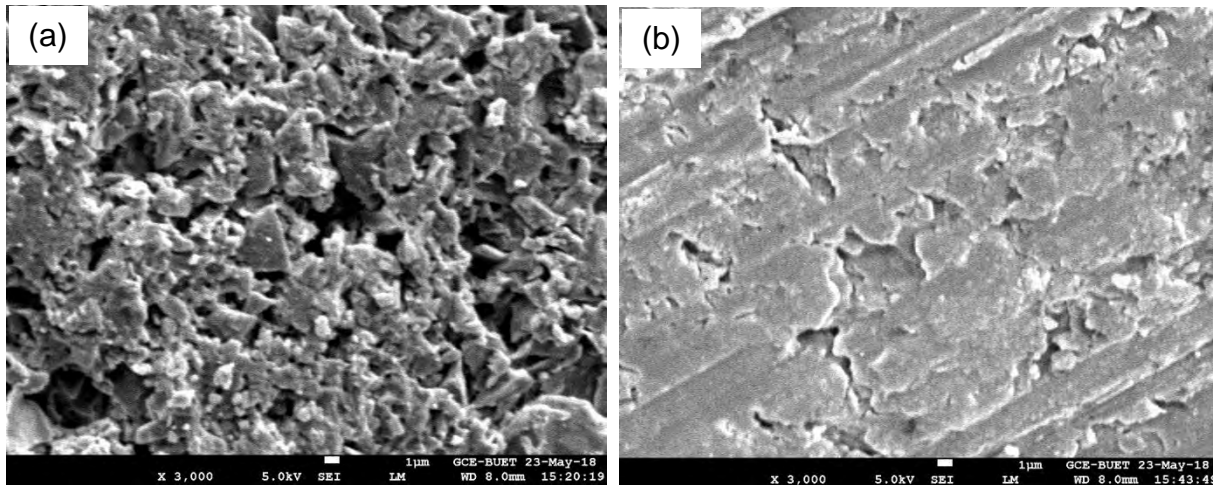


**Figure 3.7** Typical SEM images for the surface of (a) pristine PLA and (b) crosslinked PLA.

This type of porous structure of PLA surface is responsible for its brittleness failure behavior. Figure 3.7 (b) corresponds to FE-SEM image of crosslinked PLA and here it is clearly observed that the 2D-crosslinkers are dispersed homogeneously in PLA matrix without any significant agglomeration. The SEM image of 0.33% crosslinked PLA depicted in figure 3.7 (b) displays a well arranged surface and the crosslinkers are embedded and tightly held in the polymer matrix. This phenomenon can be explained in terms of strong interfacial adhesion between crosslinkers and PLA because of the covalent bonding between oxygen containing functional group of crosslinker and PLA.



### 3.8 Thermogravimetric analysis (TGA)

Thermogravimetric analysis (TGA) gives information on the weight loss due to degradation as a function of temperature. Figure 3.8 represents the weight loss curves of PLA, GO-PLA and crosslinked PLA. For comparison purposes, the TGA profile of the pure compounds are also included in the plot. The results of the thermogravimetric analysis (TGA) of PLA, GO-PLA and crosslinked PLA are shown in fig 3.8. Thermal degradation of neat PLA and GO-PLA take place in a single weight loss step, which can be evidence from the TGA curves.

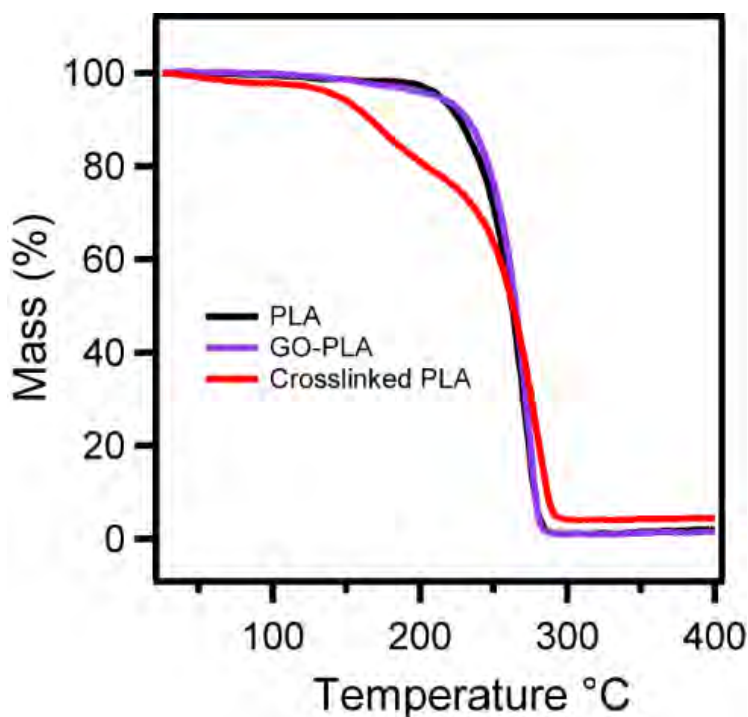


**Figure 3.8.** Thermogravimetric analysis of PLA, GO-PLA and crosslinked PLA

The profile for the pure compounds showed that the PLA has lower thermal stability than GO-PLA, because its degradation peak was at 205 °C and it was completely decomposed at 284 °C, while GO-PLA showed peak degradation at 227 °C and was fully degraded at 285 °C. On the other hand crosslinked PLA exhibits different behavior as compared to that of PLA and GO-PLA. Thermal degradation of the crosslinked PLA takes place in triple weight loss steps. In the first step, the slight degradation range 70 °C to 140 °C for physically absorbed water and the second step degradation starts at the temperature 140 °C and completed at 235 °C due to pyrolysis for oxygen

containing functional group. In the third step Weight loss of crosslinked PLA increasing continuously after 250 °C and completely decomposed at 291 °C.

### 3.9 Thermal behaviors of polymers using Differential scanning calorimetry (DSC)

The DSC heating thermograms of neat PLA, GO-PLA and crosslinked PLA are summarized in Figure 3.9. The curves of plasticized PLA exhibited two thermal transitions, i.e., glass transition ( $T_g$ ), and melting ( $T_m$ ) temperatures. Neat PLA possibly exposed a  $T_g$ , and  $T_m$  peak located at 154 °C and 273 °C, respectively. The glass transition temperature ( $T_g$ ) of GO-PLA was decreased compared to neat PLA from 154 °C to 137 °C.

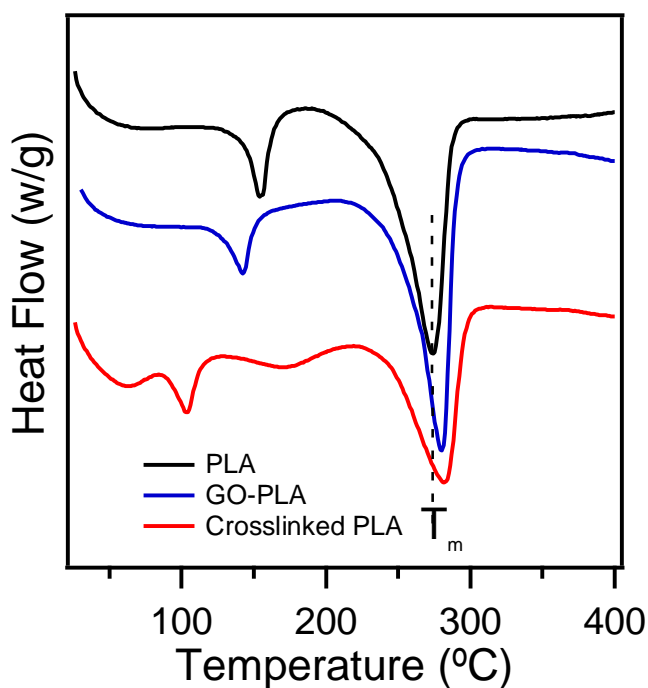


**Figure 3.9.** DSC thermograms for the PLA, GO-PLA and crosslinked PLA

For crosslinked PLA the glass transition temperature ( $T_g$ ) also decreased significantly from 154°C to 103°C. The significant decrease in  $T_g$  of crosslinked PLA was substantial may due to higher chain length of crosslinked PLA mentioned from the surface topography of AFM. The melting temperature ( $T_m$ ) was recorded 275°C and 283°C for GO-PLA and crosslinked PLA respectively. It is higher than the  $T_m$  of net PLA. For crosslinked PLA we got a different curve, while the GO-

PLA and neat PLA exhibited same DSC curves illustrated graphically in figure 3.9. It may be due to some chemical changes during crosslinking. However, DSC thermograms require more study and further investigation.

### 3.10 Mechanical strength measurement

Comparative mechanical properties were tested using universal testing machine (UTM) of pristine PLA, 0.1%, 0.2% and 0.33% crosslinked PLA, and untreated pure GO based PLA.

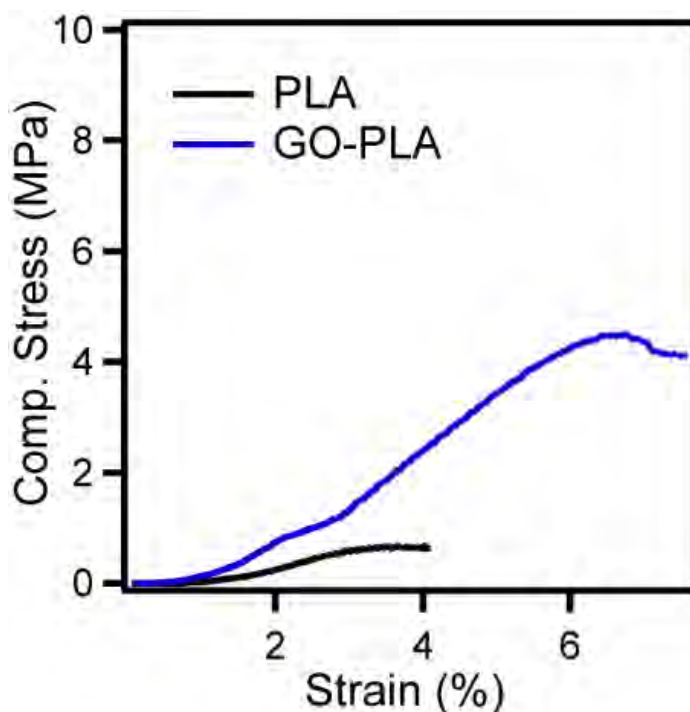


**Figure 3.10.** Stress vs. strain curve of pristine PLA and pure GO based PLA (GO-PLA)

To confirm the accuracy of comparison cylindrical pellets were made applying same pressure and temperature in order to measure compressive strength. The results are also presented in more detail in separate figures. Compressive stress (MPa) vs strain (%) curves are depicted in Figure 3.10 and 3.11. The figure clearly shows that both compressive stress and strain (%) have become higher of GO-PLA compared to pure PLA. So, loading GO in the PLA has increased the compressive strength as well as the strain (%). Mechanical properties of 0.1 and 0.2% crosslinked PLA have represented in figure 3.11 In this case no specific numerical stress and strain data were found,

because the UTM maximum load cell was 1 KN which was unable to break the 0.1 and 0.2 % crosslinked pellets. From the curve (figure 3.11), when PLA was crosslinked the compressive stress and strain (%) was increased significantly from neat PLA and GO-PLA.

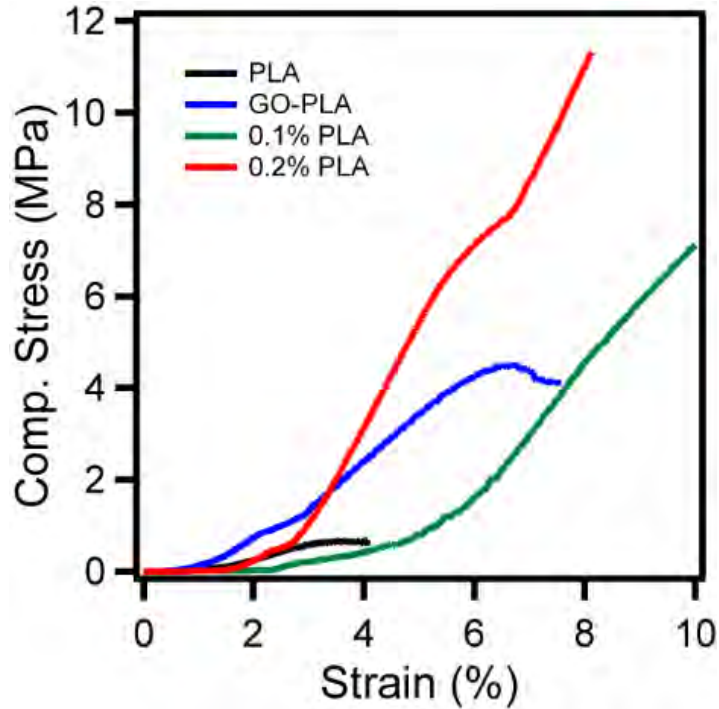


**Figure 3.11.** Stress vs. strain curve of pristine PLA and pure GO based PLA (GO-PLA), 0.1 and 0.2 % crosslinked PLA.

According to the reading of 1 KN load cell UTM, the numerical values of stress and strain (%) values are summarized in table 3.5. It is seen that, the strain percentages are 12 and 8.1 for 0.1 and 0.2% crosslinked PLA whereas the compressive strength was 7 and 11 MPa respectively. The mechanical values of crosslinked PLA, which are at least 15 times greater mechanical strength than PLA and 3~ times than pure GO based PLA. The mechanical performance of crosslinked polymer is expected to depend on the formation of covalent bond between 2D-crosslinker and PLA chain, amount of crosslinker loadings, stress transfer efficiency of the interface. The increase in strength is an indication of strong stress transfer throughout the interface, which means that there is practically chemical bonding between the crosslinker and PLA matrix. Figure 3.12 corresponded clearly the compressive strength of the polymer samples.

**Table 3.5** Stress vs. strain curve of pristine PLA and pure GO based PLA (GO-PLA), 0.1 and 0.2 % crosslinked PLA.

Samples	Strain %	Compressive Strength (MPa)
PLA	4.0	0.7
GO-PLA	6.5	4.5
0.1 % PLA	12.14	7.0
0.2 % PLA	8.1	11

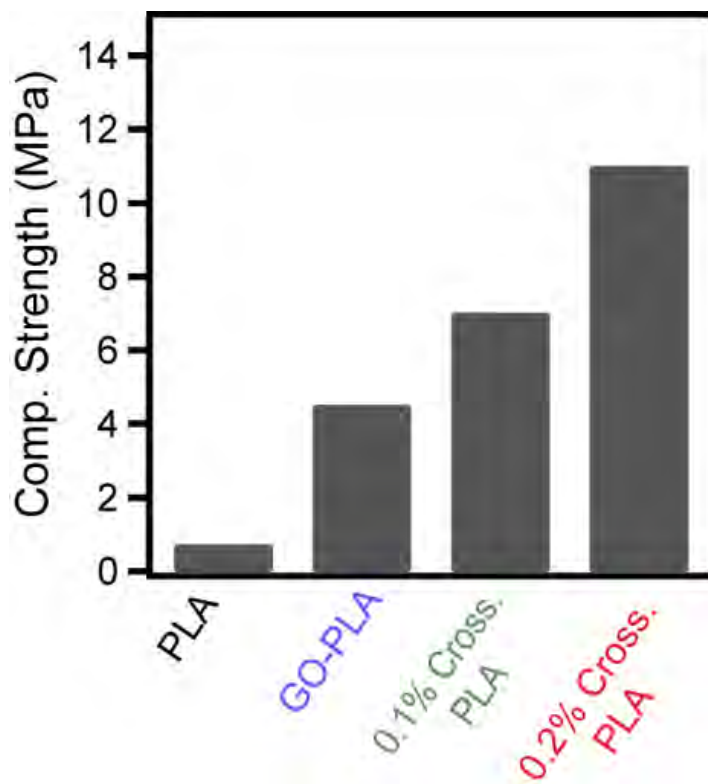


**Figure 3.12.** Comparison of the compressive strength of PLA, GO-PLA, 0.1, 0.2% crosslinked PLA.

Graphene-crosslinked PLA exhibited at least ~15 times greater mechanical strength than PLA, and ~3 times greater than GO-PLA. However, the mechanical properties is requires more details study to determine the numerical data. An interesting matter happened for 0.33% crosslinked PLA during compression. When forced was applied on it total energy was dissipated throughout the samples. From the compressive stress vs. strain (%) curve (Figure 3.13), it is comprehended that compressive strength was very low but interestingly strain percentage was measured more than 40%. If we can report this data after repeating experiment again than 0.33% crosslinked PLA would be widely used as a food packaging materials. However, it is an unusual behavior from the 0.1 and 0.2% crosslinked PLA that's why 0.33% crosslinked PLA is still under investigation and will be repeated.

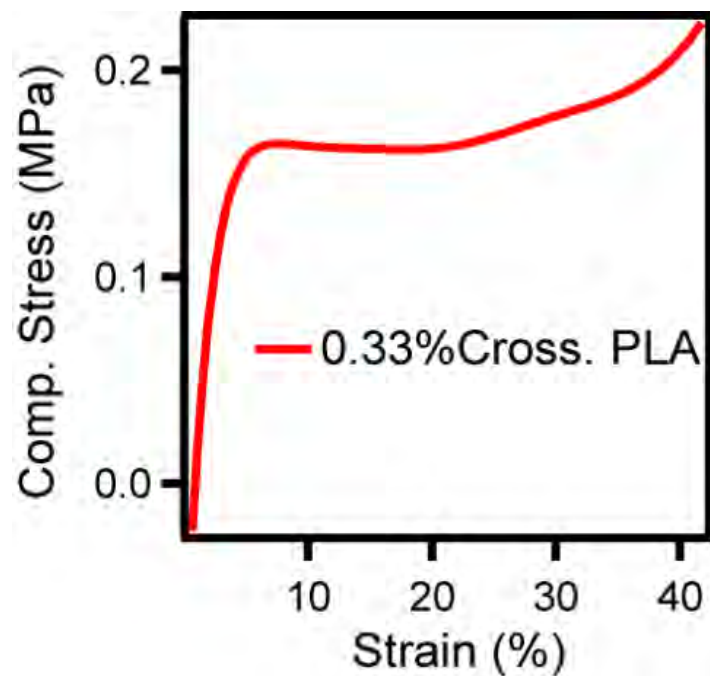


**Figure 3.13.** Compressive stress vs. strain (%) curve of 0.33% crosslinked PLA.

Physical appearance of the pellets of neat PLA and 0.33% crosslinked PLA is depicted in figure 3.14 during compression.

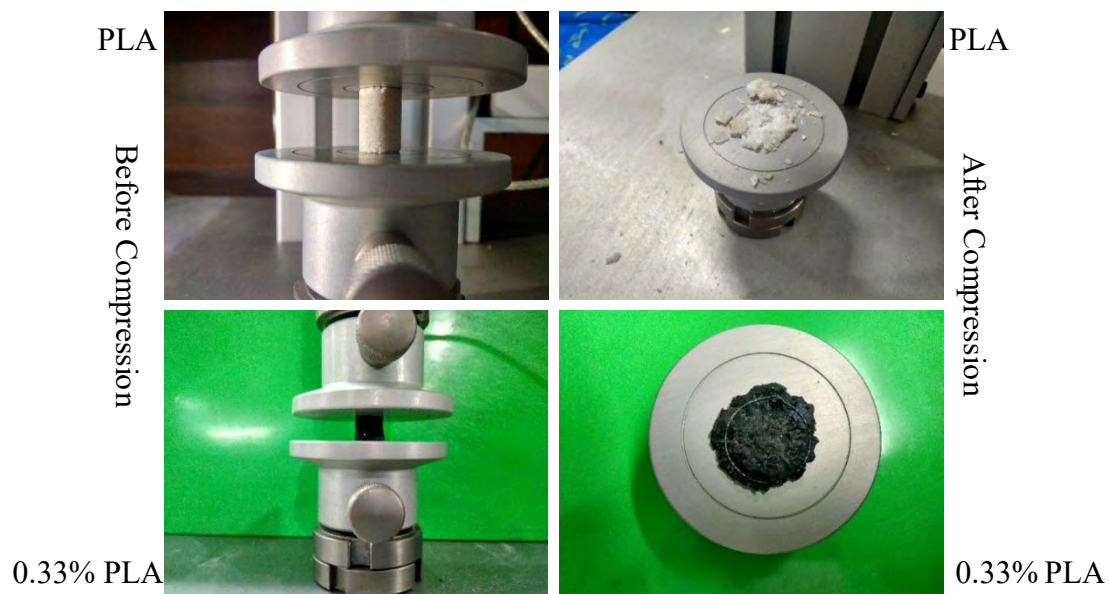


**Figure 3.14.** Compressive stress vs. strain (%) curve of 0.33% crosslinked PLA.

Figure 3.14 shows that the pure PLA pellet was broken like shard after compression in UTM, while 0.33% crosslinked PLA was unbroken and energy was dissipated through the sample. Finally, from the mechanical data it is seen that, our Graphene-crosslinked PLA exhibited at least ~15 times greater mechanical strength than PLA, and ~3 times greater than GO-PLA and 0.33% crosslinked PLA exhibited more than 40% of strain.

### 3.1.2 Conclusion

In this research GO, with further modification was properly covalently functionalized by biocompatible LA. We have successfully synthesized neat PLA, crosslinked PLA and pure GO based PLA via one step based on in situ polycondensation reaction of the commercially available LA monomer. The morphology of the fabricated polymers and graphene crosslinker was characterized by atomic force microscopy (AFM) and scanning electron microscopy (SEM). We found from SEM study that crosslinkers are homogeneously dispersed in polymer matrix without agglomeration as well as the surface thickness and diameter was determined by AFM analysis. XPS and FTIR studies specified the elemental composition and the presence of functional group that the oxygen-containing functional group of GO showed active enough to participate the polycondensation of LA and thus PLA was covalently bonded in the surface of GO-LA-LA. Samples were thermally characterized by TGA and DSC thermograms. As one of the most important biocompatible and biodegradable material, PLA bonding with the high performance GO based two dimensional crosslinker grant the improvement of mechanical properties and may multipurpose of PLA. Mechanical properties were tested by universal testing machine (UTM). Compressive strength was determined as mechanical properties making cylindrical pellets. 01, 0.2 and 0.33% crosslinked PLA were fabricated and showed excellent compressive strength compared to the neat PLA and pure GO based PLA and it was ~15 times greater mechanical strength than PLA, and ~3 times greater than GO-PLA and 0.33% crosslinked PLA exhibited more than 40% of strain.



**References**

- [1] A. K. Geim and K. S. Novoselov, "The Rise of Graphene," *Nature Materials*, vol. 6, pp. 183, (2007).
- [2] G. Brumfiel, "Graphene Gets Ready for the Big Time," *Nature*, vol. 458, pp. 390-391, (2009).
- [3] E. C. H. Sykes, "Graphene Goes Undercover," *Nature Chemistry*, vol. 1, pp. 175, (2009).
- [4] A. A. Balandin, S. Ghosh, W. Bao, I. Calizo, D. Tewwdebrhan, F. Miao and C. N. Lau, "Superior Thermal Conductivity of Single-Layer Graphene," *Nano Letters*, vol. 8, pp. 902-907, (2008).
- [5] K. I. Bolotin, K. J. Sikes, Z. Jiang, M. Klima, G. Fudenberg, J. Hone, P. Kim and H. L. Stormer, "Ultrahigh Electron Mobility in Suspended Graphene," *Solid State Communications*, vol. 146, pp. 351-355, (2008).
- [6] M. D. Stoller, S. Park, Y. Zhu, J. An and R. S. Ruoff, "Graphene-Based Ultracapacitors," *Nano Letters*, vol. 8, pp. 3498-3502, (2008).
- [7] S. Park and R. S. Ruoff, "Chemical Methods for the Production of Graphenes," *Nature Nanotechnology*, vol. 4, pp. 217, (2009).
- [8] I. Yoshito and T. Hideto, "Biodegradable polyesters for medical and ecological applications," *Macromolecular Rapid Communications*, vol. 21, pp. 117-132, (2000).
- [9] I. Armentano, N. Bitinis, E. Fortunati, S. Mattioli, N. Rescignano, R. Verdejo, M. A. Lopez-Manchado and J. M. Kenny, "Multifunctional Nanostructured PLA Materials for Packaging and Tissue Engineering," *Progress in Polymer Science*, vol. 38, pp. 1720-1747, (2013).
- [10] K. K. Yang, X. L. Wang and Y. Z. Wang, "Progress in Nanocomposite of Biodegradable Polymer," *Journal of Industrial and Engineering Chemistry*, vol. 13, pp. 485-500, (2007).
- [11] F. E. Kohn, J. W. A. van den Berg, G. van de Ridder and J. Feijen, "The Ring-Opening Polymerization of D,L- Lactide in the Melt Initiated with Tetraphenyltin," *Journal of Applied Polymer Science*, vol. 29, pp. 4265-4277, (1984).

- [12] K. K. Woong and W. S. Ihl, "Synthesis of High- Molecular- Weight Poly(L- lactic acid) by Direct Polycondensation," *Macromolecular Chemistry and Physics*, vol. 203, pp. 2245-2250, (2002).
- [13] D. C. Marcano, D. V. Kosynkin, J. M. Berlin, J. M. Berlin, A. Sinitskii, Z. Sun, A. Slesarev, L. B. Alemany, W. Lu and J. M. Tour, "Improved Synthesis of Graphene Oxide," *ACS Nano*, vol. 4, pp. 4806-4814, (2010).
- [14] J. I. Paredes, S. Villar-Rodil, A. Martínez-Alonso and J. M. D. Tascon, "Graphene Oxide Dispersions in Organic Solvents," *Langmuir*, vol. 24, pp. 10560-10564, (2008).
- [15] J. Chen, B. Yao, C. Li and G. Shi, "An Improved Hummers Method for Eco-friendly Synthesis of Graphene Oxide," *Carbon*, vol. 64, pp. 225-229, (2013).
- [16] W. Song, Z. Zheng, W. Tang and X. Wang, "A Facile Approach to Covalently Functionalized Carbon Nanotubes with Biocompatible Polymer," *Polymer*, vol. 48, pp. 3658-3663, (2007).
- [17] J. T. Yoon, S. C. Lee and Y. G. Jeong, "Effects of Grafted Chain Length on Mechanical and Electrical Properties of Nanocomposites Containing Polylactide-grafted Carbon Nanotubes," *Composites Science and Technology*, vol. 70, pp. 776-782, (2010).
- [18] A. L. Goffin, J. M. Raquez, E. Duquesne, G. Siqueira, Y. Habibi, A. Dufresne and P. Dubois, "From Interfacial Ring-Opening Polymerization to Melt Processing of Cellulose Nanowhisker-Filled Polylactide-Based Nanocomposites," *Biomacromolecules*, vol. 12, pp. 2456-2465, (2011).
- [19] S. Stankovich, D. A. Dikin, R. D. Piner, K. A. Kohlhaas, A. Kleinhammes, Y. Jia, Y. Wu, S. T. Nguyen and R. S. Ruoff, "Synthesis of Graphene-based Nanosheets Via Chemical Reduction of Exfoliated Graphite Oxide," *Carbon*, vol. 45, pp. 1558-1565, (2007).
- [20] D. R. Dreyer, S. Park, C. W. Bielawski and R. S. Ruoff, "The Chemistry of Graphene Oxide," *Chemical Society Reviews*, vol. 39, pp. 228-240, (2010).
- [21] X. Yu, Z. Xiong, J. Li, Z. Wu, Y. Wang and F. Liu, "Surface PEGylation on PLA Membranes Via Micro-swelling and Crosslinking for Improved Biocompatibility/hemocompatibility," *RSC Advances*, vol. 5, pp. 107949-107956, (2015).
- [22] C. Vergne, O. Buchheit, F. Eddoumy, E. Sorrenti, J. D. Martino and D. Ruch, "Modifications of the Polylactic Acid Surface Properties by DBD Plasma Treatment at

- Atmospheric Pressure,” *Journal of Engineering Materials and Technology*, vol. 133, pp. 030903-030910, (2011).
- [23] T. Maharana, B. Mohanty and Y. S. Negi, “Melt–Solid Polycondensation of Lactic Acid and its Biodegradability,” *Progress in Polymer Science*, vol. 34, pp. 99-124, (2009).
- [24] Y. Sun and C. He, “Synthesis, Stereocomplex Crystallization, Morphology and Mechanical Property of poly(lactide)-carbon Nanotube Nanocomposites,” *RSC Advances*, vol. 3, pp. 2219-2226, (2013).
- [25] W. Li, Z. Xu, L. Chen, M. Shan, X. Tian, C. Yang, H. Lv and X. Qian, “A Facile Method to Produce Graphene Oxide-g-poly(L-lactic acid) as an Promising Reinforcement for PLLA Nanocomposites,” *Chemical Engineering Journal*, vol. 237, pp. 291-299, (2014).
- [26] S. Stankovich, D. A. Dikin, G. H. B. Dommett, K. M. Kohlhaas, E. J. Zimney, E. A. Stach, R. D. Piner, S. T. Nguyen and R. S. Ruoff, “Graphene-based Composite Materials,” *Nature*, vol. 442, pp. 282, (2006).